Stony Brook University

A Climatology of Convection in the Northeast U.S. during the Warm Season

A Thesis Presented

by

John Christopher Murray

to

The Graduate School

in Partial Fulfillment of the

Requirements

for the Degree of

Master of Science

in

Marine and Atmospheric Science

Stony Brook University

August 2009

Stony Brook University

The Graduate School

John Christopher Murray

We, the thesis committee for the above candidate for the

Master of Science degree, hereby recommend

acceptance of this thesis

Dr. Brian A. Colle – Thesis Advisor

Associate Professor, School of Marine and Atmospheric Sciences

Dr. Minghua Zhang

Professor, Associate Dean, Director of Institute for Terrestrial and Planetary Atmospheres, School of Marine and Atmospheric Sciences

Dr. Sultan Hammed

Professor, School of Marine and Atmospheric Sciences

This thesis is accepted by the Graduate School

Lawrence Martin

Dean of the Graduate School

Abstract of the Thesis

A Climatology of Convection over the Northeast U.S. During the Warm Season

by

John Christopher Murray

Master of Science

in

Marine and Atmospheric Science

Stony Brook University

2009

The goal of this research is to highlight the spatial distribution and evolution of deep convection over the Northeast U.S. during the warm season (April through September). There is little knowledge of where convection is initiated over the Northeast U.S. in relation to the terrain, coastal, and urban areas. It is also not well known how convection evolves diurnally and as the warm season progresses. A convective climatology was constructed for the Northeast U.S. using 2km by 2km resolution NOWrad radar data from 1996-2007 as well as cloud-to-ground lightning from the National Lightning Data Network (NLDN) from 2001-2007. The lightning counts were interpolated to a 10km by 10km resolution grid centered over the Northeast U.S.

The frequency of convection at each grid point over the Northeast U.S. was obtained by summing composite reflectivity data in 15-min intervals with values of at least 45 dBZ. There are preferred regions for convection within the Hudson Valley, western and southeast Pennsylvania, central New Jersey and into the Delmarva Peninsula. A favored initiation area includes the immediate lee of the Appalachians. There is a sharp gradient in convective frequency immediately west of the coast (around New York City) as a result of the cooler marine boundary layer. There is a large interannual variability, with more convection towards the coast for years with more offshore (westerly) flow. As the warm season progresses, the convective activity shifts more towards the coast, which is consistent with the warming sea surface temperatures. During the mid-day period (18-00 UTC), the maximum convection is clearly over inland areas, but by late at night (06-12 UTC) the convective maximum shifts more offshore from the southern New England coast extending southwest across the waters through the

vicinity of the Chesapeake Bay. Composites using the North American Regional Reanalysis (NARR) highlight some of the flow patterns associated with convective enhancement in areas of upslope flow and decay with the advection of cooler air from the ocean. The various life cycles of convection over the Northeast are analyzed to highlight genesis and decay regions using hovmoller diagrams. Furthermore, convection on days of severe weather (forecasted and/or reported) are compared to the "null" convective days to compare synoptic differences and the resulting variance of the spatial distribution of convection.

Table of Contents

List of Tables

List of Figures

Acknowledgments

I would like to thank the School of Marine and Atmospheric Sciences at Stony Brook University, especially Dr. Brian Colle, who provided great support and guidance. In addition, I would like to thank Dr. Matthew Parker of North Carolina State University for his help in processing the NOWrad data. I would also like to thank the National Weather Service for my rewarding operational experiences with severe weather which helped inspire and motivate my desire to do this research, as well as the National Science Foundation for providing funding for research in convective evolution. I would also like to thank my family and friends for their tremendous support during my graduate studies.

Chapter 1 – Introduction

a. *Background*

Although severe convection is not as common over the Northeast United States as the Central Plains, Ohio Valley, and parts of the Southeast (Doswell et al 2005), accurate convective forecasts for the Northeast U.S. are still important considering the high population density in this region. Convection across the Northeast causes major flight delays at the major airport terminals (Evans and Robinson 2005). For example, Newark, NJ International Airport (as shown in Figure 1 along with other airports) experienced 41 % of its delays in arrival time from September 1998 through August 2001 due to convective weather around the New York-New Jersey area (Allan et al 2001). Also, convection can result in flash flooding as well as strong winds and hail, and this problem is multiplied in the highly urban areas of New York City, Philadelphia, and Boston. The impact is compounded by the gradients in urban development, terrain heights, soil properties, and degree of foliation across the Northeast.

Convection may be modulated by the terrain, urban, and coastal areas of the Northeast U.S. The majority of the Appalachians over the Northeast U.S. have terrain heights of less than 1200 m, and there are numerous peaks and valleys from west to east that can modify convection (Fig. 2). Topography impacts convection by providing a mechanism for lifting air to its level of free convection (LFC), generating thermal circulations, as well as creating areas of enhanced flow convergence via deflection, blocking, and perturbation of downstream air flow. Mountain wave and gravity waves

can be generated by the topography and can influence convection downstream of elevated terrain (Johnson and Mapes 2001).

Some severe weather events across the Northeast U.S. have been influenced by the higher terrain and valleys. For example, an EF3 tornado in Great Barrington, Massachusetts, on 29 May 1995 was spawned by a supercell that intensified while crossing over the Hudson Valley (Bosart et al 2006). The south southeasterly flow that was channeled by the terrain allowed for a greater amount of veering of the low level winds, which thereby increased the storm relative helicity (Bosart et al 2006). Channeled low-level flow was shown for two other Northeast tornado events: a F3 tornado in Mechanicsville, NY on 31 May 1998 (Lapenta et al 2005) and a F4 tornado in Windsor Locks, CT on 3 October 1979 (Riley and Bosart 1987). David (1976) found that tornadoes from 1968-1974 across the Northeast (Maryland and Pennsylvania through Maine) occur mostly in the summer with a west southwest flow from 850 through 500 hPa according to the closest upper air stations to the tornado touchdown.

From April through September for 1996-2006 over the Northeast U.S., there were 493 tornado reports, 4545 large hail reports (>1.9 cm in diameter), and 13074 high wind reports ($\geq$ 25.5 m s^{-1}) during the warm season from April through September (Fig. 3). Most of the annual reports occur during this warm season period over the Northeast U.S. (91% of tornadoes, 97 % of hail, and 92 % of wind). This is consistent with those times when there are warmest temperatures and highest convective available potential energy (CAPE in J kg^{-1}) on average. The spatial pattern of storm reports in Fig. 3 may not reflect the actual distribution of severe weather due to possible population biases and

inconsistencies in reporting; thus, this analysis is not too useful in understanding the spatial distribution of convection across the Northeast.

b. *Previous convective climatologies using radar and lightning*

There have been some previous studies to understand the distribution of convection over parts of the Northeast U.S. Using manually digitized radar data from 1978-1981, Falconer (1984) showed an increasing number of thunderstorm days extending southwest across the lower Hudson Valley, parts of northeast New Jersey, to the NYC metropolitan area. His radar sample was rather limited, so he could not explore the variability of the convection both diurnally and throughout the warm season. Croft and Shulman (1989) used digital radar data to quantify thunderstorm activity from 1978-1982 around the New Jersey region. They found the largest daily frequency of thunderstorm activity located over southeastern Pennsylvania, southwestern New Jersey, and northern New Jersey, with the maximum in severe thunderstorm activity over north-central and western New Jersey. The convective activity shifted to the southeast towards the ocean from July to August as temperature differences between the land and sea diminished. Relatively higher frequencies were also seen over urban areas (Croft and Shulman 1989).

Doppler radars (WSR-88Ds) were installed across the U.S. during the modernization of the National Weather Service in the 1990s. They can also be used to understand the distribution of convection, but all convective climatological studies using

this modern radar network have been outside the Northeast U.S. Carbone et al (2002) used the WSR-88D reflectivity data to identify convective complexes from the Rocky Mountains to the Appalachians. These episodes initiated primarily from elevated heating near the Rocky and Appalachian Mountains during the day. As a result, there is a convective peak during the late afternoon over the Rocky Mountains, while the Northern Plains peaks after sunset (Carbone et al 2002). Parker and Ahijevych (2007) also studied the spatial distribution of convection in the East Central U.S. from the central and southern Appalachians to the coastline. The convection over the Appalachians and along the North Carolina coast reached a maximum at 2100 UTC. They identified areas of enhanced convective activity that moved through the eastern Piedmont and coastal plain during the afternoon and evening hours. Above average vertical wind shear between the surface and 700 hPa contributed to 90% of their convective episodes, mostly in the summer during a period of conditional instability (Parker and Ahijevych 2007). No reason was given for the variability of the convection or to the geographic distribution of the convection in the Northeast.

Lightning has also been used to quantify the frequency of deep convection by summing the number of cloud-to-ground flashes per unit area. Zajac and Rutledge (2001) showed that the diurnal cycle of lightning activity was more pronounced in the mountainous western U.S. and adjacent High Plains, as well as the coastal regions of east of the Appalachians from Florida northward through the Delmarva Peninsula. Orville and Huffines (2001) mapped 216 million lightning flashes across the nation and highlighted a south to north gradient of decreasing lightning flashes from Florida to the northern portions of the Eastern Seaboard, with significant lower values over the

Appalachian and Rocky Mountains. Along the Gulf of Mexico and the Atlantic Seaboard, with the exception of Florida, the maximum flash rate abruptly shifts from evening hours to the morning hours over the water. Over the inland areas, the time of maximum flash rate is between 1200 and 2000 local time, with the exception of the northern Plains. Both of the aforementioned lightning studies did not provide exact reasoning for the distribution of the lightning activity. Across central New York State and western New England, Wasula et al (2002) showed nearly double the amount of lightning strikes when the flow at 700 hPa was from the southwest versus the northwest on days in which severe weather was reported from 1989-1998 throughout this region.

A few studies have linked the evolution over the Northeast U.S. to different terrain and coastal features. Convective genesis regions over the eastern U.S. are favored over the higher terrain over the Appalachians and the lee-side pressure trough (Bosart et al 2006; Weisman 1990). The valleys of the Hudson and Mohawk were shown by Wasula and Bosart (2002) to influence convection through channeled flow and increased shear at low-levels. Croft and Shulman (1989) noted that the higher frequency of convection over southeast Pennsylvania, southwest New Jersey, and occasionally northern New Jersey can be attributed to the land-sea temperature differences, variations in day length, and the change of air mass. Cannon (2002) studied the F1 and F2 tornado touchdowns in northern New England and found that most formed out ahead of cold fronts along a pre-frontal trough with wind shear confined to the surface to 850 hPa layer. He also found that tornados seemed to cluster to the east of the Appalachians, with good apparent correlation between north-south valleys and lakes to tornado touchdowns. However, convection sometimes initiates or intensifies over the coastal areas. This

usually occurs during the late summer when land and sea surface temperatures have diminished (Croft and Shulman 1989). Convection occurring across the coastline has also been shown to be the manifestation of land circulations during the night (Wallace 1975).

Synoptic conditions favoring severe weather outbreaks in the Northeast U.S. have also been noted for an approaching surface pressure trough axis oriented northeast to southwest as well as a quasi-stationary front oriented west-northwest to east-southeast (Johns 1984). These are related to northwest flow at 500 hPa, which have been associated with strong tornado events (F3 or greater) from Virginia through New York (Giordano and Fritsch 1991). Elevated mixed layers from the Rocky Mountains may also be important for severe weather over the Northeast U.S. (Banacos and Ekster 2006). These develop when elevated terrain heats and forms a surface based mixed layer, which advects eastward over the continental U.S. There is often a capping inversion in between the elevated mixed layer and the moist layer near the surface so that the CAPE can be stored and released later in the day.

Urban heating and associated wind circulations can enhance the low-level buoyancy and convergence zones around a major city. Loose and Bornstein (1977) presented a case study suggesting that thunderstorms can split around NYC, but only one case was presented and no evidence was presented to suggest the city was really responsible for the storm split. Changnon et al (1976) found a significant increase in thunderstorms and hail over and just east of St. Louis, Missouri. Other studies have shown urban effects on convection in Houston, Texas (Shepard and Burian 2003; Orville

et al 2000) and in Atlanta, Georgia (Bornstein and Lin 2000). This effect has not been investigated in much detail for the NYC area.

c. *Motivation*

In order to understand the evolution of convection across the Northeast, the location and timing of convective initiation and decay must be ascertained. It is known that there is some topographic and coastal dependence to the Northeast convection, but the spatial distribution of convection relative to these features needs more investigation. There are not many studies that have shown how convection varies at the hourly, daily, monthly, and annual timescales across the Northeast U.S. This knowledge is needed for accurate short term forecasts of convection that can lead to longer lead times for warnings and watches of severe convection. This thesis will address the following questions:

1) Where are the preferred regions for convective activity across the Northeast and how do they vary diurnally and during the warm season?

2) How does convection evolve around terrain, coastal geometry, and urban areas?

3) What is the role of the marine boundary layer on the convective evolution near the coast?

4) What are the large scale and local ambient conditions associated with severe convection around coastal areas, such as Long Island, New York?

Chapter 2 will describe radar, lightning, and reanalysis data and the methods to answer the aforementioned questions. Chapter 3 will highlight the spatial distribution of convection throughout the warm season, annually, monthly, and diurnally, as well as providing some physical mechanisms for these results using composites. A summary and conclusions will conclude the thesis in Chapter 4 to summarize the relevance of knowing convective evolution and how this can improve short term forecasting of convection.

Chapter 2 – Data and Methods

a. *Radar and lightning products*

The radar data used for this study consists of the National Operational Weather radar (NOWrad) provided by Weather Services Incorporated (WSI) and the National Centers for Atmospheric Research (NCAR) as well as the Upton, New York (OKX) NEXRAD (Next Generation Weather Radar System) WSR-88D Level III Doppler radar data from 1996-2007. The NOWrad is a composite of all the WSR-88D radars since 1996, which is derived from the interpolation of the raw WSR-88D data. The temporal resolution is 15 minutes and the composite reflectivity interval is 5 dBZ. Each composite reflectivity value at a grid point is the largest measured above that point from any surrounding Doppler radar. Priority is given to radars that are within 230 km of a point. For the "cone of silence" (lack of data) directly immediately surrounding a Doppler radar, the extended range data to 459 km is used from adjacent radar (Parker and Ahijevych 2007). The WSR-88D data used in this study includes radars across the northeastern quarter of the United States (Fig. 4). The WSR-88D radar data for individual stations includes all 9-11 vertical scans and is available for download at the NCDC (National Climatic Data Center).

Figure 4 shows the radar coverage at 2 and 3 km above ground level (AGL) (from Maddox et al 2002). At 2-km AGL, there is an absence of radar coverage near the Appalachians in northwest Virginia, the northeastern end of the Appalachians in Pennsylvania, as well as the Green and White Mountains near Vermont and New Hampshire, where the 0.5° beam elevation overshoots portions of these higher terrain

areas. At 3-km AGL, nearly the whole Northeast region is covered, except for a small area along the Appalachians in northwest Virginia (Maddox et al 2002). Thus, a climatology using this data can represent the spatial distribution of convection, with the caveat that the convection is deep enough (to 3 km AGL) to be observed in some terrain areas.

Another challenge of using a radar dataset is removing the non-meteorological echoes, which can lead to abnormal reflectivity counts and gradients (Joss 1990). These false returns are caused by radar artifacts, ground clutter, and anomalous propagation (AP). The false echoes can result from insects, birds, and regions of the atmosphere with high refractive index gradients (Wilson et al 1994). Anomalous propagation results from the different densities of the layer of atmosphere that intersect the radar beam. If the index of refraction decreases with height (which would be signs of warmer, less dense air overlaying relatively cooler, denser air), then the radar beam would be deflected anomalously towards the ground (super-refraction). Trapping occurs with extreme cases of super-refraction when the radar beam intersects the ground or objects at the Earth's surface. This radar signal interference is typically apparent from the lowest vertical levels of the Doppler radar (Steiner and Smith 2002). This problem can sometimes be observed from the Upton, NY (KOKX) radar during the warm season around sunrise along the New Jersey coastline, NYC when the near-surface air is cool from radiational cooling, as well as near higher topography. For example, clutter within Manhattan can arise from super-refraction of the KOKX radar beam that intersects the tall skyscrapers.

Erroneous data is filtered out by automated computer algorithms at WSI and manually removed by radar meteorologists. Some clutter is still persistent even after these quality control protocols, so one still has to use the data with care. For Parker's convective study (2005), the exclusion of the ground clutter had very little effect on the statistical results, which were averaged over areas much larger than one pixel. Also present within the dataset are WSR-88D's with slightly different calibrations, which can lead to some variation (few dBZ) in reflectivity between neighboring radars (Parker and Knievel 2005).

Cloud to ground lightning was also used to understand the spatial distribution of convection, since it does not suffer from the terrain blocking and other radar problems. The Institute for Terrestrial and Planetary Atmospheres at Stony Brook University has archived the cloud-to-ground lightning data since 2001. This data is from the National Lightning Detection Network (NLDN) and was interpolated to a grid with a resolution of 10x10 km^2 grid centered over the Northeast U.S (outlined box in Fig. 5a). There are at least 130 total lightning sensors, each capable of detecting cloud-to-ground lightning flashes out to at least 400 km. These sensors are magnetic direction finders, which determine a direction towards an electromagnetic discharge and its location from triangulation between the different direction finders. There are also sensors which record the time of arrival of the peak lightning signal and calculate the location from the difference of arrival time between at least four sensors (Christian and McCook 2009). The topographic data used in the analysis maps has a resolution of 5 minutes (or ~10 km) and it is a merged bathymetric and topographic dataset from the National Geophysical Data Center (NGDC).

b. *North American Regional Reanalysis (NARR) composites*

In order to determine the ambient conditions that favor convection in certain regions, atmospheric composites were created using the North American Regional Reanalysis (NARR). The NARR dataset was used to determine synoptic flow regimes, moisture, and instability evolution associated with the distribution of convection over the Northeast U.S. NARR data is available since 1979 at a horizontal grid spacing of 32km with 45 and vertical layers. The NARR is available every 3 hours and it incorporates many different observational types using the NCEP operational Eta model and the 3-DVariational Data Assimilation System (Mesinger et al 2006).

c. *Methods*

The NOWrad data was used for the Northeast U.S., which includes WSR-88D coverage from Ohio eastward to Virginia and northward to Maine. The NOWrad composite reflectivity data was converted from a cylindrical equidistant polar grid to a latitude-longitude grid to display in GrADS (Grid Analysis and Display System; Doty 1995). A GrADS program was written to select NOWrad composite reflectivity values ≥ 45 dBZ and then sum them across each hour and day during the warm season (April through September) from 1996-2007. Similar to Parker and Knievel's (2005) study on reflectivity statistics, and Parker and Ahijevych's (2007) study of East Central U.S. convective episodes, the frequency was divided by the total number of 15-minute time segments (N) of the dataset to give the probability that a certain point had a thunderstorm at any 15-minute period, Pr_{storm},

$$Pr_{storm}(x,y) = (1/N) \sum i_{45}(x,y,t) \text{ from } t=1 \text{ to } t=N,$$

where i_{45}= 1 when dBZ $\geq$ 45 and 0 when dBZ < 45

This statistic represents the frequency that point (x,y) had a thunderstorm at a randomly chosen time (every 15 minutes or one day). For all warm seasons in the dataset from 1996-2007, the number of 15-minute time segments is 210816 without any missing data. For each of those time segments, if composite reflectivity was $\geq$ 45 dBZ, the counter was incremented by one. Similarly, the number of thunderstorm days was computed by limiting all occurrences of convective frequency to only once per day. NOWrad data was missing for April 2001 and September of 2007. Frequencies were also computed for each hour, month and year. Many other studies used a threshold of $\geq$ 40 dBZ to identify thunderstorm cells (Parker and Knievel 2005; Fowle and Roebber 2003). The 45 dBZ threshold chosen for this Northeast analysis represent a compromise between depicting intense well-defined convection, minimizing ground clutter and bright banding (melting snow aloft), as well as having a large number of samples.

A bootstrap method was used to test for statistical significance of the results (Hesterberg et al 2009), since convective frequency may not be described by a normal distribution. This is done for all warm season days such that differences in daily means of convection between two 1° latitude by 1° longitude areas are tested for the significance of their difference at the 95 % confidence level, using 100,000 random samples.

Similarly, the lightning data from the NLDN was summed on a monthly and annual basis between the years of 2001 and 2007 to compare with the radar composite

imagery over the same period. Individual cloud to ground lightning strikes were summed within 10x10 km^2 boxes in the Northeast U.S.

In order to better understand the propagation and evolution of convection over the Northeast, hovmoller diagrams were constructed for each week of all warm seasons from 38.5º N and 41.5º N and from central Indiana to offshore of the Delmarva Peninsula and the waters south of Long Island. The goal was to determine the favored longitudes of convective initiation and decay. For this study, the echo frequency of composite reflectivity ≥ 45 dBZ was calculated, similar to Carbone et al (2002), to show the percentage of time an echo ≥ 45dBZ is observed at a particular longitude and hour of the day. The movement and development of convection on the hovmoller plot is depicted as a "streak" of enhanced convective frequencies ≥ 45 dBZ. On each hovmoller plot, the location of the origin (O) and decay (D) were manually recorded in 1 degree longitude bins for each streak that was at least 3º in longitudinal width and exhibited continuous echo frequencies ≥ 30 % as shown in Fig. 6. The criterion of 3º longitudinal width does not include any non-continuous areas, where convective systems may decay and reform. The frequency of origins and decays of the convective episodes were plotted for different longitudes. In addition, three types of objects were identified. Short-lived (SL) events persisted and were visually isolated for less than a day (Fig. 7a), while long-lived (LL) events had to persist at least one day over at least the same 3 degree longitude area (Fig. 7b). Serial convective events (SC) had at least 3 streaks evident over 4 consecutive days (Fig. 7c). A streak had to deviate from a straight horizontal line on a hovmoller plot in order to be as considered propagating. When streaks are purely horizontal, the

convection initiated everywhere in the domain during that hour and would not be propagating.

To investigate the diurnal evolution of convection for various subregions across the Northeast U.S., convective frequency ($\geq$ 45 dBZ) was summed for each hour of the day within several boxes over the Northeast (Fig. 8). A quantitative comparison of the areal sums and averages between two adjacent boxes around Long Island was conducted for 24 hour periods that had frequencies > 1 standard deviation greater than the mean of one of the boxes. This was done to focus on the more convectively active days and eliminate days contaminated with ground clutter. After the significant days were indentified, convection in the adjacent box was compared and only days in which the adjacent box had 50 % less convection were recorded. Boxes across western and eastern Long Island were also tested for days in which both boxes had convection greater than 1 standard deviation. For each of these days, only the maximum hour of convection was recorded. In addition, to better depict intense convection, reports of severe weather were also recorded for the boxes.

Knowing the ambient conditions associated with convectively active regions can help better forecast these events. The 3-hourly NARR data closest to the peak time of the convection and reports of severe weather within a box was composited (averaged). Low level conditions at 925 hPa were averaged including the geopotential height, equivalent potential temperature (Θe), and average CAPE between the surface and 180 hPa above. Upper level conditions were also averaged, which included the 500 and 300 hPa geopotential heights, and wind speeds, and 500 hPa absolute vorticity.

NARR data was also used to separate synoptic-scale flow regimes, such as that the spatial distributions of convection in a particular region can be plotted for each regime. Four points around each area of interest were chosen where there were large gradients in convective frequency. The convective events were separated using four different wind direction bins at 925 hPa and 500 hPa, helping identify the terrain forcing and 500 hPa large scale flow regime. The points for each level are shown as X's and O's on Fig. 9. The wind directions were categorized as follows: South-Southeast to Southwest (145º - 225º), Southwest to West-Northwest (225º - 315º), Southwest to West (225º - 270º), West to Northwest (270º - 315º).

To determine the spatial distribution of convection over the Northeast U.S. during periods of severe weather days, the days in which there was either a warning issued and/or storm report were recorded. The storm reports and warnings issued by the National Weather Service are available from verification and storm database (http://verification.nws.noaa.gov). The fraction of convection on severe weather days was calculated for the regions surrounding the New York NY (OKX), Mount Holly NJ (PHI), State College PA (CTP), Binghamton NY (BGM), Albany NY (ALB), Sterling VA (LWX) and Taunton MA (BOX), National Weather Service offices as shown in Fig. 10.

Chapter 3 – Northeast U.S. Convective Climatology Results

a. *Warm season average*

First, the spatial distribution of convection averaged from April-September 1996-2007 was calculated over the Northeast U.S. Figure 11 shows the percent of time (for all 15 minute time periods) that the reflectivity is greater than or equal to 45 dBZ over the Northeast U.S. during the warm seasons of 1996 through 2007. Some care has to be made when interpreting these results, since some ground clutter still exists around some of the radar locations and along the coast (e.g. coastal New Jersey), and there is some beam blockage by terrain (radial spokes on image). In addition, there is a ring of relatively higher ≥ 45 dBZ frequencies (over eastern PA) associated with the Mount Holly (KPHI) radar, which might be a radar calibration issue or a radar mosaic problem in the WSI composite product. The most active convective areas exist along the coastal plain from southeast Maryland northeastward to southwest Connecticut, southeast Pennsylvania near the lee of the Appalachians, just west of the windward Appalachians in southwest Pennsylvania, and the Hudson and Mohawk Valleys of New York in between the Catskill and Adirondack Mountains (see Figure 2 for locations). In these areas, the percentage per 15-minute interval for composite reflectivity ≥ 45 dBZ varies between 0.18 and 0.27%. In contrast, the percentage is a relative minimum (< 0.15%) over parts of northeast Pennsylvania, eastern New England, and the coastal waters around Long Island, extreme southern New Jersey, and the Great Lakes. All of these locations are influenced by the relatively cool sea surface temperatures during the warm season. The daily convection for a few 1° latitude by 1° longitude areas across southwest

Pennsylvania and western Long Island were found to be significantly different at a 95 % confidence level compared to other areas of equal dimension in eastern Long Island and northwest Pennsylvania, using 100,000 random resampling methods.

Since the average percentage may be influenced by a few very active days, only the percentage of days exceeding 45 dBZ was calculated (Fig. 12). This leads to a somewhat smoother analysis that highlights the maximum (coastal plain, southeast PA, western PA, and Hudson and Mohawk River valleys) and minimum (eastern New England, coastal waters, Great Lakes, central Appalachians from VA to PA) areas as well. The percentages in the active areas varies from 10 to 13 %, while the minimum areas have percentages generally < 8 %.

Other thresholds of composite reflectivity were tested to determine the sensitivity of these radar results and determine the convective frequency for stronger and weaker events (Fig. 13). When the composite reflectivity threshold was lowered to 40 dBZ, as done over the mid-Atlantic in Parker and Ahijevych (2007), the convective frequencies (0.45-0.65 %) are 2-4 times greater than the ≥ 45+dBZ threshold (Fig. 13a). The 40 dBZ has less of a gradient of convection across Long Island, which is likely because 40 dBZ includes many weakening convective events and some heavy stratiform areas associated with the radar bright band (melting level) aloft. Many of the other maximum and minimum areas are similar to the 45 dBZ threshold. For the 50 dBZ threshold, which represents the more vigorous convection, the maximum percentage ranges from 0.06 to 0.11 % (Fig. 13b), which is approximately a third of that of the 45 dBZ threshold. The maximum areas for 50+dBZ frequencies are in the same general locations as the ≥ 45

dBZ thresholds; however, the maximum region is somewhat more widespread across southeast Pennsylvania and southeast New Jersey, and the maximum in the Hudson Valley is more well-defined than lower thresholds.

Given some of the radar quality control issues, it is important to validate the above results against an independent data source. Fig. 14 compares the NOWrad 15-minute interval composite reflectivity percentage $\geq$ 45 dBZ and the percentage each month per km^2 obtained by the cloud to ground lightning strikes over the same 2001-2007 warm seasons.[1] There is general agreement between the maximum and minimum locations of convection using the radar and lightning data; however the convective areas are somewhat better defined in the lightning data, since this dataset is less susceptible to heavy stratiform precipitation influences. There are maximum areas of cloud to ground strikes in east-central Maryland, southwestern Pennsylvania, and northern West Virginia (> 0.70 %), which are somewhat farther to the south than the reflectivity data. There are secondary maxima between 0.50 and 0.70 % in southeastern Pennsylvania and in the vicinity of New York City.

The lightning data provides more defined gradients of convection in areas of terrain than the composite reflectivity, so the lightning data was used to better understand the mesoscale details around the region (Fig. 14b). For example, the lightning percentage decreases rapidly (by at least 60%) from southwest Pennsylvania (0.70-1.10 %) to the

[1] The lightning data from 2001 through 2007 has a few missing months (April from 2001 and 2003-2007, May 2001, September 2006, and September 2007).

immediate lee of the Appalachian crest over central Pennsylvania (0.30-0.50 %). There are localized maxima (0.50-0.60 %) and minima (0.30-0.40 %) on the southern and northern side of the smaller ridges, respectively, such as enhancement at points A, C, and D, and a reduction at point B. This modification at A, B, and C is consistent with the orographic upslope enhancement expected for a low-level southerly flow component, interacting with the south (windward) and north (lee) side of the ridges. The convective maximum near Albany, NY (Point D), suggests an enhancement that develops with westerly flow down the Mohawk Valley towards the Berkshire Mountains. Finally, the maximum over Maryland is primarily just west of Chesapeake Bay, which is consistent with a sea breeze to the west of the Bay helping to enhance convective frequency.

When the lightning frequency is recalculated as a daily percentage (Fig. 15), many of the same convective features are present. However, the convection is more enhanced over the windward side of the Appalachians (western Pennsylvania and West Virginia) than other areas. Meanwhile, the maximum areas to the east such as the Chesapeake, urban locations, and to the lee of the Appalachians are somewhat less pronounced than the 30-minute lightning frequencies in Fig. 14. Thus, some of the maxima using the 30-minute data above are the result of a few very active lightning periods, rather than a large number of lightning days.

b. *Annual analysis*

The spatial patterns for the convective frequency shown above also vary interannually. The quantity plotted in Figs 16 and 17 are the total number of composite reflectivities ≥ 45 dBZ and lightning strikes each year, respectively. For those areas denoted in Fig. 8, the annual trends show the variation each year and that the relatively higher years of convection have a periodicity of 2-4 years (Fig. 16). The lightning data is only available for the years 2001-2007, but an annual trend of lightning strikes for the same areas shows approximately the same periodicity of relatively more active years of lightning of 2-4 years (Fig. 17).

The areas across the Northeast were analyzed for annual trends in convection during the warm season to quantify the interannual variance. For example, comparing regions 1 (northeast Pennsylvania), 5 (eastern Long Island), and 8 (northwest Pennsylvania), shows that eastern Long Island experienced more convection in the years 1998-2001 (Fig. 16). With the exception of the year 2000, eastern Long Island has between 1 and 2 times more convection than northwest or northeast Pennsylvania. Region 4 (western Long Island), also has between 1 and 2 times the convection in northeast Pennsylvania and northwest Pennsylvania for the years 1998, 2000, and 2001. Within the years 2002-2007, convection across eastern Long Island was between 25-75 % less than other interior regions such as northwest and northeast PA. Regions 2 and 3 (Delmarva Peninsula and northern New Jersey, respectively) have the largest frequency of convection annually. The interannual variability of western Long Island follows the Delmarva Peninsula and northern New Jersey more closely than for eastern Long Island.

Northern New Jersey consistently shows higher convective frequency each year compared to western Long Island and is higher than eastern Long Island for all of the years except for 1999, when they have nearly the same value. The 2001 warm season for eastern Long Island was a relatively more active convective year compared to other areas. Eastern Long Island deviates from the interannual trend of both northern New Jersey and western Long Island. For eastern Long Island, the 2001 warm season was a relative increase from the previous year unlike northern New Jersey and western Long Island. This shows the greater interannual variability across eastern Long Island than across northern New Jersey, which suggests that eastern Long Island is more sensitive to the synoptic variability each year. This subsequently controls how much marine air is encountered by convection as it approaches Long Island.

The interannual variability in convection over the Northeast U.S. likely results from variations in instability, origin of the ambient flow (onshore vs. offshore flow), and the strength of the synoptic forcing. The warm seasons of 1998 and 2005 are good examples of the variation in the spatial distribution of convection within a warm season (Fig. 18). The warm season of 1998 had more active convection in coastal areas with convective frequencies of 0.24 to 0.36% from southeast Pennsylvania, central New Jersey as well as across eastern Long Island and southern Connecticut. The frequency of convection was between 0.15 to 0.24% across much of New England east of the Berkshires. The 1998 warm season showed the majority of the larger 45+dBZ frequencies in a west southwest to east northeast orientation from the Delmarva Peninsula through Eastern Long Island, Southern Connecticut and Southern Rhode Island, where convection was 2 to 3 times as frequent as locations farther in the interior (Fig. 18a).

Strong synoptic forcing in the month of June 1998 is shown from a composite of the mean sea level pressure anomalies for that month using the NARR reanalysis, which shows that mean sea level pressure is 4 hPa less than the June mean (1996-2007) around Long Island (Fig. 19a), while the 500 hPa geopotential height is approximately 50-60 meters below the mean over the same region (Fig. 20a). The 500 hPa heights are also anomalously low in July, when they were 5-10 m below the July mean (Fig. 20b), with sea level pressure ~1.0 hPa below the July mean around Long Island (Fig. 19b). In contrast, there is a substantial west to east gradient in the warm season of 2005, with convective frequencies of 0.24-0.33% throughout the Mohawk Valley of New York State with isolated areas towards the Delmarva Peninsula and southern New Jersey with frequencies of < 0.12 % across eastern Long Island, with < 0.15 % across much of New England east of the Berkshires. The mean sea level pressure in June of 2005 on average was closer to the 1996-2007 June mean than June of 1998 as well as for the 500 hPa geopotential height, both averaging slightly above the mean (Figs. 19c,20c respectively). Likewise for July of 2005, the pressure was 0.8 to 1 hPa above the mean in the Long Island region (Fig. 19d). This shows that on average there was more synoptic forcing in the warm season of 1998 during June and July, which related to the larger amount of convection across the coastal regions during those periods. In 2005, the greater positive pressure anomalies relative to the mean indicate less synoptic forcing on average and therefore a greater marine influence in the gradient of convection towards the inland areas.

c. *Monthly variability*

It is hypothesized that the spatial distribution of convection over the Northeast U.S. varies throughout the warm season as the ambient conditions change (wind shear, moisture, lift) and the sea surface temperatures warm. There is an overall minimum in convective activity in April (Fig. 21a), since the atmosphere over the Northeast U.S. is still relatively stable as evidenced from low values (< 100 J kg^{-1}) of average CAPE in the lowest 180 hPa (Fig. 21b). The relatively cool April sea surface temperatures of 5-10º C along the coast also prohibit much convection (Fig. 26a). Even with cool sea surface temperatures, embedded convection can occur across the coastal areas (Fig. 22a). The 45+ dBZ composite reflectivity frequencies are still relatively higher across Long Island. From inspection of many cases, this is due to "bright banding" associated with heavy stratiform rainfall with synoptic low pressure systems (Fig. 22b). From the case example shown in Fig.22b, there are only a few pixels of 45 dBZ as opposed to 40 dBZ, where the areas are much larger. This was taken into consideration in using a threshold of composite reflectivities ≥ 45 dBZ to diagnose convection instead of composite reflectivities ≥ 40 dBZ.

In May and June, convection increases, and becomes more widespread and thus resembles more of the total warm season signal (Figs. 24 a,c). As compared to April, there is at least twice as much convection over inland areas across the windward and leeward side of the Appalachians, central New York State, along the Berkshire Mountains, north-central New Jersey and the Delmarva Peninsula than eastern New England, eastern Long Island and offshore. There is also approximately five times the

amount of lightning strikes for inland areas compared to coastal and offshore areas for the months of May and June (Fig. 24a). When compared to total warm season convection (Figs. 11, 14b), 40-60% of the warm season convection occurs along the Alleghany Plateau near the border between north-central Pennsylvania and south-central New York State as well as portions of New England towards southern Vermont and New Hampshire during May and June (Fig. 25 a,b). The convection is more frequent across interior areas due to the greater instability across these sections compared to along the coast. Only those convective events supported by a strong jet streak would be able to persist along the coastline. There is a ~100 km shift towards the coast from May to June in the lightning frequencies. For western Long Island, the lightning frequencies increase from 0-0.40 % in May (Fig. 23a) to 0.40-0.80 in June (Fig. 23b). The offshore waters of the Atlantic Ocean are still relatively cold in May with average sea surface temperatures ranging from 7 to 12º C (Fig. 26b), but this increases to 12 to 22° C by June (Fig. 26c). In fact, the average low level CAPE from 0 to 180 hPa above the ground increases in June along the coastal plain from Delaware through the New York City Metropolitan Area, with average values ranging between 300 and 500 J kg^{-1} (Fig. 27a).

For July and August (Fig. 24 b,d), convection increases by 50-150 % compared to May and June over many land areas, and the convection is more extensive along the coast and offshore. The July and August periods have a maximum in the 45+dBZ frequencies in the same areas as May-June, but are now more widespread across New England and offshore. The marine influence is less pronounced during this portion of the warm season since sea surface temperatures in the Atlantic Ocean extending 200-300 km offshore south of Long Island and east of New Jersey range from 20° to 27° C (Fig. 26 d,e). The

lightning data from July to August shows the maximum areas exceeding 0.4 shift farther east of the Berkshires in central New England and across Long Island Sound, as well as the offshore waters extending 200-300 km south of Long Island. From July to August, the lightning decreases across most of the Alleghany Plateau and portions of the central Appalachians by approximately 50-70 % compared to May and June. However, there are some finite interior areas which experience 200-400 % increases in lightning near the Tug Hill Plateau just east of Lake Ontario as well as east central PA and just north of Manhattan where the monthly rate of lightning increases by 0.40-0.80. Coincidently, lightning increases offshore by 0.20-0.30 from May and June to July and August (Fig. 24c). The lightning over the Chesapeake Bay itself almost doubles from July to August, since the sea surface temperatures in the Chesapeake Bay are in excess of 25º C by August (Fig. 26d). The number of lightning strikes across the offshore waters 200-300 km south of Long Island during July-August accounts for 50-80% of the warm season lightning total (Fig. 25d). On the other hand, those areas which had active areas of convection in May and June, such as along the Alleghany Plateau and central Pennsylvania, experience less than 50 % of their convection during July and August (Fig. 25 c,d).

In agreement with the higher convective frequencies in July, the average CAPE from 0-180 hPa above ground over the Northeast U.S. in July reaches a maximum of 300 to 700 J kg^{-1} along the coastal plain and along the windward side of the Appalachians (Fig. 27b). By August, the CAPE over the ocean areas maximize to ~300 J kg^{-1}, while inland CAPE decreases by 50 to 100 J kg^{-1} (Fig. 27c). This is reflecting the shorter

daytime heating periods towards northern New York State and New England during the second half of the warm season.

By September, convection decreases by at least 50% across New York State, western and central PA, and all of New England (Fig. 28a). The most noticeable changes are for the domain north of the Alleghany Plateau through the Hudson Valley and Berkshire and Green Mountains. This could represent the decrease in diurnal heating with the reduction in decreasing daylight hours and more synoptic cool periods from the north and west. Relatively higher frequencies are located primarily near northwest PA, southeast PA, central NY State east of Binghamton, the southern part of the Delmarva Peninsula, and across most of Connecticut. Sea surface temperatures for the Atlantic Ocean and Long Island Sound still range from 20 to 25ºC with slightly higher SSTs in the Chesapeake Bay (Fig. 26f). However, the average 0-180 hPa above ground CAPE for September is < 250 J kg^{-1} across the domain from Pennsylvania through the Delmarva Peninsula and Long Island, which is greater than April and slightly greater than May (Fig. 28b).

d. *Diurnal analysis*

The spatial distribution of convection also varies as a function of the time of the day. Figures 29 and 30 show the diurnal variability (every 6-h) of composite reflectivity ≥ 45 dBZ and lightning strikes over the Northeast U.S, respectively. During the early morning to early afternoon period (12-18 UTC), convection begins mainly across the

coastal plain, the windward side of the Appalachians, a portion of the Hudson Valley and across western Long Island (Figs. 29a, 30a). The lightning data more clearly shows some of these enhancement areas, which includes the lee of the Appalachians over eastern Pennsylvania, the windward side of the Berkshires to the east of Albany, NY, and the central spine of Long Island (Fig. 30a). The enhancement over Long Island is suggestive of a convection initiated by a sea breeze, in which southerly and northerly flow from Long Island Sound and the Atlantic Ocean converge over the center of the island to trigger convection. The minimum locations are located primarily along higher portions of the Appalachian terrain and east of the Berkshire and Green Mountains throughout central New England, as well as most of the ocean waters within the domain. This is representing those areas which are able to sustain enough stability throughout the first heating of the day.

Convection occurs most frequently from 18-00 UTC across the Northeast U.S. (Fig. 29b, 30b), thus the spatial patterns are similar to the daily total. The largest convective frequencies are located just west of the Appalachians over western Pennsylvania, over some of the windward (south side) ridges of the east-central Appalachians, eastern Virginia northward to eastern Pennsylvania, Hudson and Mohawk River valleys, and some of the urban areas (New York City and Boston, Massachusetts) in the lightning data. The convection rapidly decreases towards eastern Long Island and offshore, with decreases from near NYC to eastern Long Island of 90% in the 45+dBZ frequencies and approximately 97% in the number of lightning strikes.

From 00-06 UTC (Figs. 29c, 30c), the frequency of convection is approximately 50% less than the 18-00 UTC period within most of the lower Hudson Valley, central New York State and western Pennsylvania. The decreases are between 80-90 % east of the Berkshires into New England as well as over the central Appalachians in Pennsylvania. Convection across the Delmarva Peninsula, parts of southeast Pennyslvania, parts of central New Jersey, and Long Island only decreases by 30-50 % from the 18-00 UTC to the 00-06 UTC period with a few localized areas where convection increases. The 45+dBZ and lightning more than doubles across the south fork of Long Island and also across the offshore waters just to the south as compared to the previous 6 hour period.

Through the remainder of the overnight period (06-12 UTC), convection is more suppressed across the Northeast (Figs. 29d, 30d). Convective frequency decreases across southeast Pennsylvania by 50-60 % in 45+dBZ and 80-95 % in lightning relative to 00-06 UTC. Convection remains active across western Pennsylvania west of the Appalachians, where it only decreases between 25-50 % from 00-06 to 06-12 UTC, and across the far offshore waters to the southeast of Long Island, where it actually is 2-3 times greater in some locations in the lightning data and between 10-50 % greater in the 45+dBZ frequency. Other active areas are also located just downwind of Lake Ontario and across the western end of the Mohawk Valley, where again lightning only decreases by approximately 33 % with < 30 % decreases in 45+dBZ frequencies.

The diurnal cycle of convection over the Northeast U.S. can also vary through the warm season (Fig. 31). Between the first half of the warm season (April, May, June) and

the second half (July, August, September), convection from 06-12 UTC increases over portions of the offshore waters south of Long Island by more than 50 % during the second half as compared to the first half (Fig. 31d). Between 12-18 UTC (Fig. 31a), convection increases also occur offshore south of Long Island and across the northern portions of Long Island from the first to the second half. The increases in convection offshore during the second half account for the majority of the total convection during the 12-18 UTC timeframe. This implies a weakening of the cool marine boundary layer as sea surface temperatures warm later in the summer. The Great Lakes also warm during the summer with a resulting maximum in convection downwind of the Great Lakes during the second half of the warm season. Between 18-00 UTC (Fig 31b), the greatest convective increases during the second half are found along the coastal plain from Delaware and southeast Pennsylvania through northern New Jersey and also along southern parts of the Hudson Valley. The second half increase is about 40% of the total convective frequency during the warm season between 18-00 UTC (Fig. 31b). The increase over the coastal plain could be due to the increasing low level temperatures during the second half of the warm season. This results in increases of the coastal water temperature and the development of some surface troughs in the lee of the Appalachians, which have been shown to trigger convection (Bosart 2006). The 00-06 UTC period has the least amount of change in 45+dBZ frequency between the first half and the second half of the warm season across the Northeast. There are a few noticeable areas which had higher totals during the second half, such as in southeast Pennsylvania and the southern portion of the Chesapeake Bay (Fig. 31c).

The diurnal cycle of convection for various subregions across the Northeast U.S. was analyzed further for a series of eight 1º latitude by 1º longitude boxes across Pennsylvania, near the Delmarva Peninsula, New Jersey, New York City, Long Island, New York State, and New England (Fig. 32). The actual number of occurrences of 45+dBZ is used instead of the Pr_{storm} quantity to compare the total number of convective occurrences. Generally, the peak hour of convection for those regions farther inland (Regions 1, 6, and 8) occurs during the mid to late afternoon hours (19-21 UTC). For these regions the magnitudes and duration of convection is less than region 3 over northern New Jersey and New York City. The convective peak shifts 6 to 12 hours from locations farther to the west across western Long Island and the interior Northeast for most coastal offshore areas (e.g. Region 5) including Long Island as well as the Great Lakes (Fig. 33a, b). For the coastal locations, the peak is 40-60 % less than inland areas (e.g. Regions 1, 6, and 8) with an e-folding decrease in convection occurring 2 hours later.

Convection increases rapidly after 16 UTC, with the increased warming of the day. The first region to reach one of its peaks in convection is northwest Pennsylvania (Region 8) between 19 and 20 UTC, and there is a second peak between 23 and 00 UTC. This region has a higher hourly rate compared to the other regions through the afternoon hours, and it also declines rapidly between 00 and 02 UTC, similar to northwest Pennsylvania, northeast Pennsylvania (Region 1), and near Albany, New York (Region 6). Region 2 in Maryland has convection initiating between 18-19 UTC and it has the most convection compared to the other areas, reaching a frequency above 30 occurrences of 45+dBZ from 20 to 02 UTC. The peak of convection occurs between 00 and 01 UTC,

which is the maximum of convection for all regions. There is a sharp decline of convection nearly 50 % until 03 UTC.

For region 3 in northern New Jersey, the peak at 21-22 UTC occurs a few hours before central Maryland, and then there is a slow and steady decline of 50% by 04 UTC. Similar to the other regions, the convective activity over region 3 reaches a minimum thereafter through the following morning. Region 5 on eastern Long Island has a peak time of convection much different than the surrounding regions to the west, since it does not exhibit any increase of convection during the afternoon. The most rapid increase for this region occurs after 00 UTC, reaching multiple peaks throughout the night between 01-02 UTC, 04-05 UTC, and 07-08 UTC. In contrast, just 50-100 km to the west for region 4 on western Long Island, diurnal trends in convective activity resemble more those inland regions to the west, although convective activity does not increase until 18 UTC and reaches its peak at 00 UTC.

Region 7 in western Massachusetts is farther away from the marine layer than Long Island, so the convection increases at a greater rate during the afternoon than the coastal areas to the south. However, this region has less total convection compared to regions 1, 2, 3, 6, and 8. The peak for convection in this region occurs between 22 and 23 UTC. This region has the least amount of convection during much of the night than any other regions.

Fig. 33 shows the maximum hour of convection both for composite reflectivities ≥ 45 dBZ and for lightning. These both show a shift in the time of peak convection from 18-00 UTC across New York State, Pennsylvania, and northern New England to offshore

areas and the Great Lakes from 04-12 UTC. The maximum lightning hour plot is more detailed than the reflectivity data and helps show some of the convective initiation across portions of the Appalachians, Adirondacks and just to the lee of the Berkshires from 16-20 UTC.

e. *Severe weather events*

A fraction of the 45+dBZ events above produced severe convection, which is defined as a thunderstorm producing hail of at least 0.02 m (0.75 inch) diameter, wind gusts of at least 25 m s^{-1} (50 kts or 57 mph), and/or a tornado of any magnitude (Doswell 2001). This section highlights the spatial distribution of convection for days (0000-0000 UTC) in which severe weather was either reported and/or warned by a National Weather Service forecast office. Fig. 34 shows the number of severe weather days through the warm seasons of 1996-2007 for seven forecast offices, Baltimore/Washington D.C. (LWX), State College, PA (CTP), Mount Holly, NJ/Philadelphia, PA (PHI), New York City, NY (OKX), Binghamton, NY (BGM), Albany, NY (ALY), and Taunton, MA (BOX). CTP has the most total severe weather days (482) while OKX has the least (235) during all warm seasons.

Figures 35 (a-g) shows what percentage of convection during the warm season occurs on severe weather days. The areas that have the most convection on days of severe weather are generally located in areas of complex terrain. For the CTP office (Fig. 35a), this includes the western portion of the Allegheny Plateau, where 75 to 80% of the

convection occurs on severe weather days. At LWX (Fig. 35b), there is 80-90% of convection on severe weather days over the lee of the Appalachians of western Virginia. For BGM (Fig. 35c), convection on severe weather days occurs on the windward side of the Allegheny Plateau if there is low-level northwesterly flow, where the fraction of convection is 60-70%. The PHI county warning area had 55-75% of its convection on days of severe weather along the lee of the Appalachians in eastern Pennsylvania to northwest New Jersey near the Poconos (Fig. 35d). For ALY (Fig. 34e), 60-70% of the convection occurs just south and east of Albany, New York. This location is an area of upslope for westerly flow and it is where the westerly flow out of the Mohawk Valley can converge (and trigger convection) with the more southerly Hudson Valley flow. The maximum convection for the OKX region of severe weather days is 55-60%, occurring over the hills of northern New Jersey, southern portions of the lower Hudson Valley, and over the hills just east of the Connecticut River Valley in south-central Connecticut (Fig. 35f). There is also an interesting secondary maximum of 45-55% over the New York City metropolitan area. The largest fraction for the BOX area (60-70%) occurs just downslope of the Green Mountains in southeastern Vermont and White Mountains in southwestern New Hampshire (Fig. 35g). In summary, this analysis highlights the importance of terrain (particularly the lee slopes) in focusing the convection during severe convective days over the Northeast U.S.

f. *Hovmoller analysis*

In order to quantify the number of convective episodes and their movement across the Northeast U.S., a hovmoller plot was created showing the frequency ≥ 45 dBZ for all warm season days. This was averaged between 38.5° N to 41.5º N from Indiana to the Delmarva Peninsula and Long Island as a function of time and longitude (Fig. 36). This analysis helps identify whether convection propagates in this region and the favored regions of convective genesis and decay.

From the morning to early afternoon hours (09-16 UTC), there is an overall minimum in convection stretching across the entire domain. There is a relatively higher frequency of convection towards Ohio and Indiana in the early morning hours between 9 UTC and 12 UTC. Convection then begins to develop across the domain between 18-21 UTC across Ohio and Indiana as well as eastern Pennsylvania with relative minimum areas over the western and central Pennsylvania as well as Long Island. There is a pronounced diurnal maximum from Indiana through Ohio between 21 and 00 UTC as well as over the northern Appalachians of central Pennsylvania. These regions correspond to those areas that have generally smaller terrain peaks to the west of the Appalachians and to the immediate lee of the Appalachians. Convective frequency is consistently higher throughout the entire 24-hour diurnal cycle for the western third of the domain, or from -86.5º W to -81º W. Convection persists into the early morning hours between 09 UTC and 12 UTC for the extreme western portion of the domain from -86.5º W to -85º W across Indiana. This is likely representative of nocturnal MCSs propagating into this region from the west as was noted by Carbone et al (2002). There is

a slight indication that convection propagates in the lee of the Appalachians (76º-78ºW) and propagates towards the coast from 21 to 09 UTC. This propagation is weaker than the propagating convective events from the Rockies to the Great Plains (Ahijevych et al 2002). Convection reaches a minimum first over the higher terrain regions of the Appalachians during the evening hours between 02-06 UTC. This can be explained by the more rapid nocturnal cooling over the elevated terrain regions as compared to the warmer low land areas to the west and east. In contrast, towards eastern Long Island, convection remains relatively active later at night.

As discussed in Section 2c, convective objects on the hovmoller plots were counted in order to identify individual organized convective events from west to east across the domain shown in Fig. 37. A total number of 221 objects were manually identified across the domain, with 146 objects indicating at least slight propagation. These propagating objects were used for the remainder of this analysis. The majority of the objects were short-lived with a lifecycle of less than 1 day, with 80% of the events occurring in the months of June, July, and August. There were only 3 long-lived episodes of greater than 1 day and 8 serial convective events. There were 35 individual objects that were part of the serial convective events. The year 2005 had the least amount of events (8), while 2003 had the most events (26). Approximately 55% of the 221 events originated west of Pennsylvania with subsequent decay of 42% of the events over eastern Ohio and western Pennsylvania as seen on Fig. 37. The Appalachians and to the immediate lee in central and eastern Pennsylvania comprised 40% of the event origins. The next major decay region was from New Jersey through eastern Long Island and over the ocean waters where 40 % of the events decayed.

With the genesis times of convection, the events were separated into 6 hour groups (Table 1). Similar to the diurnal analysis aforementioned in this research, the dominant timeframe for the genesis of convection was from 18-00 UTC, incorporating 49% of the events. The next common genesis timeframe was 00-06 UTC, with 25% of the events. The 06-12 UTC and 12-18 UTC time periods were relatively similar for the events, each including 12% and 14% of the events respectively. The most common time period for the decay of these convective events was 00-06 UTC, for 47% of the events, followed by 23% of the events decaying between 06 and 12 UTC, 12% of the events decaying between 12 and 18 UTC, and 18% of the events decaying between 18 and 00 UTC.

Regarding the longevity of individual convective episodes, the average length of all events increased with increased daylight. Minimum average lengths of episodes were seen from 00-06 UTC with a distance of 3.84º of longitude. Maximum average lengths with a distance of 4.25º of longitude were seen between 18 and 00 UTC. This is consistent with Parker and Ahijevych's work in 2007, with convection surviving to the coast more often when systems crossed the Appalachian terrain during the warmest part of the day.

An example of a propagating event is seen from 27 June 2007 at approximately 18 UTC through approximately 06 UTC on 28 June 2007 as shown in Fig. 38. Convection initiated across and to the lee of the Appalachians around 18 UTC. Then, the individual thunderstorms began to aggregate with each other as the coverage of convection increased, eventually forming a squall line by 20 UTC across the Alleghany

Plateau. Another less continuous squall line formed over south central Pennsylvania around 2230 UTC. The smaller maxima that are below the streak identified in this hovmoller diagram depict when the coverage of convection was greater across the domain as shown in Fig. 39. Both of these mesoscale convective systems moved towards the greater New York Metropolitan area. The northern most squall line moved into western Long Island by 1 UTC 28 June 2007 and subsequently dissipated as it moved to the south of western Long Island by 2 UTC. Meanwhile, the squall line farther to the south had moved into southeast Pennsylvania. This line weakened over southern New Jersey but was still intense over central New Jersey as it slowly moved across from 2 to 4 UTC. The front end of the system further decayed through the late night hours while an area of trailing stratiform rain on the back end persisted offshore, peripherally extending into southern portions of Long Island. This example represents one of the 30 propagating events (almost 21% of the total) which started in Pennsylvania and decayed across Long Island. There were 14 events (almost 10% of the total) which also started in Pennsylvania but lasted through the eastern end of Long Island.

g. *Dependence of convection on the regional flow regime*

It is important to understand how convection is distributed for different atmospheric flow regimes over the Northeast U.S. Flow composites (averages) were created at both a low level (e.g. 925 hPa) and upper level (e.g. 500 hPa) flow regime. The low level flow helps determine whether topography and land-water boundaries are important in modifying convection, while the upper level flow relates convection to the

large scale trough or ridge pattern over the Northeast U.S. As discussed in Section 2c, the flow regime was determined using the NARR for select points over the Northeast U.S., in which the closest 3-h reanalysis time was used closest to the time of convection.

At 500 hPa, the sampling points used to measure the wind direction were spread far apart from one another across the Northeast as indicated in Chapter 2 (Fig. 9). For a west to northwest 500 hPa flow (Fig. 40a), the distribution of convection varies more from west to east than with southwest flow. Relative maxima appear mainly to the windward side of the Appalachians where probabilities range from 0.15 to 0.25 %, with secondary maxima of half the magnitude across the Mohawk Valley, as well as portions of the Berkshires and southeast Pennsylvania. More specifically, the greatest convection is west of the Appalachians and along its windward slope across western Pennsylvania and West Virginia. This is likely the result of the northwest flow regime favoring more upslope flow and convective triggering in these regions. A minimum in convection encompasses a wide area over the central Appalachians and downwind of the Appalachians over eastern New England.

When the 500 hPa flow is from 225º-270° (southwest to west flow), the greatest amount of convection (0.35 to 0.50 % probability) was located in southeast Pennsylvania on the lee of the Appalachians (Fig. 40b). Smaller localized areas of this same magnitude are found in northwest Pennsylvania and along the Hudson Valley. The pattern closely resembles that of the total climatology for the 12 warm seasons (Fig. 12). The interior areas across the windward and leeward side of the Appalachians and the Hudson Valley have between 2-3 times the amount of convection across Long Island and eastern New

England by southeast Massachusetts. The minimum areas are located within the highest terrain in the domain across northern Virginia into western Maryland as well as southeast Long Island and southeast Massachusetts (where 45+dBZ probabilities are < 0.10 %).

Four points were chosen at 925 hPa to determine whether the convective distribution is dependent on marine air from the Atlantic Ocean (Fig. 41). For a 925 hPa wind from southwest to northwest (225°-315°) (Fig. 41a), there is a greater shift of maximum areas of convection to the north and east over New England. The largest maximum area is within the eastern Hudson Valley and Berkshires, in which a 225º-315º flow represents an upslope flow component and convective triggering in this region. Other maximum areas are located in northwest and east-central Pennsylvania, and throughout central New York State. There is also a greater shift of convection across Long Island Sound with a more westerly flow showing the decreasing influence of the marine boundary layer.

For a more southerly wind (145º-225º) and advection of cooler marine air (Fig. 41b), convection is limited east of -74º W longitude across Long Island and coastal New England. This is the result of the cooler marine air advecting into this region from the Atlantic. This can be conveyed through NARR composites of 925 hPa Θ_e and low level CAPE (0-180 hPa above the surface) corresponding to the times of southeast to southwest flow and southwest to northwest flow. The composite showing the more southerly flow has on average 100-200 J kg^{-1} less average CAPE and 1-2K less Θ_e across Long Island and coastal New England, which limits convective development. Maximum convective areas are located in southeastern Pennsylvania into northern Maryland, where

the probability of 45+dBZ is 0.35 to 0.55 %. Other maximum areas are in central and northern New Jersey, portions of the New York State near the Mohawk and Hudson Valleys as well as in northwestern Pennsylvania. In contrast, a minimum area also exists along the Alleghany Plateau where the probability of 45+dBZ ranges mostly from 0.05 to 0.20 %. This is consistent with low-level southerly flow, which enhances some of the convection along the south facing slopes of Pennsylvania and New York, while there is a minimum in the lee of the Alleghany and Catskills, where there would be downslope flow and resulting drying.

h. *Synoptic conditions associated with the most active convective days in the northeast*

In order to determine the pressure patterns, flow, and thermodynamics associated with more active convective days across the Northeast, a composite was constructed for those days in which the convection, from -80.5 °W,-70 °W and 38°N,44°N, (western Pennsylvania through Long Island and New England) exceeded 1 standard deviation of the areal mean over this region. The hour of the largest amount of convection was used for each day identified and related to the nearest 3-h NARR time. The composite geopotential height and absolute vorticity at 500 hPa illustrate a mean trough over the Great Lakes and southwest flow over the Northeast. There is positive absolute vorticity advection over much of the Northeast, which is suggestive of some forcing for quasi-geostrophic ascent aloft (Fig. 42a). At 925 hPa (Fig. 42b), there is positive advection of equivalent potential temperature from the south over much of the region, which also favors upward motion. This is associated with a surface low pressure trough that extends

southward from Lake Ontario to a secondary low centered on Maryland (Fig. 43). Meanwhile, at 200 hPa, much of the Northeast is within the right rear of a 34 m s^{-1} jet, which also favors ascent over the region (Fig. 44a). In fact, at 700 hPa, there is upward motion over a large area of the Northeast U.S. (Fig. 44b).

In order to assess the low-level stability for the large convective days, Fig. 43, shows the average CAPE between 0 and 180 hPa above the surface. There is a maximum along the coastal plain of Maryland and Delaware, which extends northward to portions of southern New England. The low-level southwesterly flow advecting warm air from the south helps to extend this axis of maximum instability just inland from the coast. This combined with the synoptic scale ascent leads to the active convective days across the Northeast U.S. The placement of the maximum instability and lift at 700 hPa is consistent with some of the more active convective areas over the Chesapeake Bay region into eastern Pennsylvania and New Jersey.

i. *Synoptic conditions associated with the evolution of convection near the coast*

Convection can evolve quite rapidly at the coast given the different ambient conditions. For example, on 1 June 2002, a squall line remained intact while crossing Long Island (Fig. 45a). Meanwhile, a squall line that developed over the lower Hudson Valley, on 1 June 2006, weakened after crossing through the New York City area (Fig. 45b). The low-level stability was quite different between these two cases. At 0000 UTC 1 June 2002, (Fig. 46b), the surface CAPE ranged from 800 to 2000 J kg^{-1} and it was

present over the Atlantic waters south of Long Island. At 0000 UTC 2 June 2006, there was a much tighter gradient of surface CAPE than the 2002 event (Fig. 46d), which was situated along the coastal plain through Manhattan, northern Connecticut, and eastern Massachusetts, ranging from 500 to 3500 J kg^{-1}. The CAPE decreases to less than 300 J kg^{-1} across of the offshore waters and most of Long Island. The June 2006 case had multiple lows along a discontinuous cold front across the Eastern Seaboard (Fig. 46c,d), while for 1 June 2002, the cold front was much more uniform (Fig. 46a,b). The magnitude of the sea level pressure differences was larger in the 1 June 2002 case, with sea level pressure values ~10 hPa lower around New Jersey, Manhattan, Long Island, and Connecticut than for the 2 June 2006 case. At 200 hPa, a stronger jet of 24 to 30 m s^{-1} is seen extending southeast from the lower Hudson Valley through Long Island on 1 June 2002 (Fig. 47a,b), while on 2 June 2006, there was only 5-15 m s^{-1} wind speed at 200 hPa across the same area (Fig. 47c,d). The 2002 event had more synoptic forcing for ascent and instability along the coast; thus the convection was able to maintain itself over this region. There are just two events presented, so these ideas are also tested below for a composite of events.

To do this composite analysis, days were recorded when the sum of convection for a 1° latitude x 1° longitude box centered over north-central New Jersey was greater than 1 standard deviation of its mean. For these days, only the days when the convection decayed by at least 50 % in an adjacent box with the same dimensions centered over western Long Island were used, as shown in Fig. 48. The peak hour of convection for the day was used to relate to the nearest time of the NARR data. The previous 12 hours from the peak time was used to derive the evolution of time of individual synoptic features.

This was repeated for cases in which convection was greater than 1 standard deviation over two adjacent boxes of 1° latitude x 1° longitude across both western and eastern Long Island.

Initially, 12 hours before the decaying events, a trough at 925 hPa is centered over the Ohio Valley with a Θ_e ridge that is developing just to the lee of the Appalachians (Fig. 50a). The average CAPE (0-180 hPa above the ground) is also increasing along the windward and lee of the Appalachians along the coastal plain from eastern Virginia through New Jersey. The CAPE difference between the coastal plain and eastern Massachusetts and Long Island is 200 to 300 J kg^{-1}. At the time of the peak convection, the average CAPE (0-180 hPa above the ground) is a maximum across eastern Virginia with values $\geq$ 1000 J kg^{-1} (Fig. 50b). This maximum gradually diminishes as it extends across north northeastward along the coastal plain and into the Hudson Valley from $\geq$ 800 J kg^{-1} to $\geq$ 400 J kg^{-1}. The CAPE is a minimum farther interior into New York State and New England as well as the eastern half of Long Island with values < 400 J kg^{-1}. The Θ_e ridge at 925 hPa is oriented right along the coastal plain extending from eastern Virginia through the lower Hudson Valley and had increased by approximately 2 K from the previous 12 hours. At this same vertical level, a 500-hPa trough is positioned in central Virginia through central Pennsylvania. The trough has deepened 10-15 m as it approached to the lee of the Appalachians during the past 12 hours. The south southwesterly flow indicated at 925 hPa results in a positive Θ_e advection along the coastal plain and therefore greater values of average CAPE with less CAPE across the coast. At the upper levels, the 500 hPa trough is approaching with southwest flow from 12 hours before to the time of peak convection (Fig. 51a). Also, the right rear exit region

of the jet at 200 hPa is over the region with wind speeds ranging from 26 to 28 m s^{-1} at the time of peak convection (Fig. 51b). This composite was computed using 60 cases out of which 73 % were between 21 and 03 UTC, showing the peak in the diurnal cycle of convection coinciding with the times of higher CAPE and Θ_e advection.

In contrast, when compositing the times when convection is greater than 1 standard deviation across Long Island, the average low level CAPE (0-180 hPa above the ground) is 50 % less across much of the interior Northeast with approximately 25 % less CAPE along portions of the coastal plain from central Delaware through New Jersey at the time of peak convection (Fig. 52b). This does not show as much of an increase from 12 hours before (Fig. 52a) as shown with the previous scenario. Farther southward along the coastal plain, the changes in CAPE are quite small. There are some finite localized increases in CAPE towards eastern Long Island and the offshore waters to the south, where CAPE ranges from 400 to 700 J kg^{-1}, increasing towards the south. This is approximately 50 % larger than with the cases of decaying convection. The trough at 925 hPa is well defined and situated closer to the coast. The geopotential height at 925 hPa across eastern Long Island and offshore is 14 to 19 m less than the 925 hPa heights for the decaying cases and this is statistically significant at the 90 % level according to paired t-test using unequal variances. The Θ_e ridge is not well defined with a large north to south gradient from northern New England to the Mid-Atlantic. The 500 hPa trough is approximately 20 m deeper than with the events that decay and the right rear quadrant of the 200 hPa jet is closer to Long Island with these events than with the decaying events both 12 hours before and at the peak time of convection. The wind speed at 200 hPa ranges between 28-30 m s^{-1} 12 hours before (Fig. 53a) and 30-32 m s^{-1}at the peak time of

the convection (Fig. 53b), which is 4-6 m s^{-1} higher than the set of days in which convection decayed. This scenario used 64 cases, of which only 31 % occurred between 21 and 3 UTC. The majority of the cases occurred between 6 and 12 UTC (50 %) and this agrees with the diurnal maximum observed towards coastal locations further to the east as evidenced in section 3f.

With the previous two examples, the evolution of convection was assessed for cases of decaying convection across Long Island for a day as well as the maintenance of convection over Long Island. However, the convection represented in these cases includes non-severe convection, including some cases of embedded convection. This is more evident with eastern Long Island, since the fraction of convection on days of severe weather ranged from 30 to 45 %, whereas for northern New Jersey 45 to 70 % of the convection occurs on days of severe weather as shown on Fig. 34f. To assess for the evolution of severe weather from northern New Jersey and the decaying cases from severe weather on eastern Long Island, severe storm reports were used for each of the areas and related to the nearest time of the NARR data as shown in Fig. 49. The events recorded for each area in the composites were mutually exclusive, but are not withheld from biases relating to population differences.

For northern New Jersey, there were 142 severe weather events with 96 % occurring between 18 and 03 UTC. The composite of these event times show a deeper trough at 925 hPa at the time of peak convection compared to including non-severe cases (Fig. 54b). However, the trough does not deepen as much from central Virginia and central Pennsylvania compared to 12 hours before the severe report (Fig. 54a). The

trough has more of a west southwest flow compared to the events decaying which include non-severe events. One recurring feature is the increase in CAPE gradient between the coastal plain and eastern Long Island and Massachusetts. For 12 hours before the severe event, 400-800 J kg^{-1} of CAPE exists on the windward and leeward side of the Appalachians (Fig. 54a). The 925 hPa Θ_e ridge starts to emerge along the coastal plain and increases 2 to 4 K by the time of the severe report (Fig. 54b) as it is advected by the west southwest flow. This allows for a slightly greater extension of the Θ_e ridge to the east along with increased CAPE values to the east across the lower Hudson Valley and southern Connecticut in comparison to the composite including non-severe events. The CAPE gradient is still steep between the coastal plain and eastern Massachusetts and eastern Long Island where CAPE differences are 600-800 J kg^{-1}. The 500 hPa trough has more of a west southwest flow with the severe events with just about the same jet speed maximum with the approaching right rear quadrant as was shown with the decaying events including non-severe convection (Fig. 55a,b).

While the synoptic conditions between northern New Jersey events that decay towards western Long Island and the severe events exclusive for northern New Jersey were relatively similar, there is quite a contrast between the convection across Long Island and the severe events across eastern Long Island. While there were only 31 severe events, differences were noted at 925 hPa, which was much more zonal compared to all convective cases across Long Island with the ridge of Θ_e oriented along the coastline from southern New Jersey through eastern New England (Fig. 56a,b). There are relatively higher CAPE initially 12 hours before the severe event along the coastal plain, ranging from 800 to 1000 J kg^{-1} near the Delmarva Peninsula through western Long

Island to 600-800 J kg^{-1} across the lower Hudson Valley, eastern Long Island, and Connecticut (Fig. 56a). The highest CAPE values extending along the coast out of any of the scenarios are shown at the time of the Eastern Long Island severe reports ranging from 1000 to 1400 J kg^{-1} across southern Connecticut into Rhode Island and portions of southeast Massachusetts as well as eastern Long Island (Fig. 56b). This can be related to the greater westerly flow and less marine air over eastern Long Island during the severe weather events. At 500 hPa, the approaching trough is more zonal 12 hours before the report (Fig. 57a) with the base of the trough along the coastal plain at the time of the severe report (Fig. 57b). The flow is westerly at 500 hPa at the event time with slightly stronger (~ 4-6 m s^{-1}) 200 hPa wind speed compared to severe events over northern New Jersey (Fig. 57b).

Chapter 4 – Conclusion

Using 12 warm seasons (April-September) of composite reflectivity data (1996-2007) and 7 years of lightning data (2001-2007) over the Northeast U.S., this thesis highlights regions that are more likely to have convection during the warm season. The composite reflectivity and lightning data produce similar results, but the lightning data is able to better locate convection relative to small-scale terrain features and it did not have ground clutter and other biases. The convection for 12 warm seasons varied spatially, with maxima located along the coastal plain extending from eastern Virginia through New Jersey to the lee of the Appalachians in eastern Pennsylvania, as well as the windward side of the Appalachians and the Mohawk and Hudson River Valleys in New York. Minimum areas were located mainly along the highest of the Appalachian terrain towards northern Virginia extending northward through the central Appalachians as well as the greater marine environment of coastal New England and Long Island.

The distribution of convection over the Northeast U.S. was also explored at various time scales from annual to the diurnal periods. On an annual basis, convection had a periodicity of 2-4 years for different areas and convective frequency increased towards coastal sections for approximately a quarter of the years analyzed in the radar data (1998-2001). Monthly variability showed that from the end of spring through summer and at the onset of autumn, areas of maximum convective activity shifted to greater distances towards the coast as the sea surface temperatures warmed. With the onset of diurnal heating, convection first maximizes over the land areas (18-00 UTC),

and eventually it moves to the south and east towards the offshore later at night (03-09 UTC). This diurnal cycle is more pronounced during the second half of the warm season (July-September), when stronger heating at the surface can more easily destabilize the lower boundary layer and lead to increases in the amount of convection that is closer to and along the coastline as sea surface temperatures warm. On severe weather days, the frequency of convection is maximized near areas of terrain, which shows the importance of terrain in each office's county warning area.

Hovmoller diagrams were used to objectively identify areas of organized convection along areas from Indiana and Ohio eastward to Long Island in order to quantify what fraction of convection comes from outside the Northeast versus the fraction of convection developing within the domain. Most convection does originate or enter in from Indiana and Ohio (58%), but a smaller fraction (42%) originated within the Northeast across the Appalachians and along the coastal plain. The decay of 51 % of the events occurred just west of the Appalachians and 34 % ended across Long Island.

Synoptic wind flow regimes were found to have a relatively important effect upon the spatial distribution of convection. Convection was most frequent over inland areas with southwest to west flow (225°-270°) at 500 hPa. With west to northwest flow (270°-315°) at 500 hPa, convection was enhanced along some of the windward slopes of the Appalachians. At 925 hPa, a greater southerly component results in a greater influx of marine air into southern New England, resulting in a larger gradient of convection from west to east. Upslope effects can be seen near the Hudson Valley and along the Appalachians with both southeast and southwest wind. Minima are seen downwind of

the corresponding maxima indicating the importance of terrain and low level wind direction.

Using synoptic scale composites, it was found that a more westerly flow was observed on average with severe weather events on eastern Long Island, which prevents onshore flow of cooler marine air and thereby allows the thunderstorms to maintain themselves. The non-severe cases on eastern Long Island can occur with more of a southwest flow and less CAPE but the thunderstorms can still be enhanced by greater synoptic lift provided by a deep trough at 925 hPa and enhanced divergence aloft from the jet stream at 200 hPa. The combination of both ample amounts of average CAPE at low levels (0-180 mb above the ground) and being relatively close to a jet speed maximum is consistent with cases of severe weather across the eastern United States.

Overall, this thesis has obtained some unique results not obtained before in previous studies, which can be summarized as follows.

1. There is a large interannual frequency of convection over the Northeast that occurs on 2-4 year time scales and it is dependent on the large scale flow regime during the warm season.

2. Lightning data is better able to depict areas for convective initiation between 12-18 UTC along the windward and leeward side of the Appalachians as well as on Long Island from sea breeze convergence.

3. There is a slight propagation of convection from the central and leeward Appalachians towards the coast throughout the evening hours.

4. Convection remains relatively more active near the coast into the night than farther inland in the Northeast, where the average convection each hour rapidly decreases.

5. For enhanced coastal convection on Long Island, the wind flow is primarily westerly, which favors the least influx of marine air so that higher Θ_e and CAPE values can be obtained.

6. Interior areas near terrain are influenced by the wind and subsequent upslope and downslope flow, which influence the areas of convective genesis and decay events, respectively.

From this climatology, there are areas for future work. The many individual maxima and minima need to be analyzed more closely in terms of initiation and duration of convection across the terrain and coastal areas of the Northeast. Urban effects also need to be considered relative to the spatial distribution of convection and its evolution. This will enable better understanding of the physical processes leading to either the rapid intensification or dissipation of convection over the terrain and coastal areas. This will enable further analysis of convective evolution through initiation mechanisms of sea breeze convergence zones and lee troughs as well as greater convective intensification perhaps through increases in potential vorticity when thunderstorms move downwind of

terrain or the dissipation of convection when gust fronts accelerate out ahead of thunderstorms in a marine environment. Analysis of these properties will require simulations of convection across the Northeast with and without terrain using numerical models of high resolution. This is in an effort to better develop a conceptual model of convection and severe weather in the Northeast so that better short term forecasts can be made with increased understanding of convective evolution.

Tables

Time Period (UTC)	Origin Frequency	Decay Frequency	Avg Length of Episodes (º longitude)
00-06	37	68	3.835
06-12	17	34	3.924
12-18	21	17	4.171
18-00	71	27	4.251

Table 1. The diurnal frequency of the origin and decay regions of all hovmoller objects (organized convective events) and the average length (in º longitude) of all events beginning for each 6 h period.

Figures

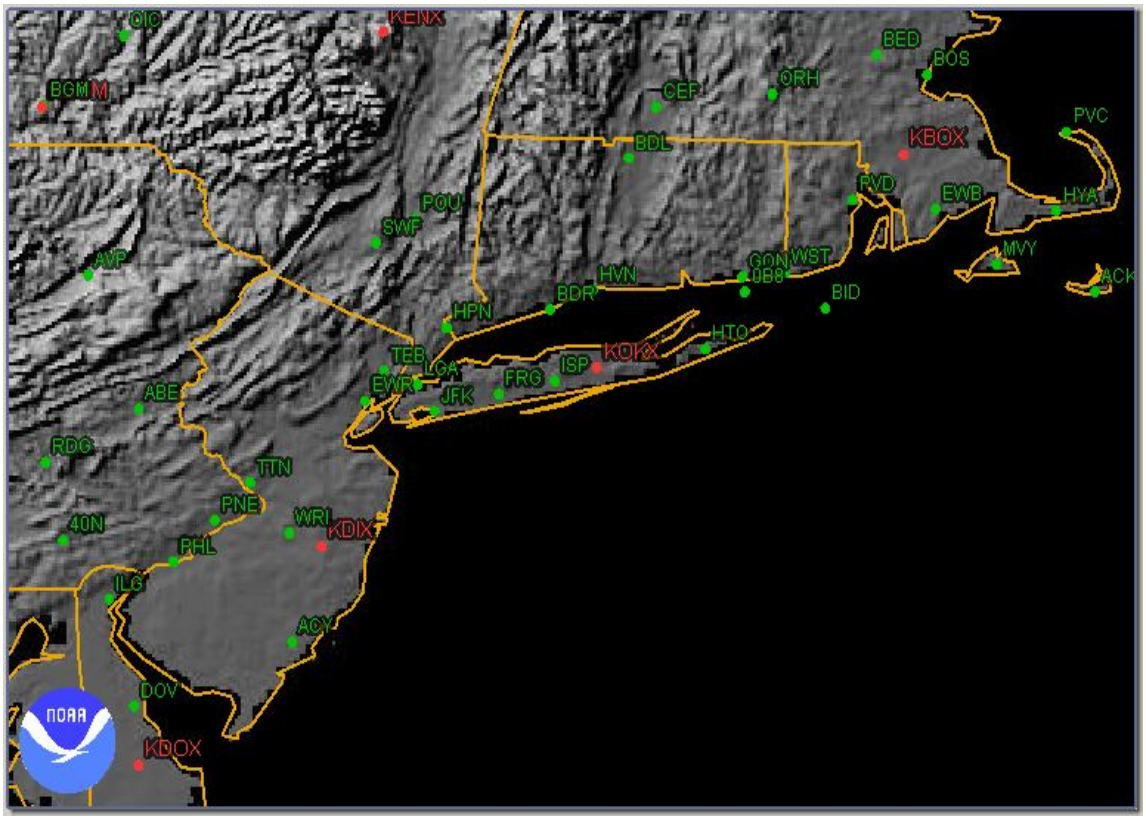

Figure 1. Airport surface stations across the local New York Metropolitan Area (green) with WSR-88D locations (red). Topography is indicated by the different shades of gray in the background (higher is whiter).

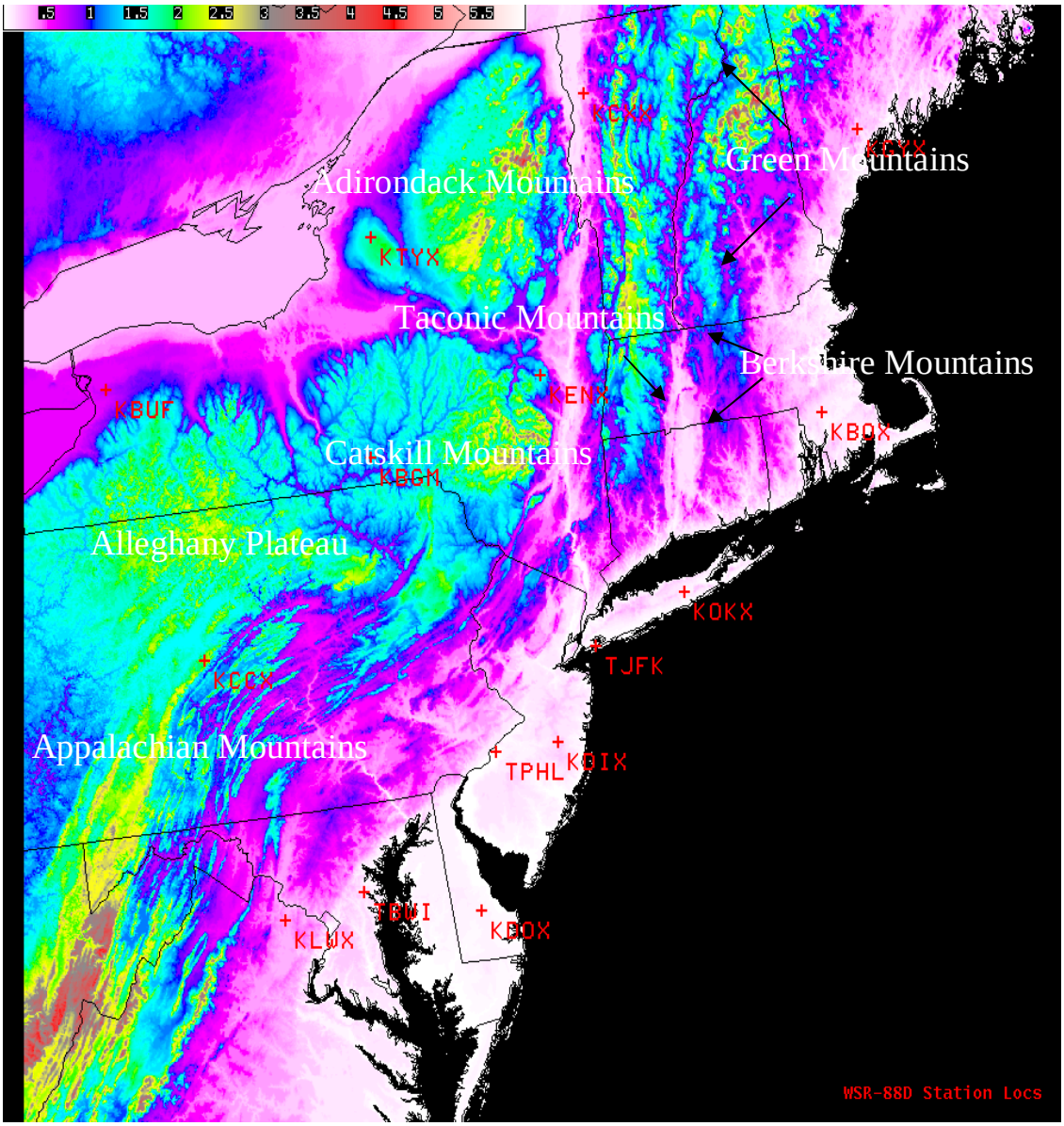

Figure 2. Topography (shaded in ft) map across the Northeast U.S. WSR-88D locations and terminal Doppler radars are overlaid.

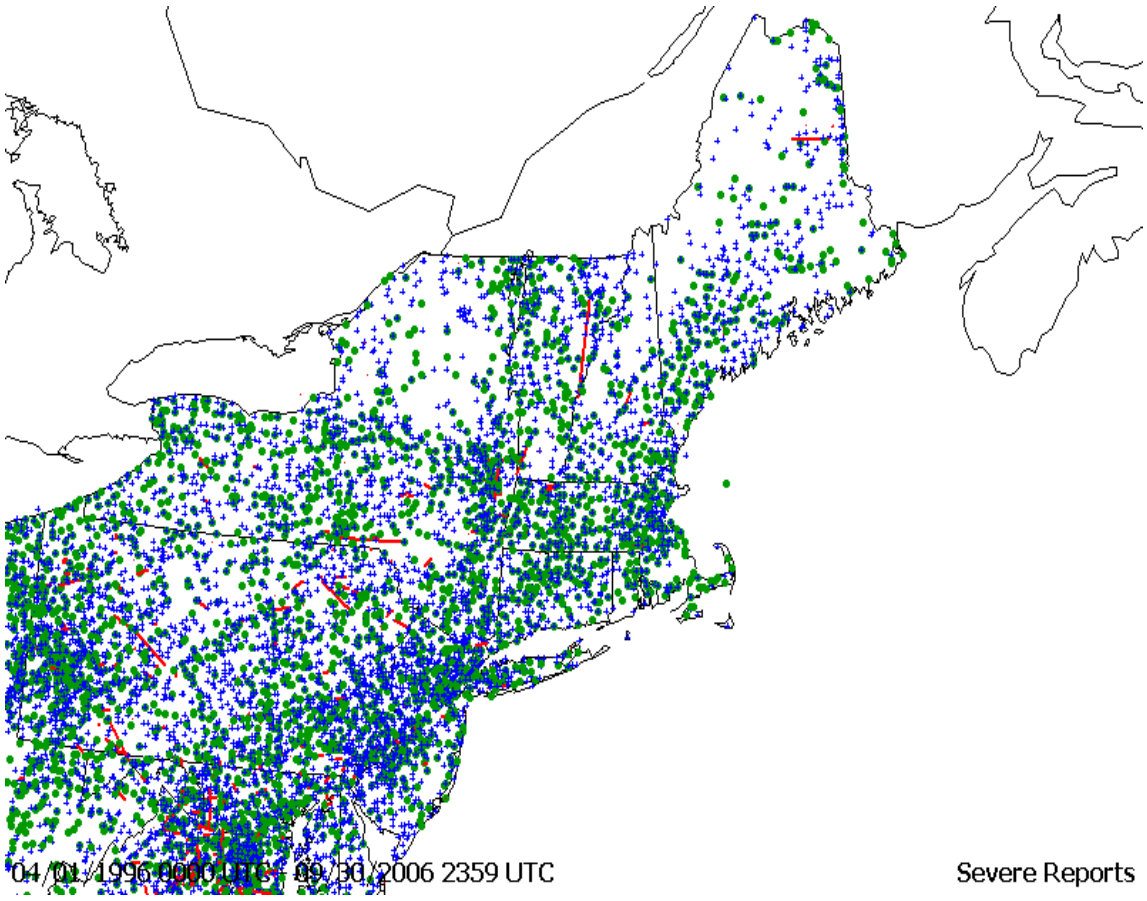

Figure 3. Severe storm reports from NCDC Storm Data across a select portion of the Northeast from 1996 through 2006 for the months of April through September using SvrPlot 2 software. Note: Red indicates tornadoes with a corresponding path length, blue indicates severe wind damage (>50 kt), and green indicates hail of diameter ¾ inch or greater.

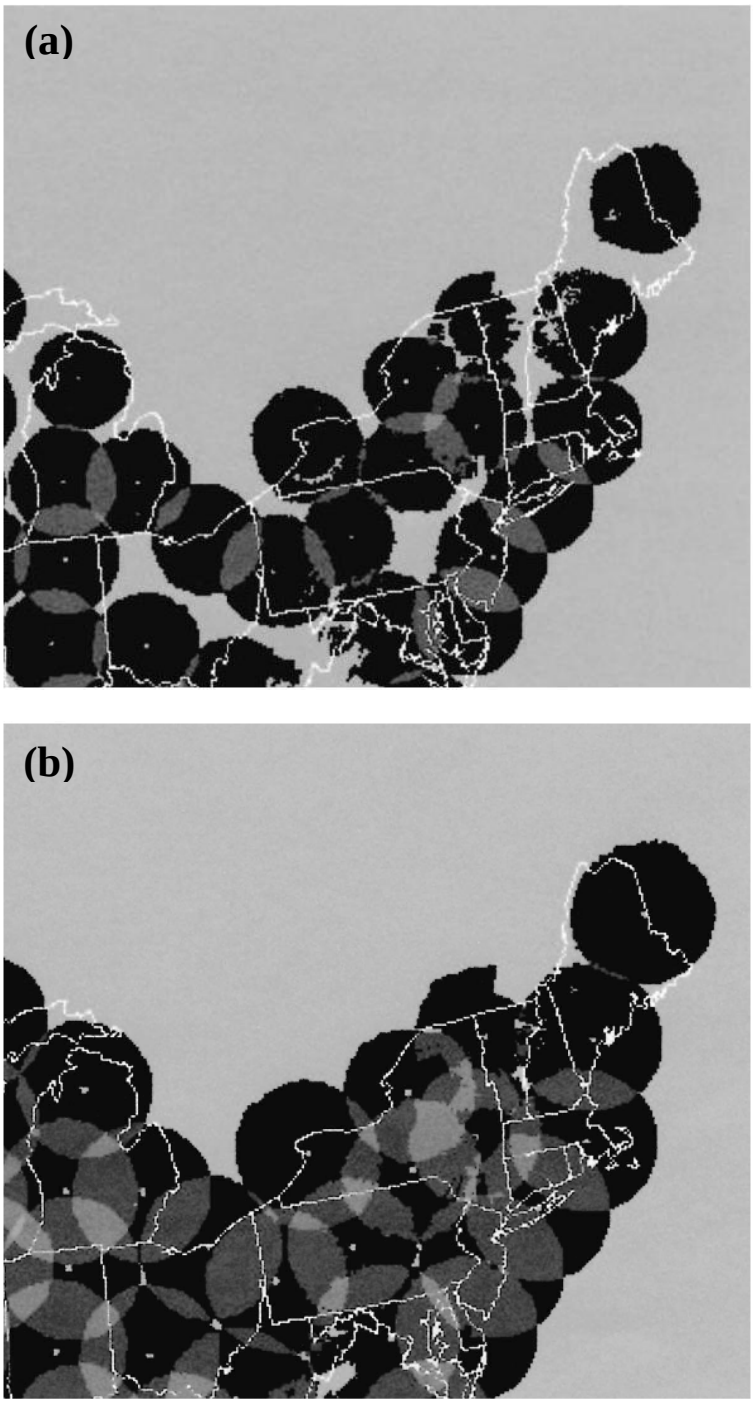

Figure 4. (a) WSR-88D coverage at 2km above ground level (AGL) (from Maddox et al. 2002). (b) WSR-88D coverage at 3km above ground level (AGL) (from Maddox et al 2002).

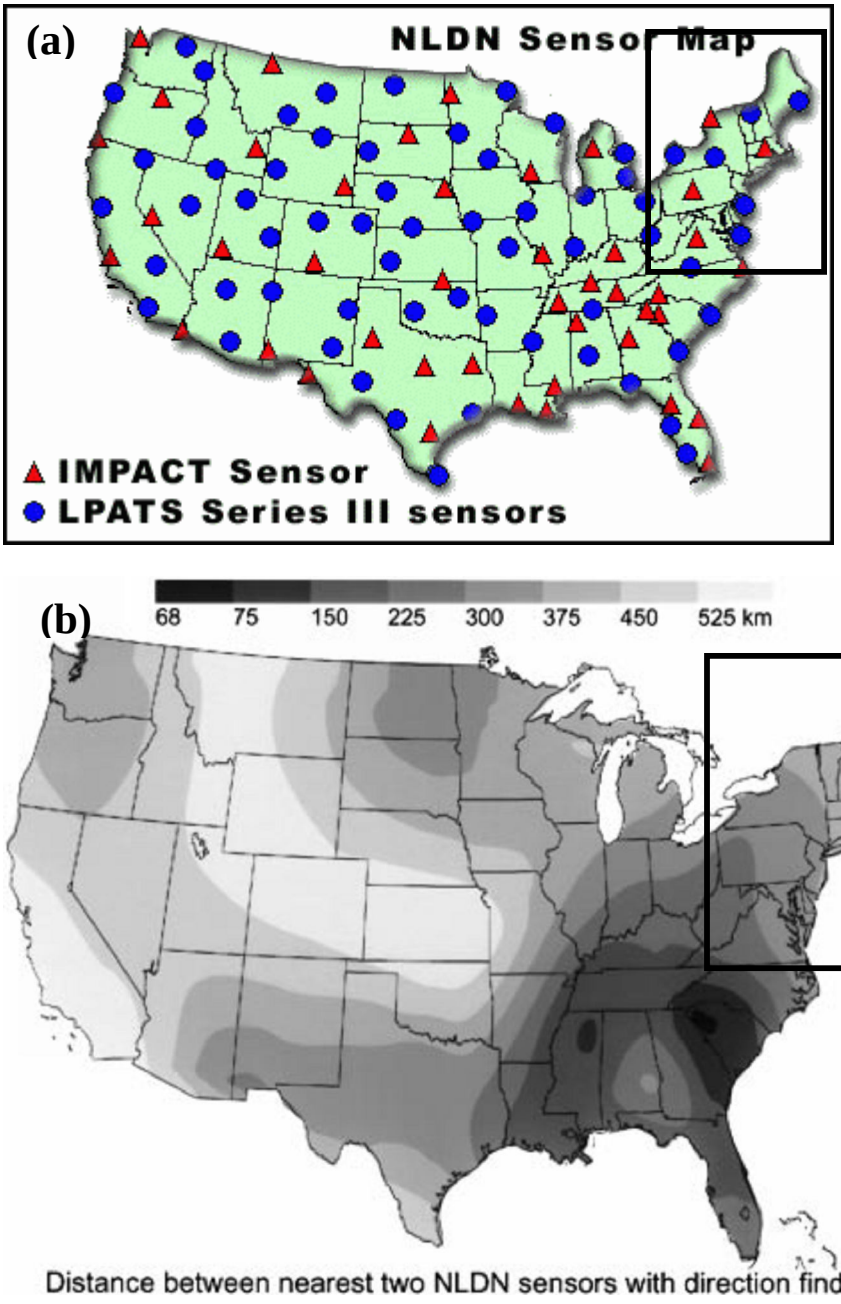

Figure 5. (a) National Lightning Detection Network (NLDN), from Global Hydrologic Climate Center. Outlined box denotes area of study. (b) Distance between nearest pair of sensor with direction finders (IMPACT) sensors (from Orville and Huffines 2001). Outlined box denotes area of study.

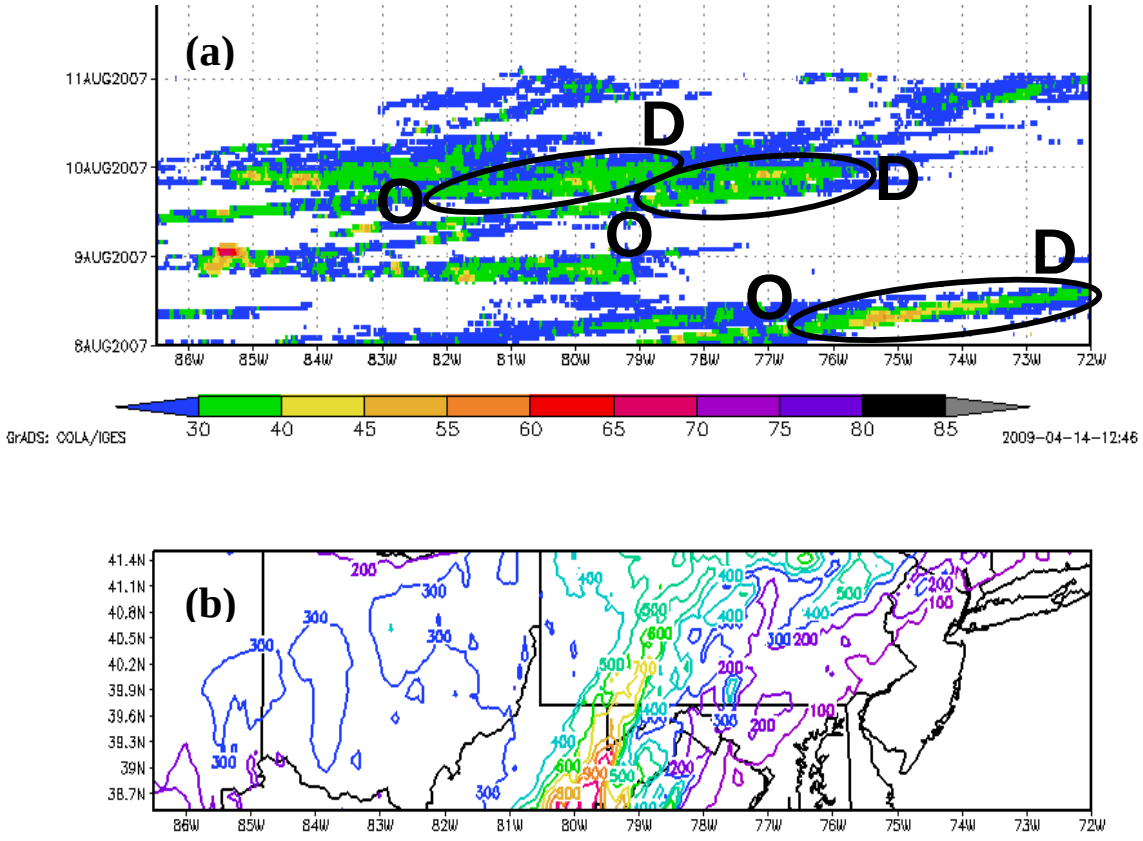

Figure 6. (a) An example of a hovmoller diagram where echo frequency ≥ 45 dBZ is plotted for the region shown in (b). The streaks indicated by the ovals represent episodes with a length ≥ 3° of longitude with initiation indicated by origin (O) and ending or decay (D) of each episode indicated.

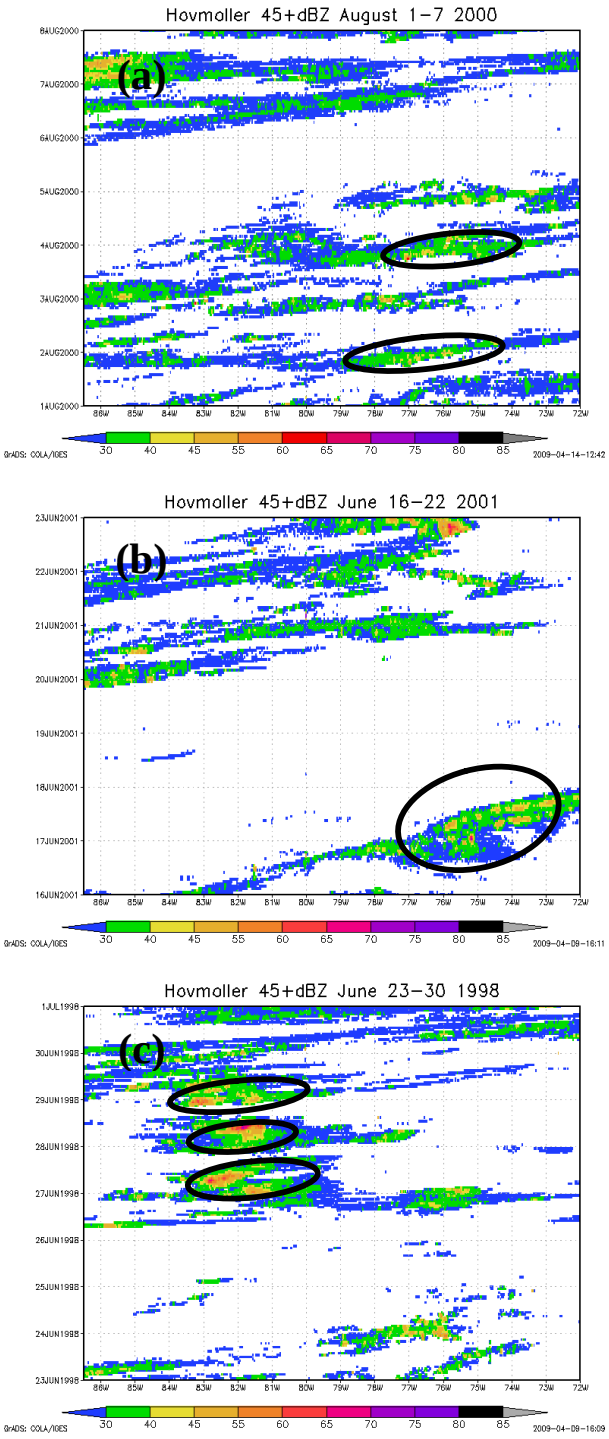

Figure 7. Examples of the types of objects identified for each of the 222 hovmoller plot streaks. (a) Short-lived (SL) convective events with duration of < 1 day, (b) Long-lived (LL) convective events with duration ≥ 1 day, (c) Serial convective (SC) events had at least 3 streaks in a 4 day period

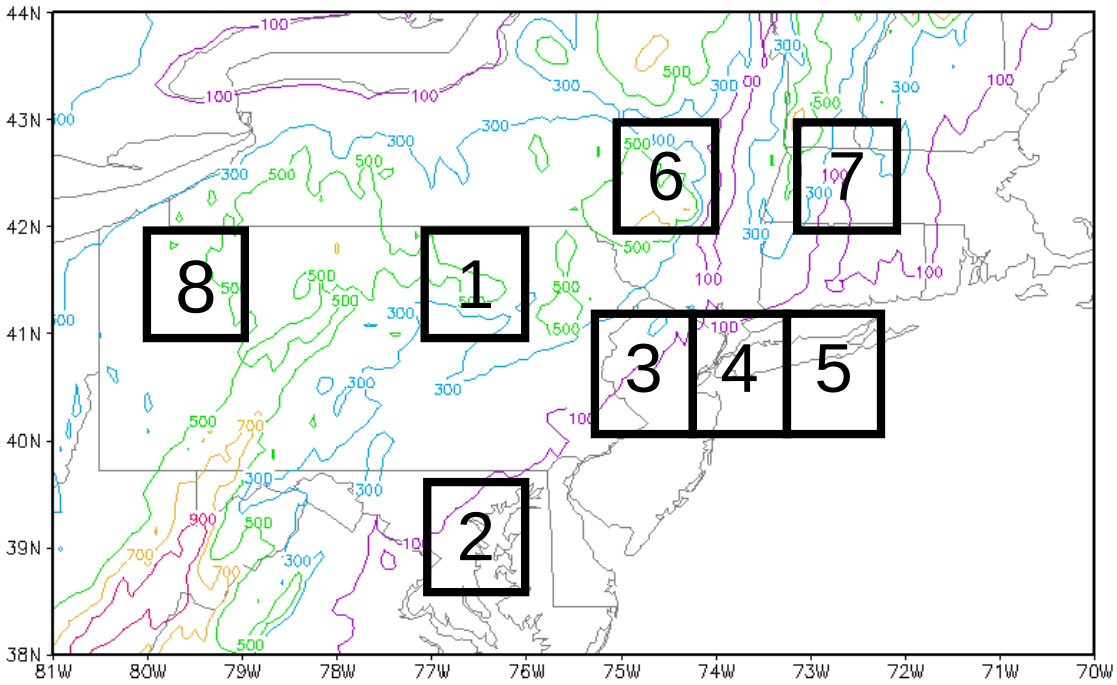

Figure 8. 1º latitude by 1º longitude boxes for select areas across the Northeast that have areal averages of frequencies of 45+dBZ computed for each hour across each of the boxes.

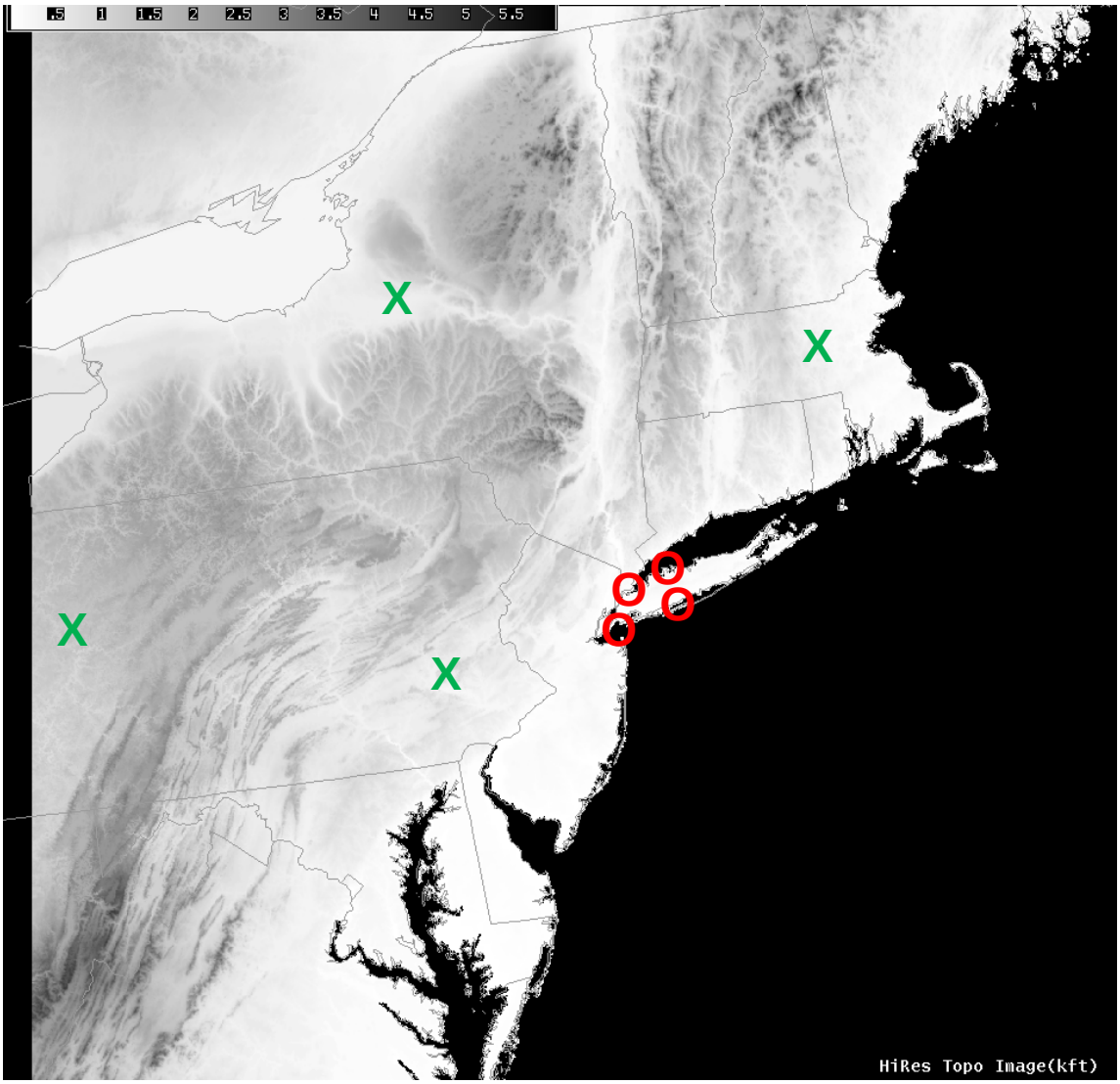

Figure 9. The green X's and red O's show the location of the sampling points for convective wind regimes from NARR data at 500 hPa and 925 hPa, respectively.

Figure 10. National Weather Service forecast offices used for the severe weather days analysis in section 3e. The stations include, New York NY (OKX), Mount Holly NJ (PHI), State College PA (CTP), Binghamton NY (BGM), Albany NY (ALB), Sterling VA (LWX) and Taunton MA (BOX). The outline boundaries represent the county warning area for each forecast office.

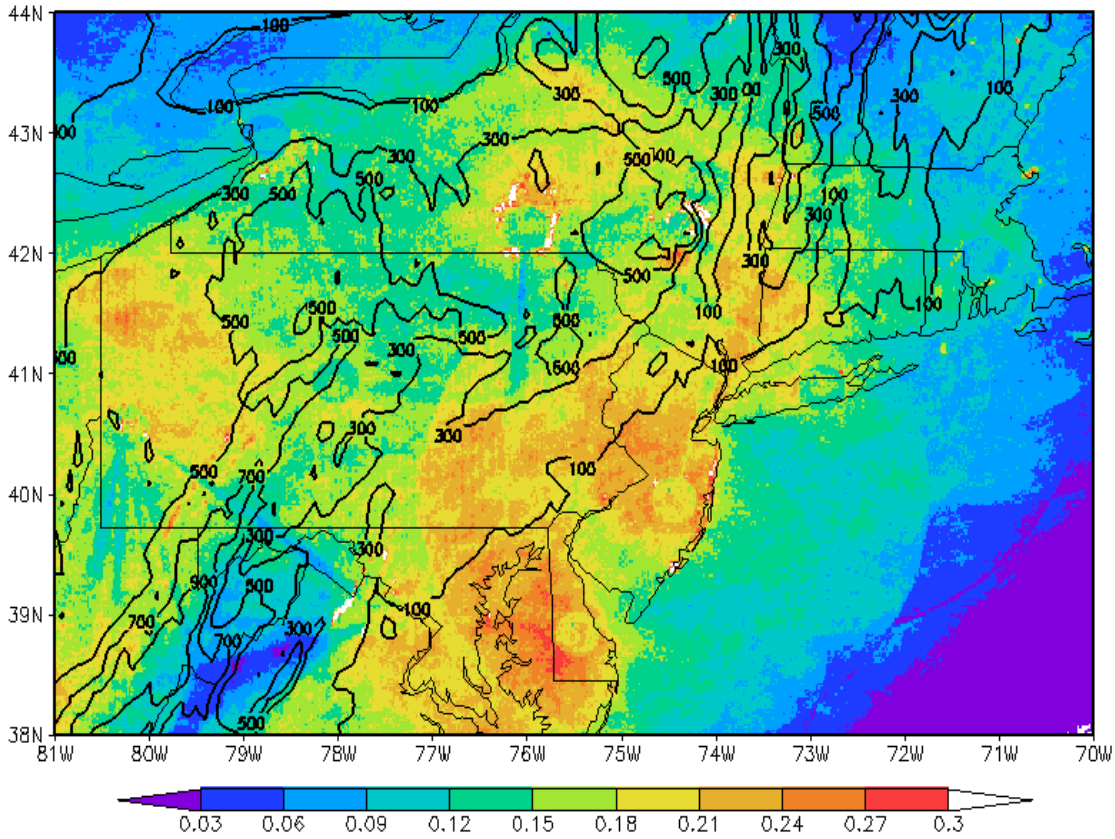

Figure 11. Pr_{storm} or storm frequency per 15 minute interval for a composite reflectivity ≥ 45 dBZ from April through September during the warm seasons of 1996-2007. Values have been multiplied by 100 and therefore are equivalent to percentages.

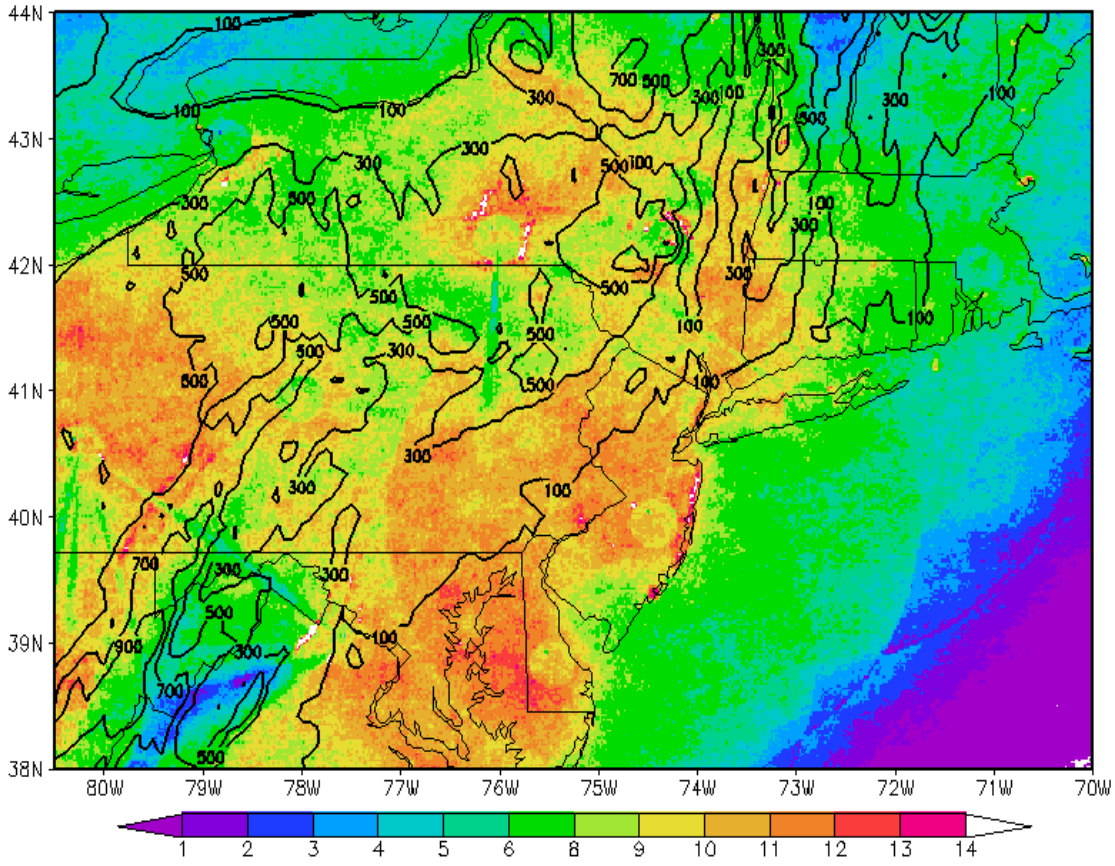

Figure 12. The percentage of thunderstorm days for the 1996-2007 warm seasons having at least 1 daily occurrence of composite reflectivity ≥ 45 dBZ.

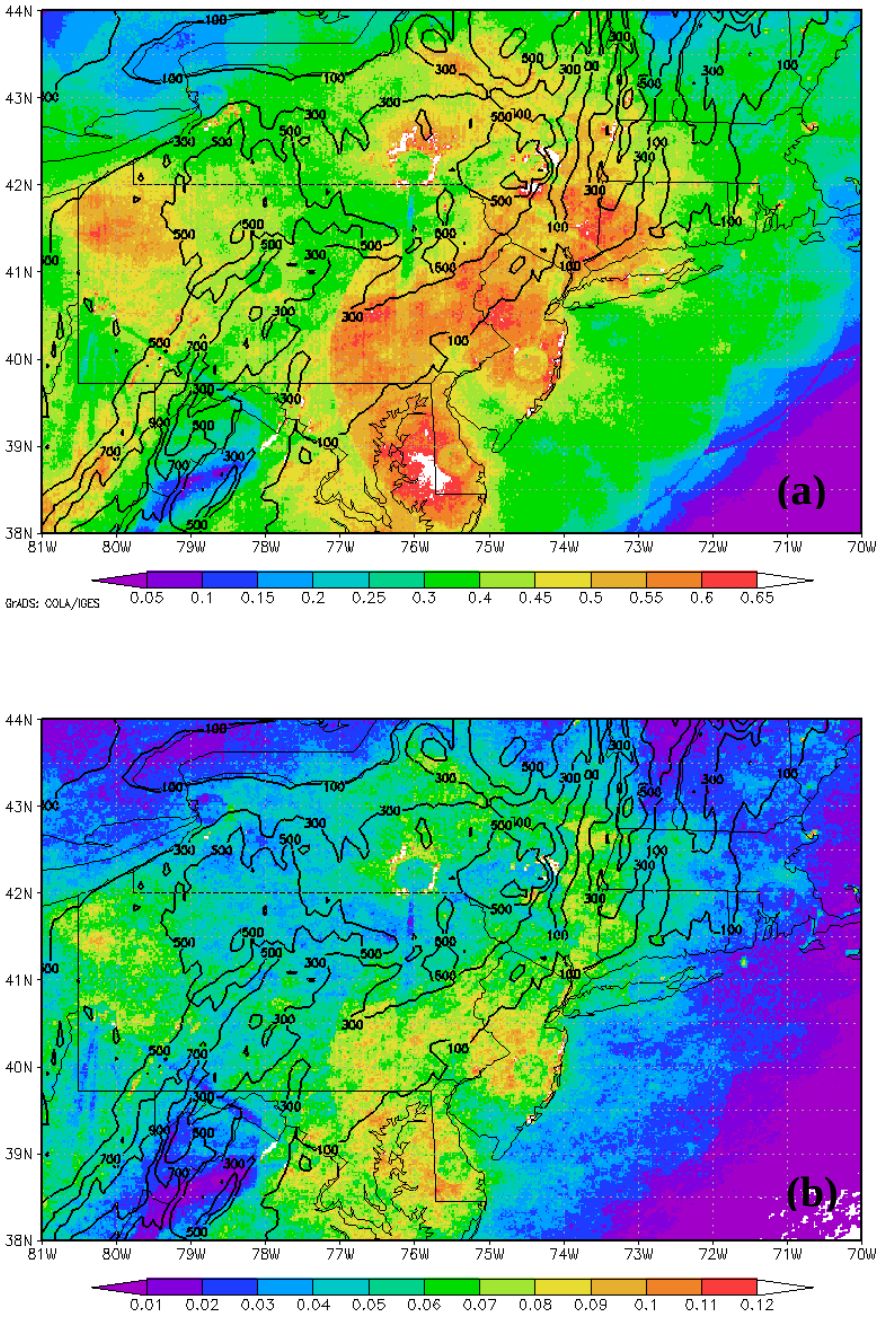

Figure 13. Same as Fig. 11 but for (a) composite reflectivity ≥ 40 dBZ and (b) composite reflectivity ≥ 50 dBZ. Values have been multiplied by 100 and therefore are equivalent to percentages.

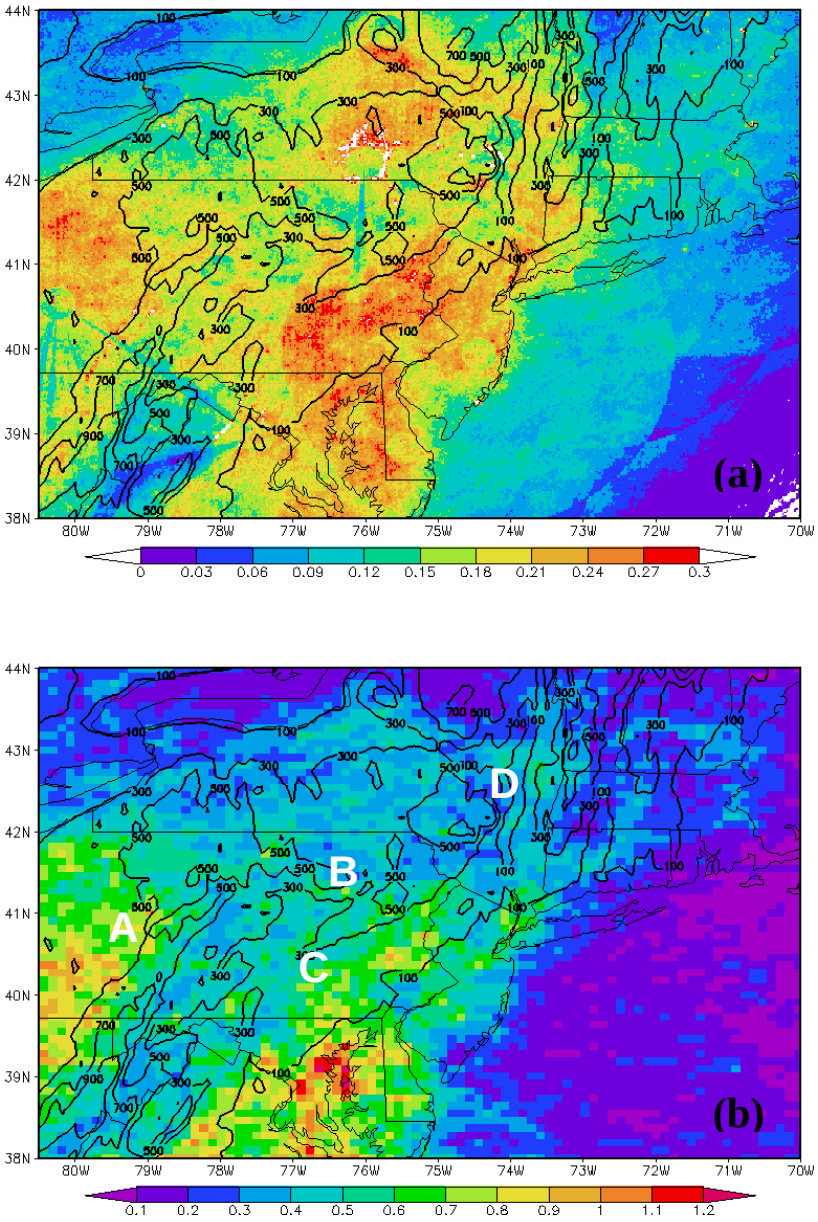

Figure 14. (a) The Pr_{storm} for composite reflectivity ≥ 45dBZ and (b) the monthly frequency per km^2 for lightning strikes number for the same months of the warm season that lightning data was available. A, B, C, and D refer to areas with more distinguished gradients in convection with the lightning data.

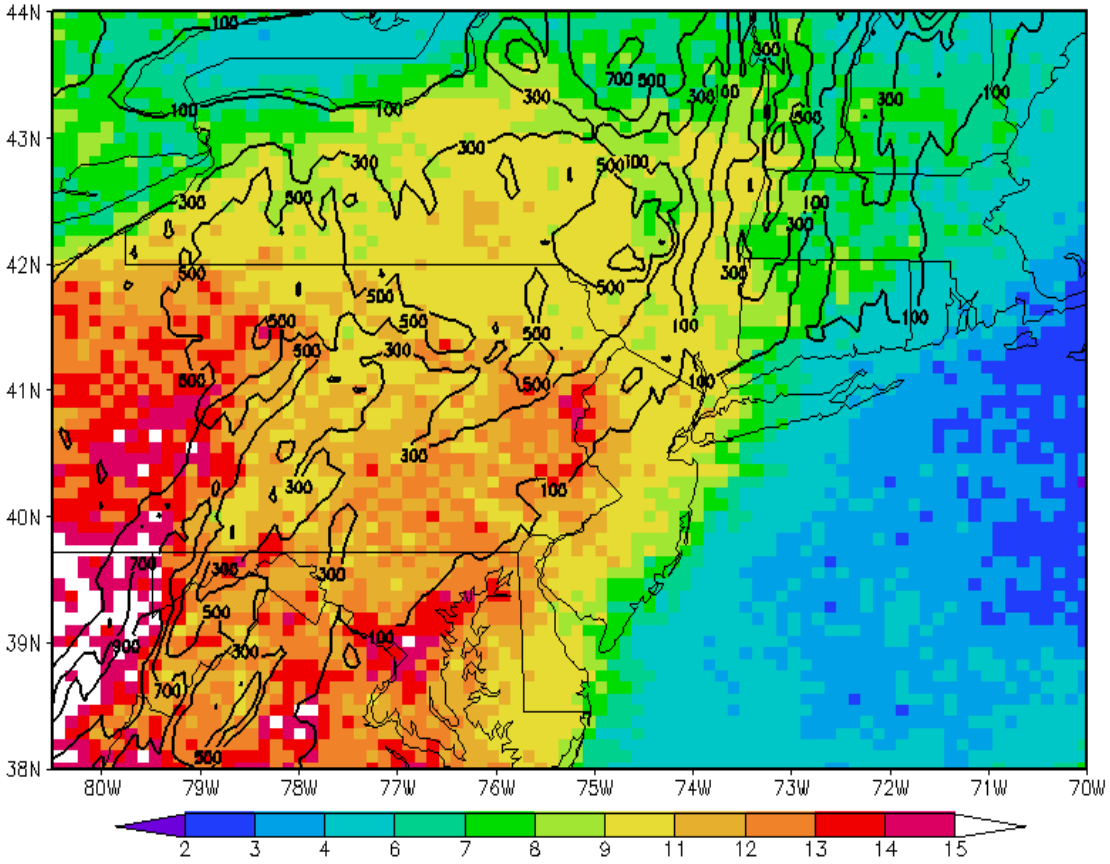

Figure 15. Same as Fig. 12, but for the percentages of days having at least 1 lightning strike of each day during the warm seasons of 2001 through 2007.

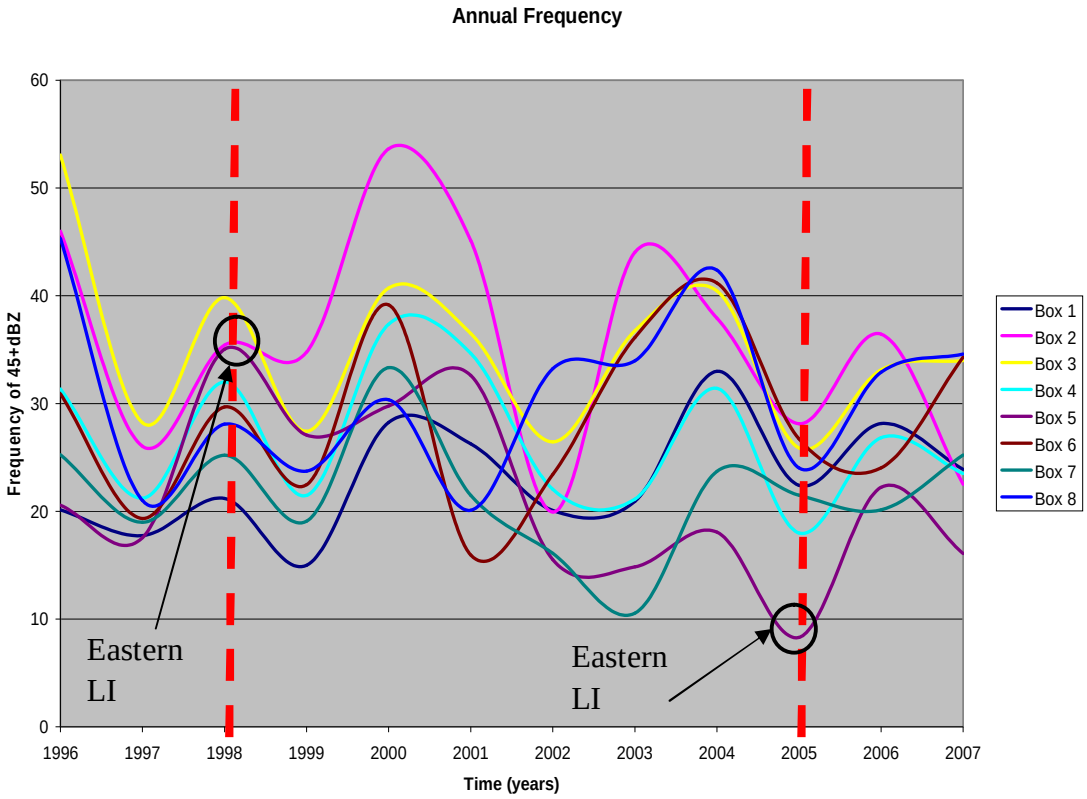

Figure 16. The frequency of 45+dBZ versus warm season (1996-2007) for the 1º latitude by 1º longitude boxes in Fig. 8. Red lines indicate years that were analyzed for synoptic and convective differences. The black arrows point to Box 5 over eastern Long Island and represent the maximum (1998) and minimum (2005) of the annual quantity of convection over that region.

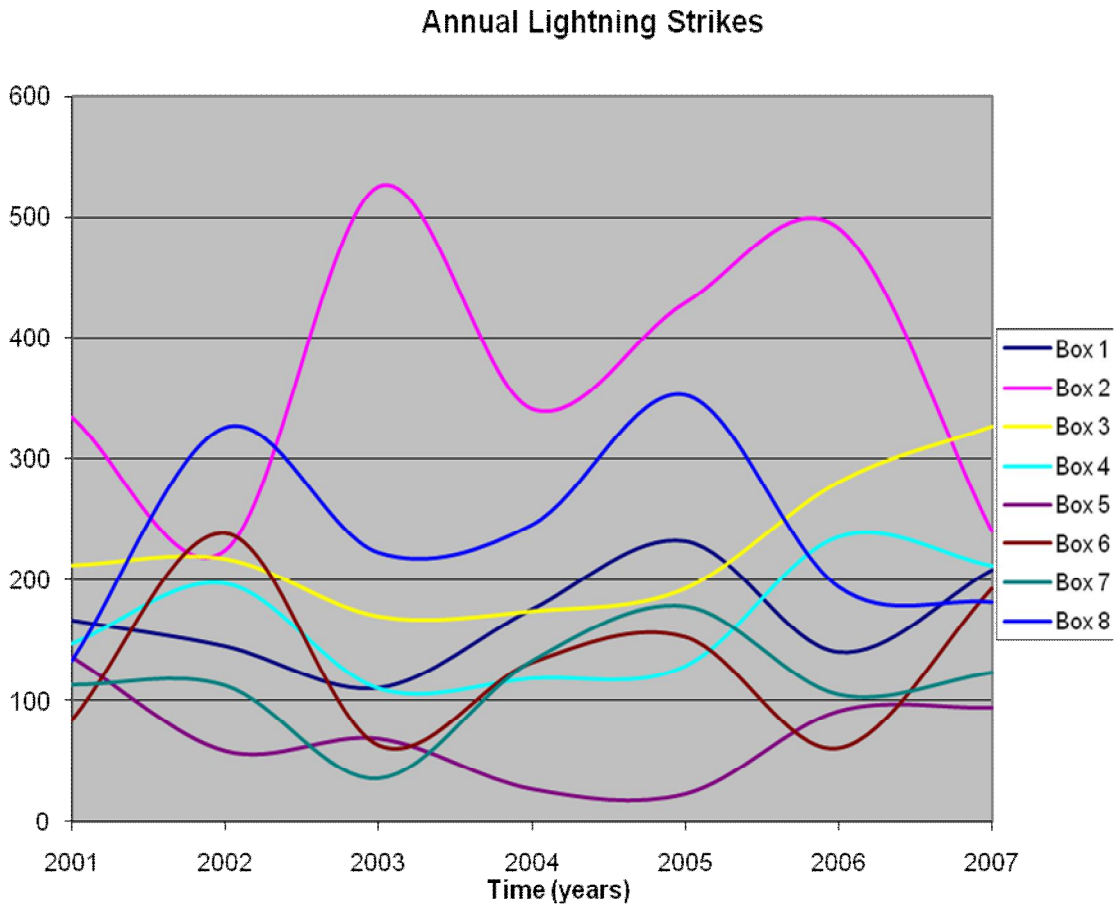

Figure 17. The number of lightning strikes versus warm season (2001-2007) for the 1º latitude by 1º longitude boxes as shown in Fig. 8.

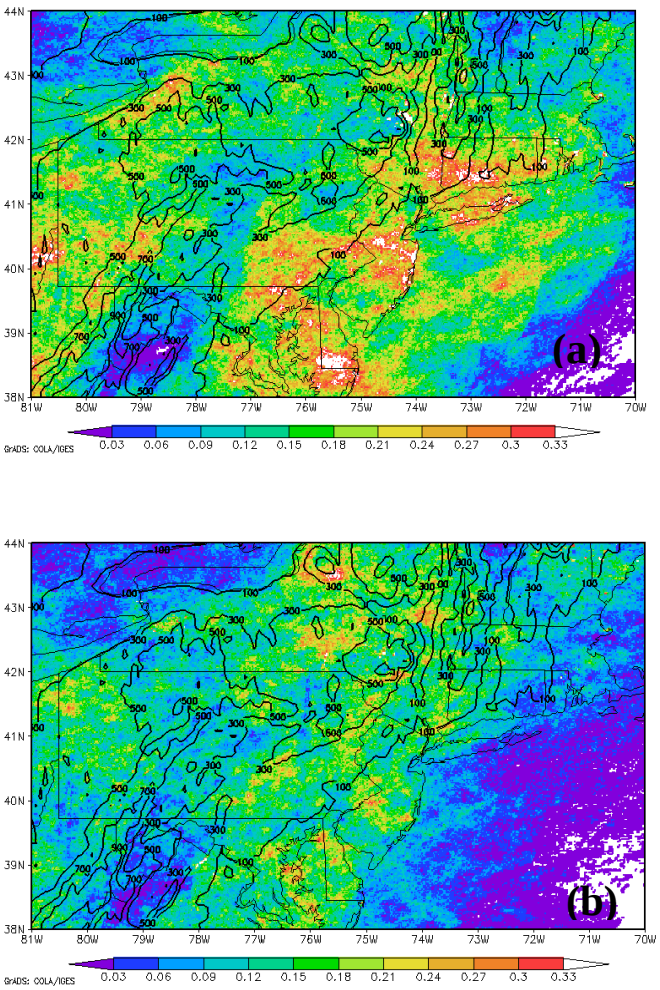

Figure 18. Pr_{storm} (45+dBZ Frequency) for the warm seasons of (a) 1998 and (b) 2005. Values have been multiplied by 100 and are therefore equivalent to percentages.

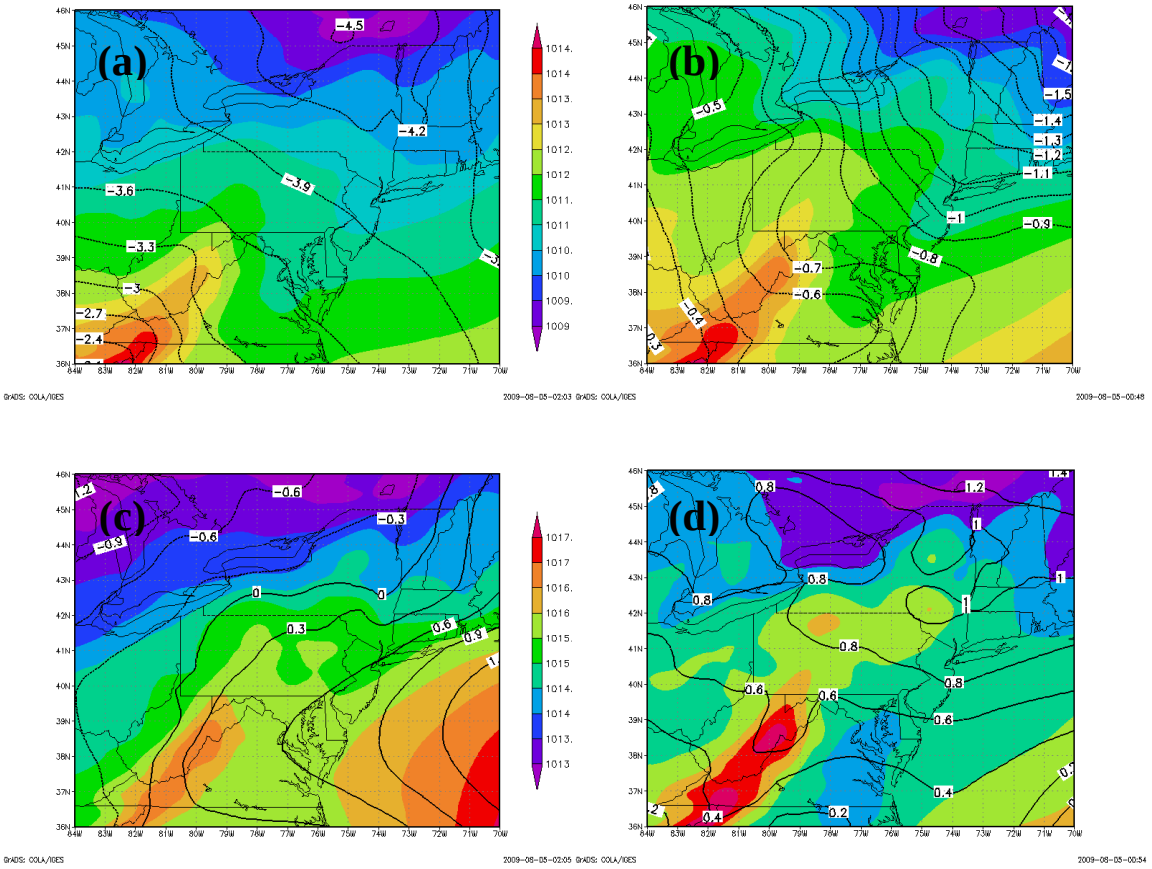

Figure 19. NARR sea level pressure (MSLP; shaded every 1 hPa) and difference with the 1996-2007 monthly MSLP climatology (contoured black in hPa) for (a) June 1998 and (b) July 1998. (c) and (d) Same as (a) and (b) except for June and July 2005.

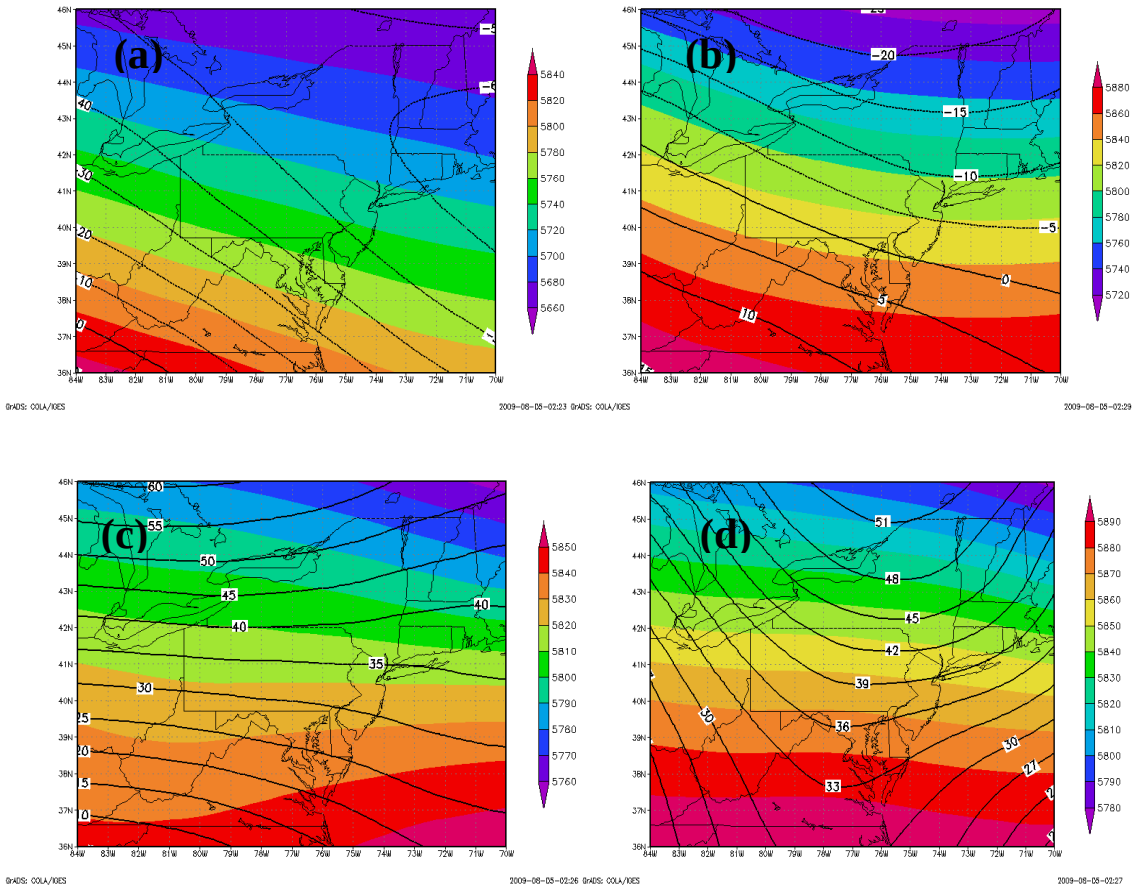

Figure 20. NARR geopotential height at 500 hPa (shaded every 5 m) and difference with the 1996-2007 monthly 500 hPa geopotential height climatology (contoured black in m) for (a) June 1998 and (b) July 1998. (c) and (d) Same as (a) and (b) except for June and July 2005.

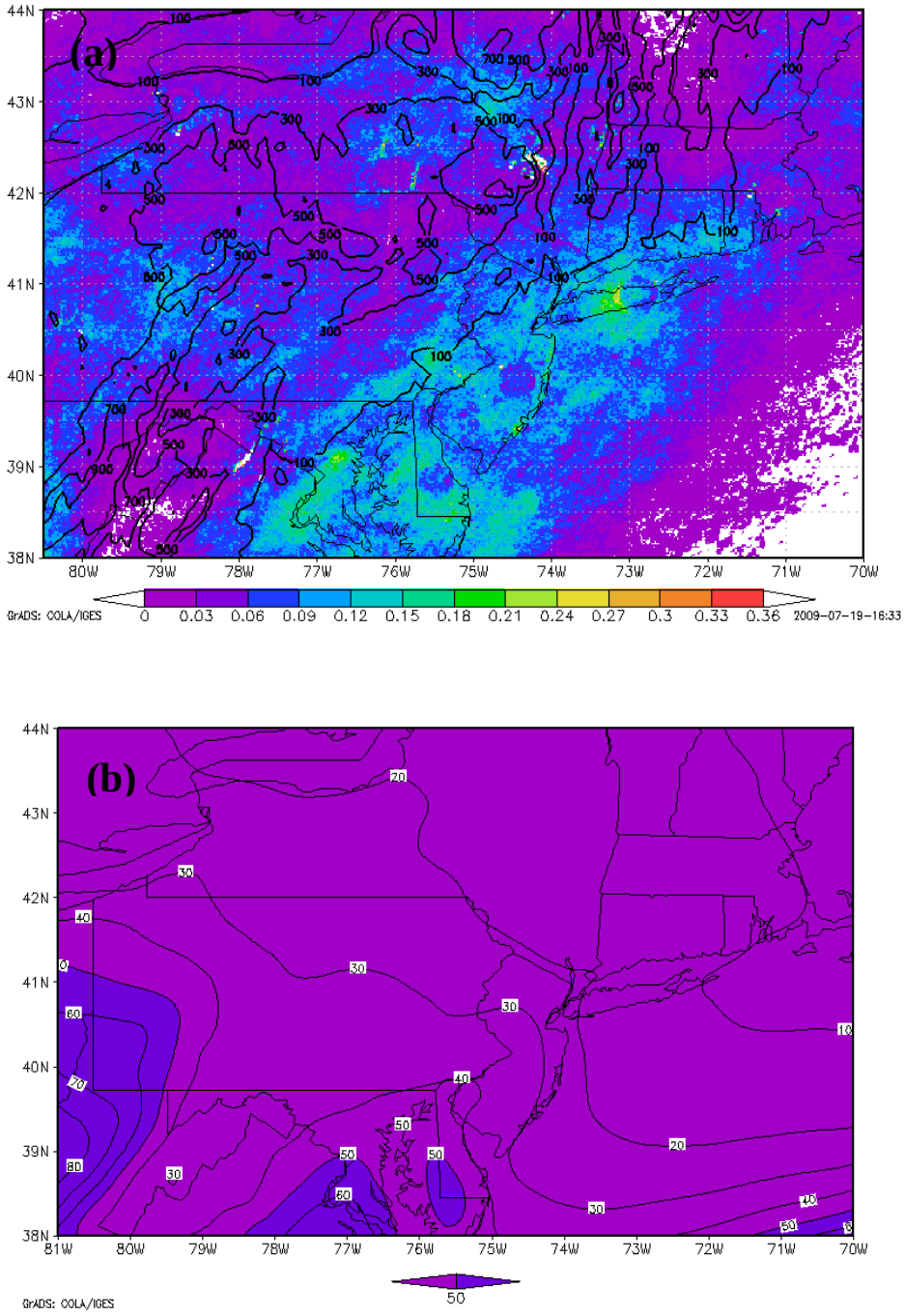

Figure 21. (a) Pr_{storm} for 45+dBZ in April (from 1996-2007) with values multiplied by 100, (b) NARR Average low level CAPE (J kg^{-1}) between 0 and 180 hPa above the ground from 1996-2007 for month of April.

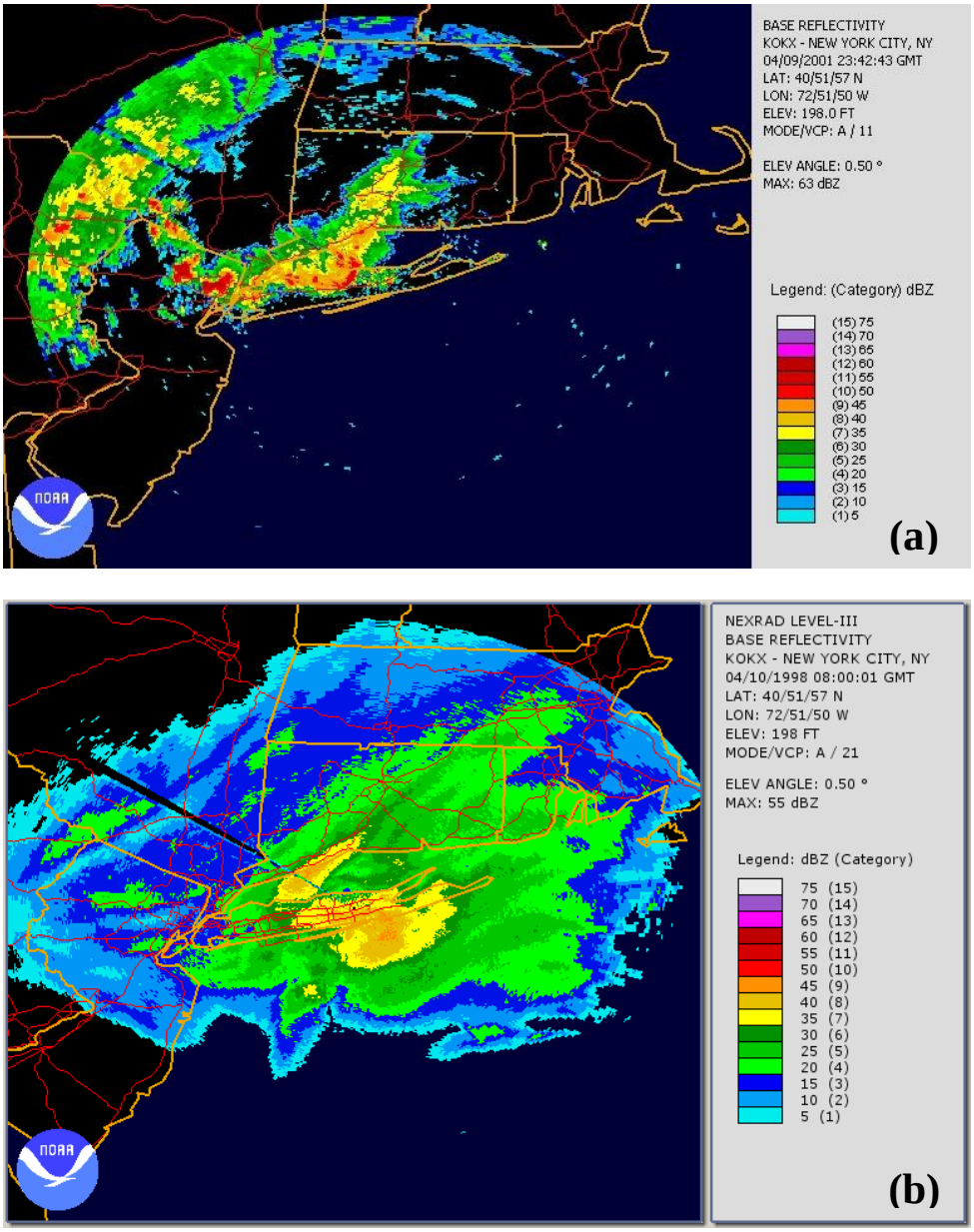

Figure 22. (a) Base reflectivity (0.5° elevation scan) from the WSR-88D at KOKX for 23:42 UTC on 9 April 2001. The higher reflectivities (≥ 45 dBZ) are more cellular shaped and correspond to embedded convection as opposed to cases of bright banding (b) where the higher reflectivities are generated because of the widespread melting of ice.

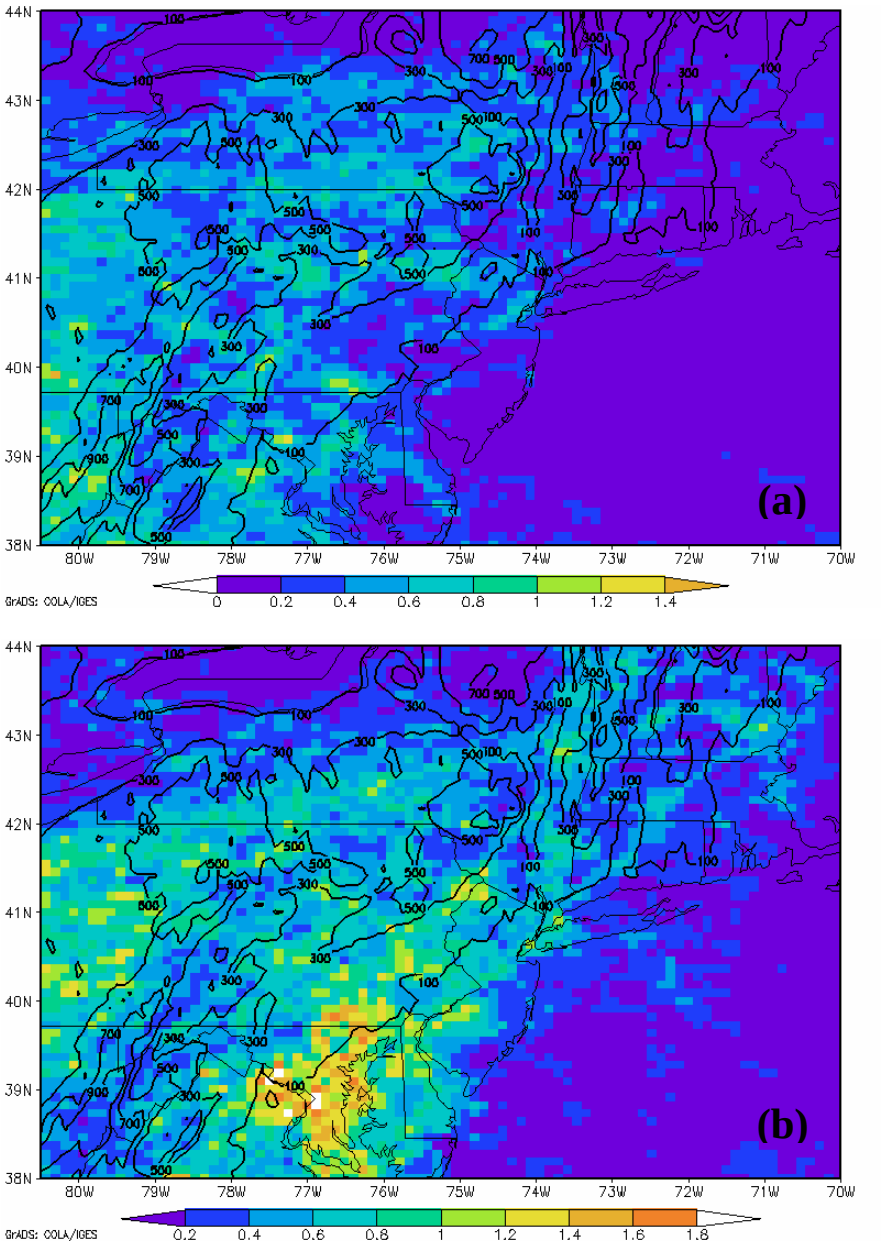

Figure 23. Monthly flash rate of lightning per km^2 for (a) May and (b) June during the warm seasons of 2001-2007.

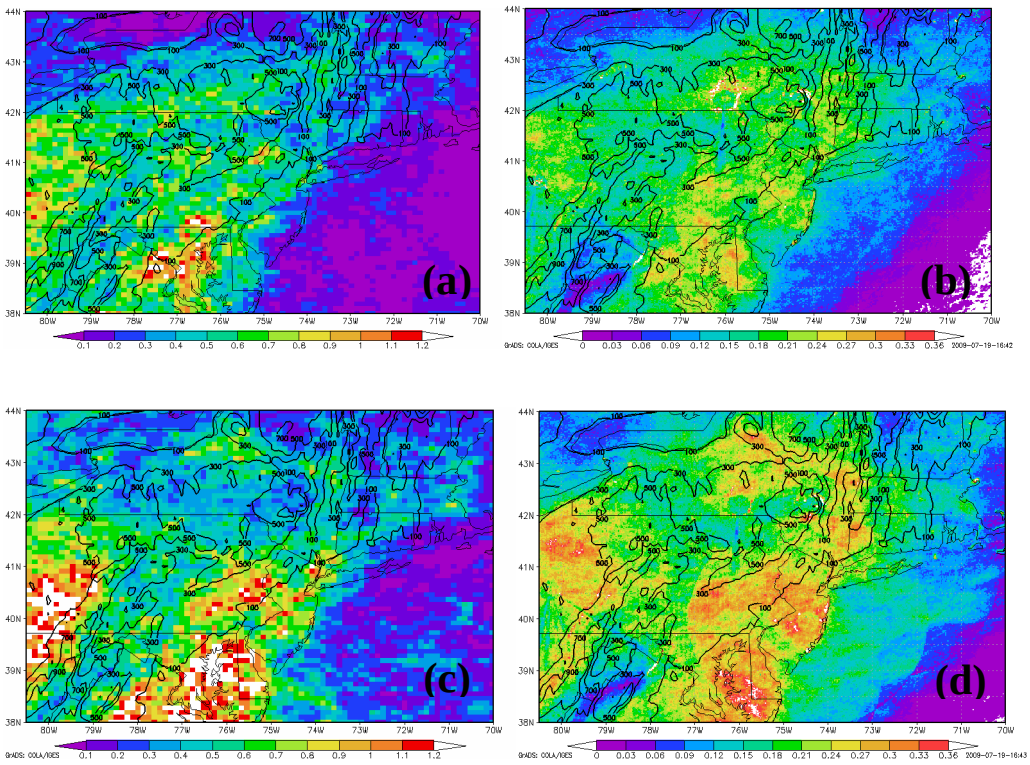

Figure 24. The monthly frequency per km^2 of lightning for (a) May and June and (c) July and August as well as Pr_{storm} of composite reflectivity ≥ 45 dBZ for (b) May and June and (d) July and August.

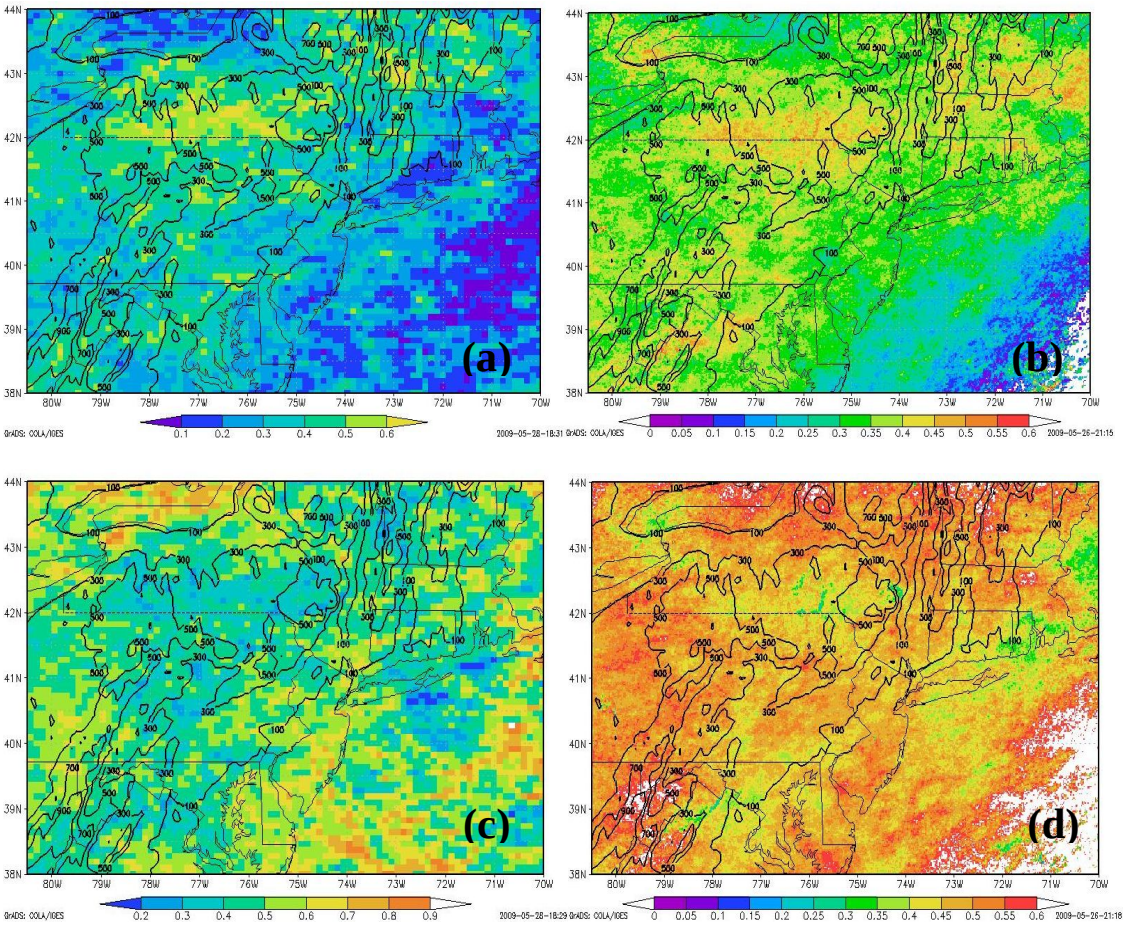

Figure 25. (a) The fraction of the total lightning strikes and (b) fraction of composite reflectivity ≥ 45 dBZ frequency for the months of May and June, as well as for July and August for the fraction of (c) total lightning strikes and (d) fraction of composite reflectivity ≥ 45 dBZ frequency.

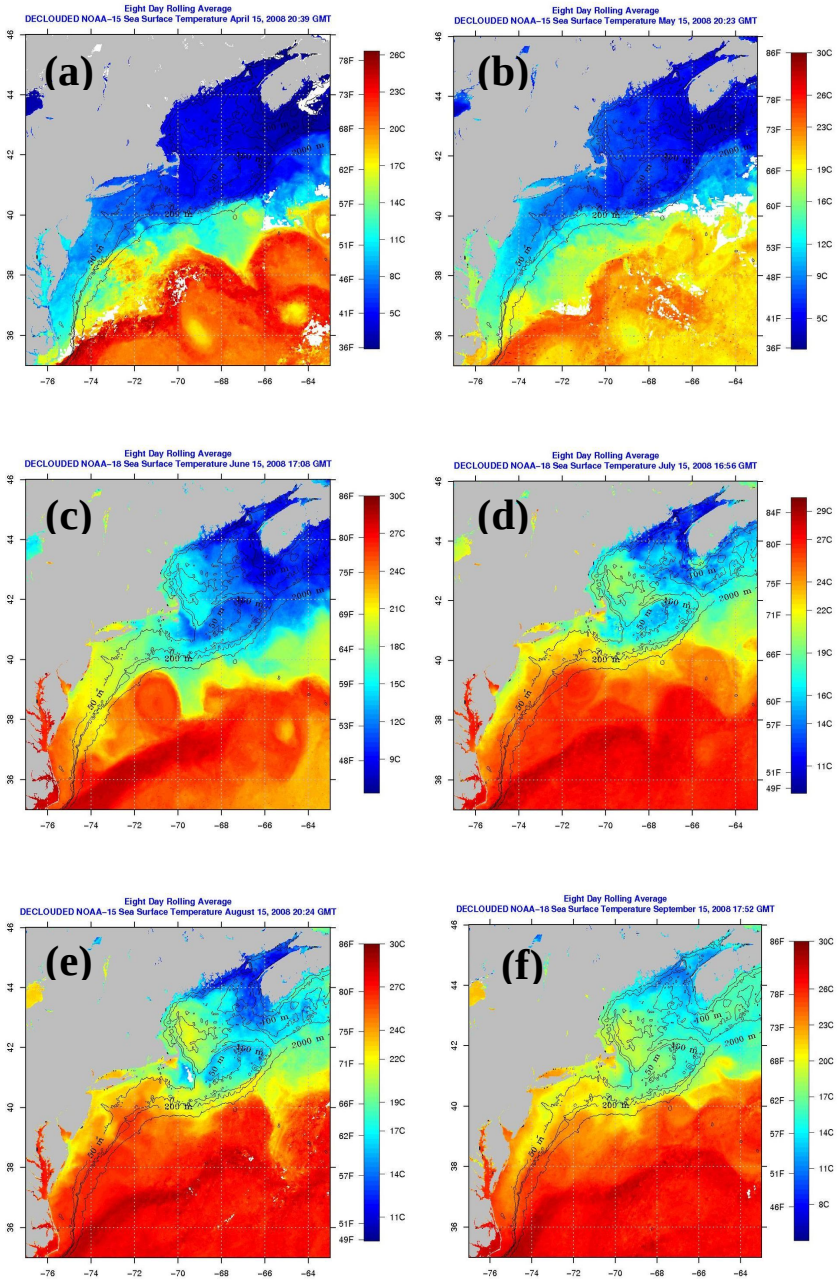

Figure 26. Eight day average of NOAA-18 Satellite (Advanced Very High Resolution Radiometer (AVHRR)) derived sea surface temperatures during the warm season of 2008. Each image is taken around the midpoint for each month of (a) April, (b) May, (c) June, (d) July, (e) August, and (f) September.

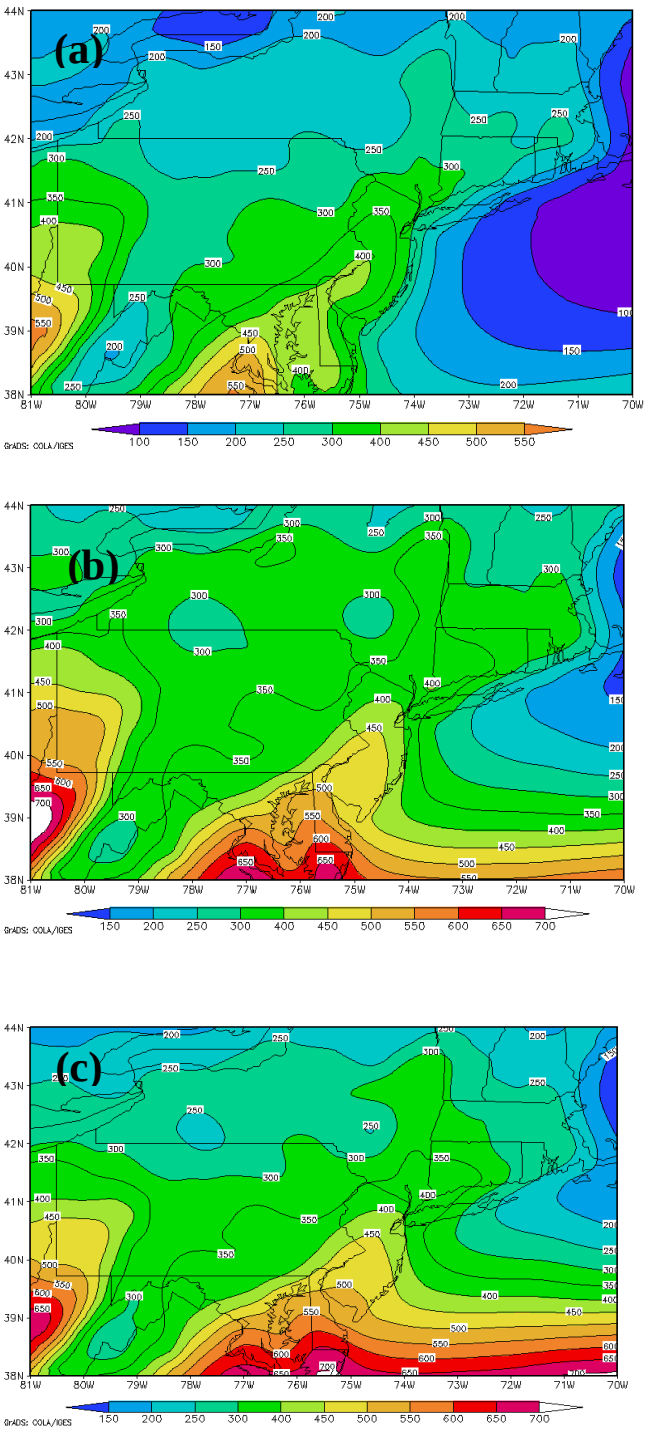

Figure 27. Averaged low level (0-180 hPa above the ground) CAPE (J kg^{-1}) from 1996-2007 for the months of (a) June, (b) July, and (c) August.

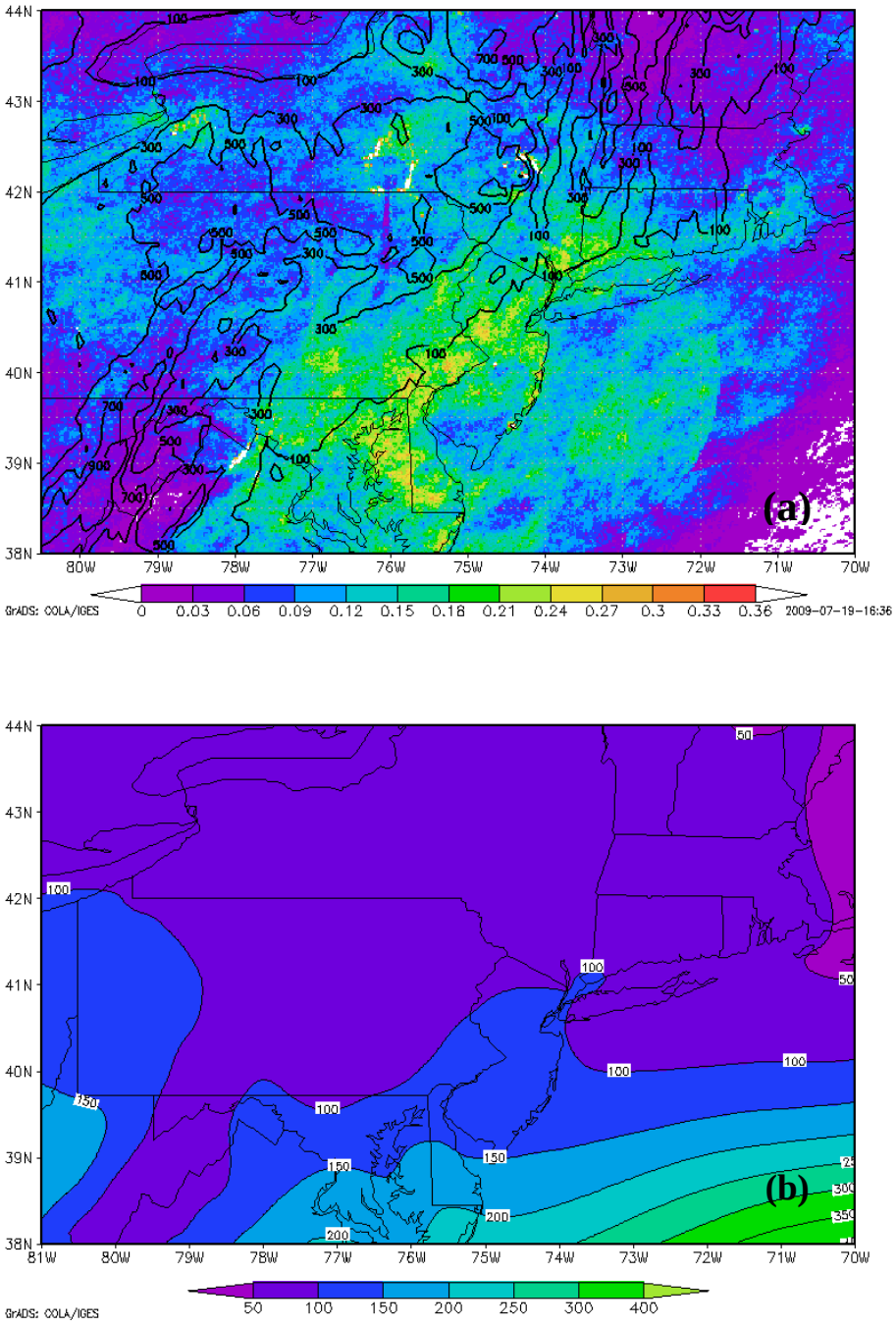

Figure 28. (a) Pr_{storm} (45+dBZ frequency) for the month of September. (b) Average low level CAPE between 0 and 180 hPa above the ground for all September months (1996-2007).

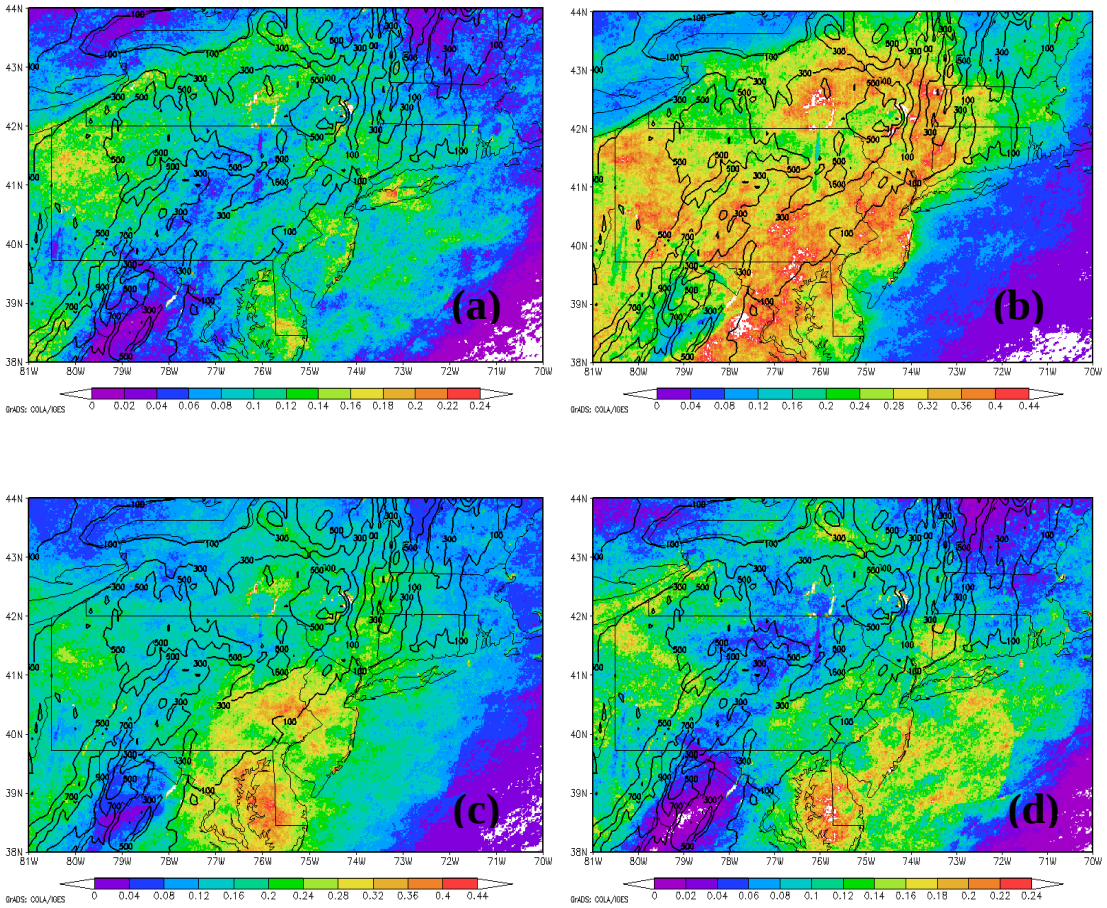

Figure 29. Pr_{storm} of composite reflectivity ≥ 45dBZ during the 1996-2007 warm seasons for the 6-h time periods of (a) 12-18 UTC, (b) 18-00 UTC, (c) 00-06 UTC, and (d) 06-12 UTC.

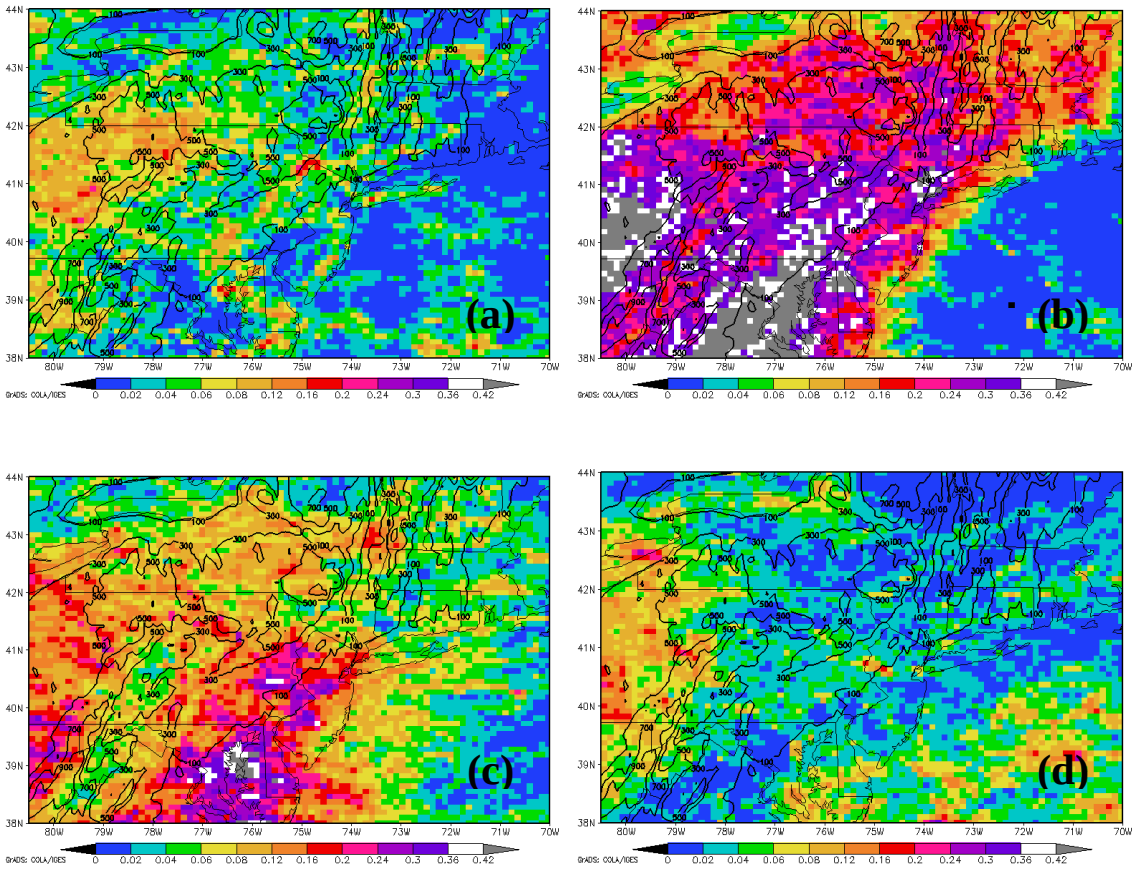

Figure 30. The monthly frequency per km^2 of cloud to ground lightning for the 1996-2007 warm seasons for the 6-h time periods of (a) 12-18 UTC, (b) 18-00 UTC, (c) 00-06 UTC, and (d) 06-12 UTC.

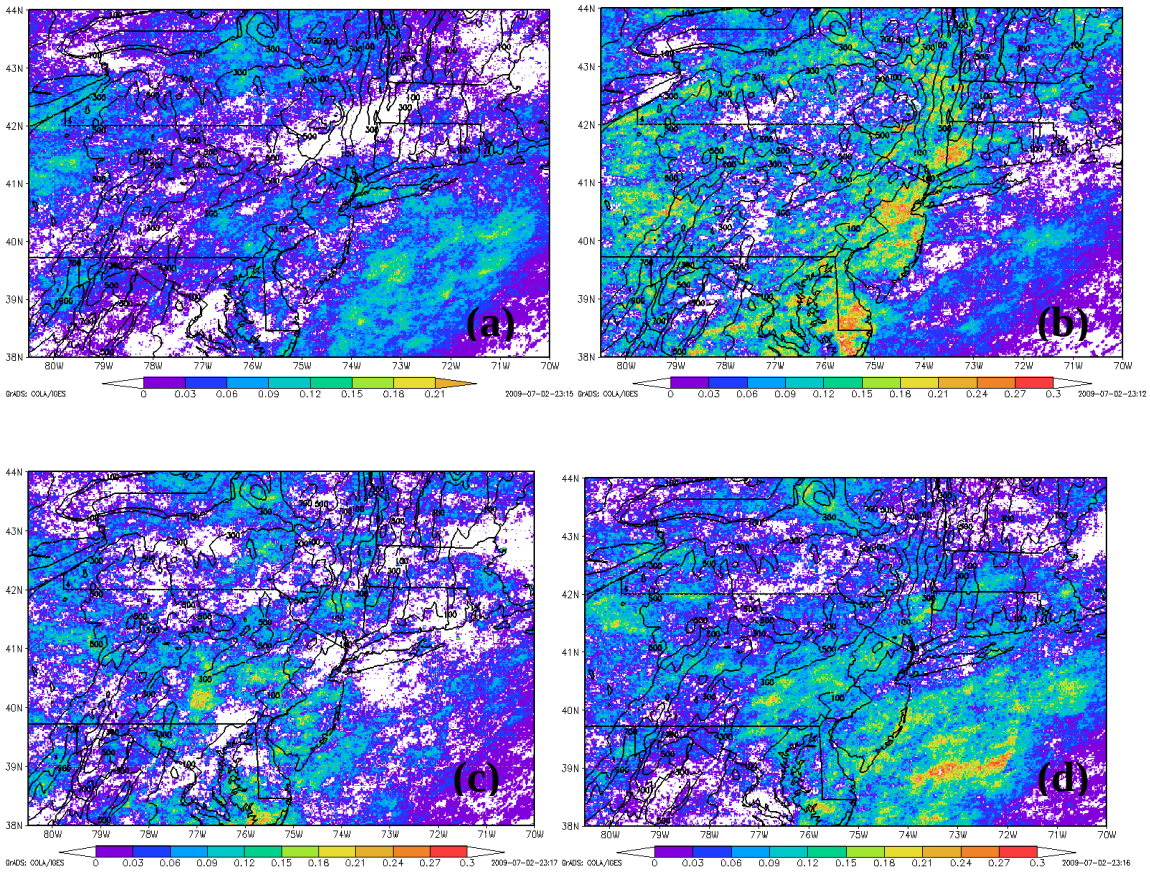

Figure 31. Differences in the Pr_{storm} for ≥ 45dBZ only for the 6-h time periods of (a) 12-18 UTC, (b) 18-00 UTC, (c) 00-06 UTC, (d) 06-12 UTC between the first half (April, May, June) and second half (July, August, September) of the warm season.

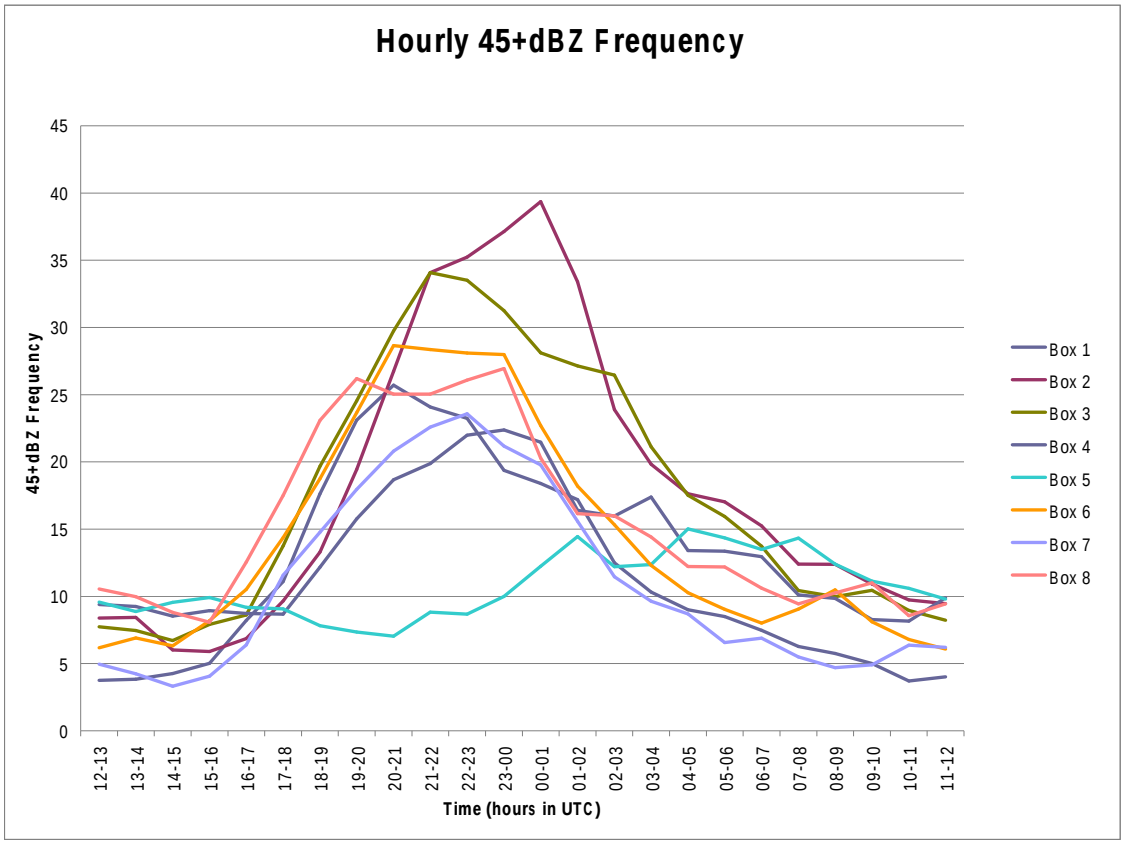

Figure 32. Areal diurnal means of 45+dBZ frequency for 1º latitude by 1º longitude boxes shown in Fig. 8.

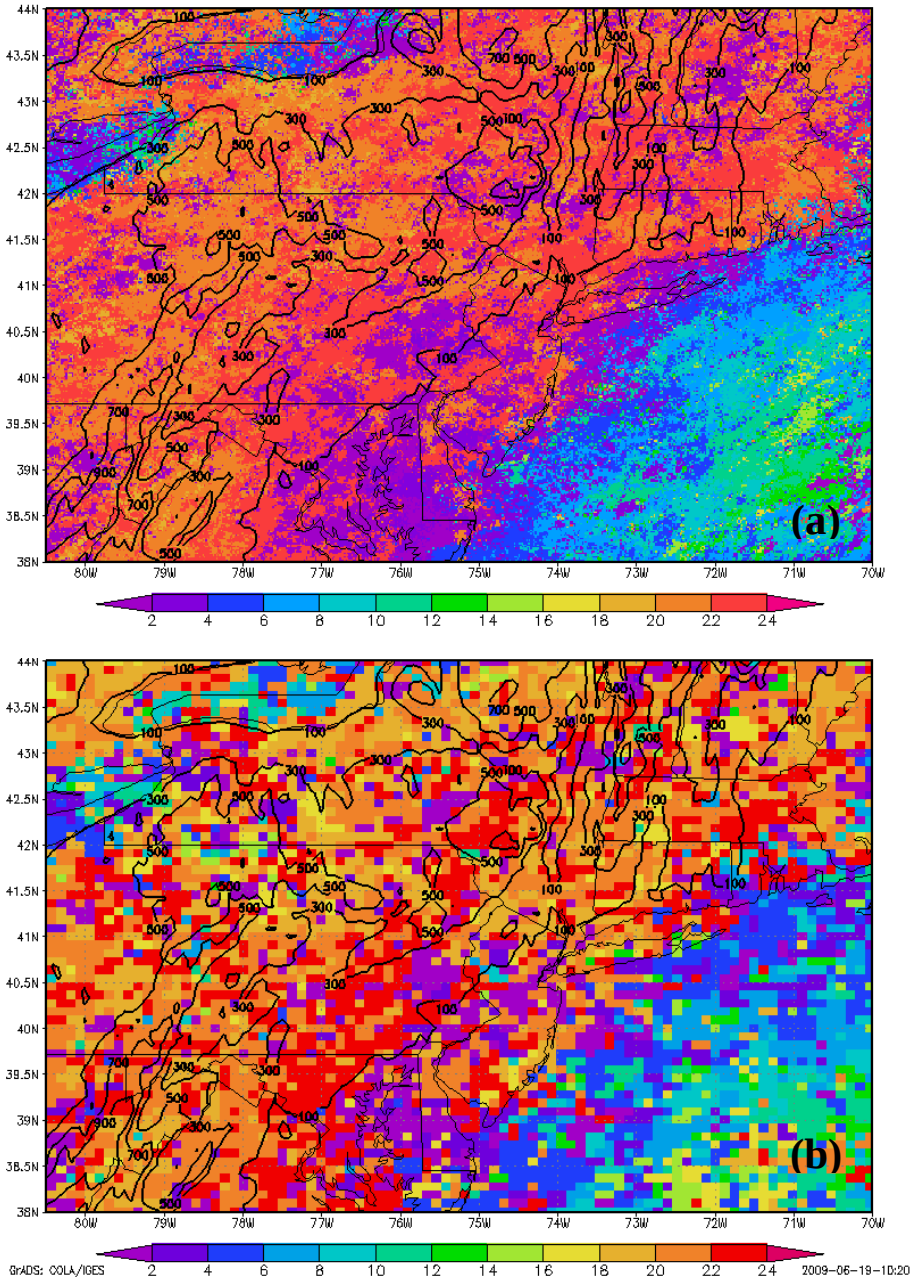

Figure 33. The hour (in UTC) of the maximum (a) 45+dBZ frequency and (b) lightning strikes.

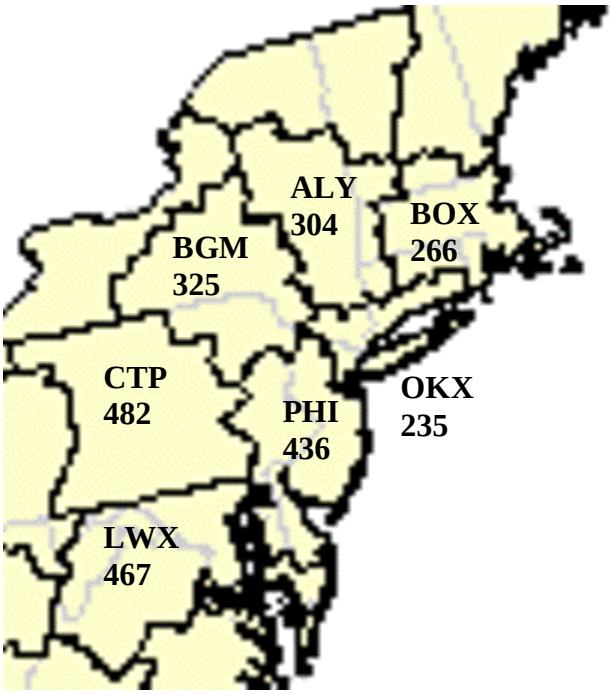

Figure 34. Number of severe weather days (severe storm report and/or severe warning days) for each NWS forecast office during the 1996-2007 warm seasons.

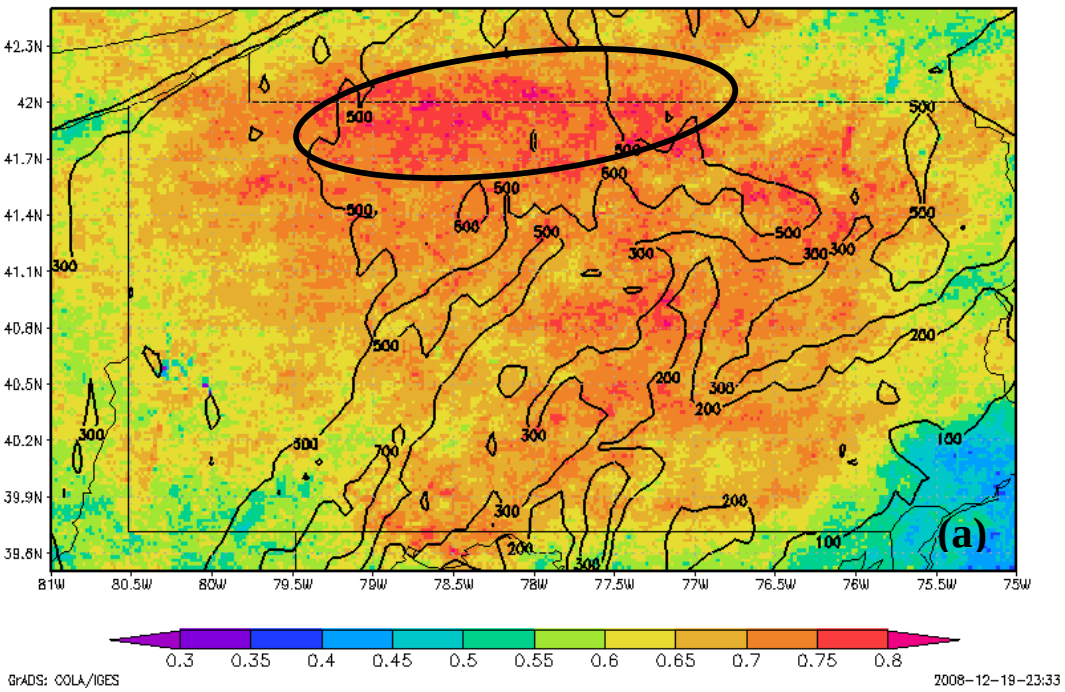

Figure 35.(a) Fraction of 45+dBZ occurrences occurring on severe weather days for forecast office CTP (State College, PA) during the 1996-2007 warm seasons. Oval indicates convective maxima along terrain features.

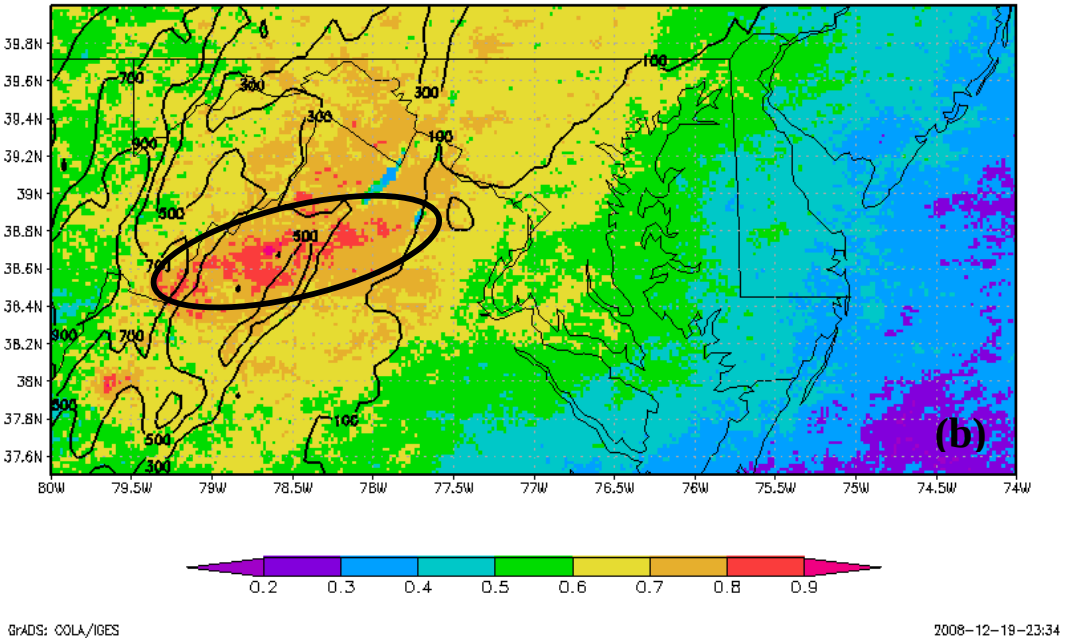

Figure 35. (b) Fraction of 45+dBZ occurrences occurring on severe weather days for forecast office LWX (Sterling, VA) during the 1996-2007 warm seasons. Oval indicates convective maxima along terrain features.

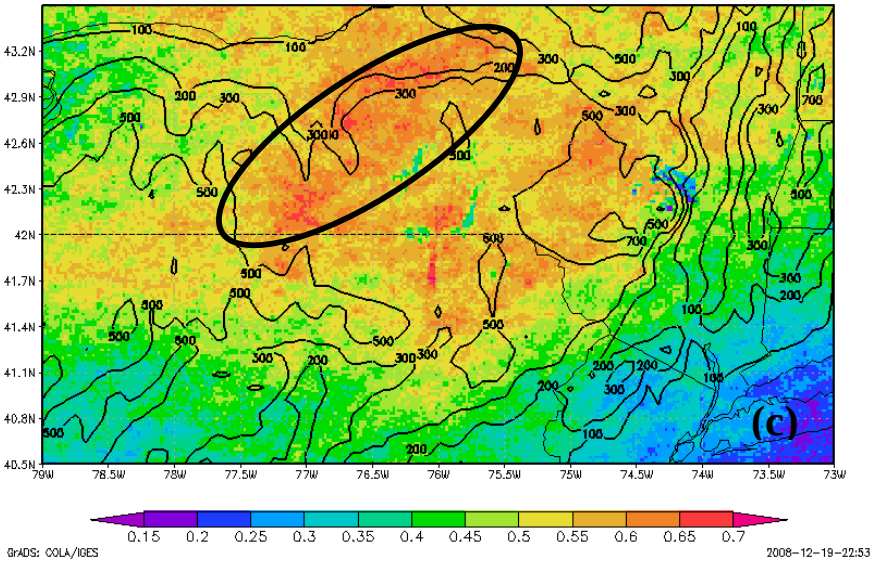

Figure 35. (c) Fraction of 45+dBZ occurrences occurring on severe weather days for forecast office BGM (Binghamton, NY) during the 1996-2007 warm seasons. Oval indicates convective maxima along terrain features.

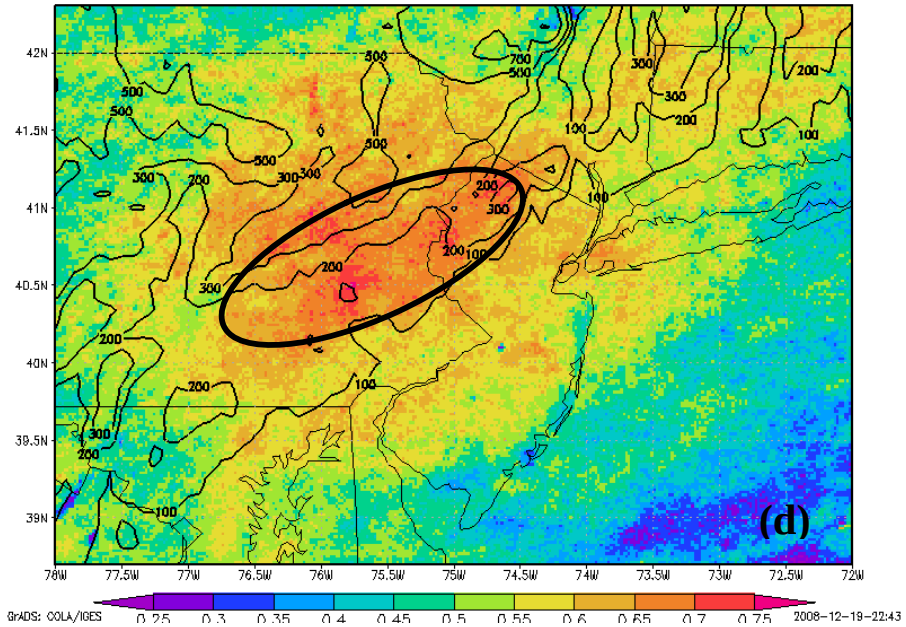

Figure 35. (d) Fraction of 45+dBZ occurrences occurring on severe weather days for forecast office PHI (Mount Holly, NJ/Philadelphia PA) during the 1996-2007 warm seasons. Oval indicates convective maxima along terrain features.

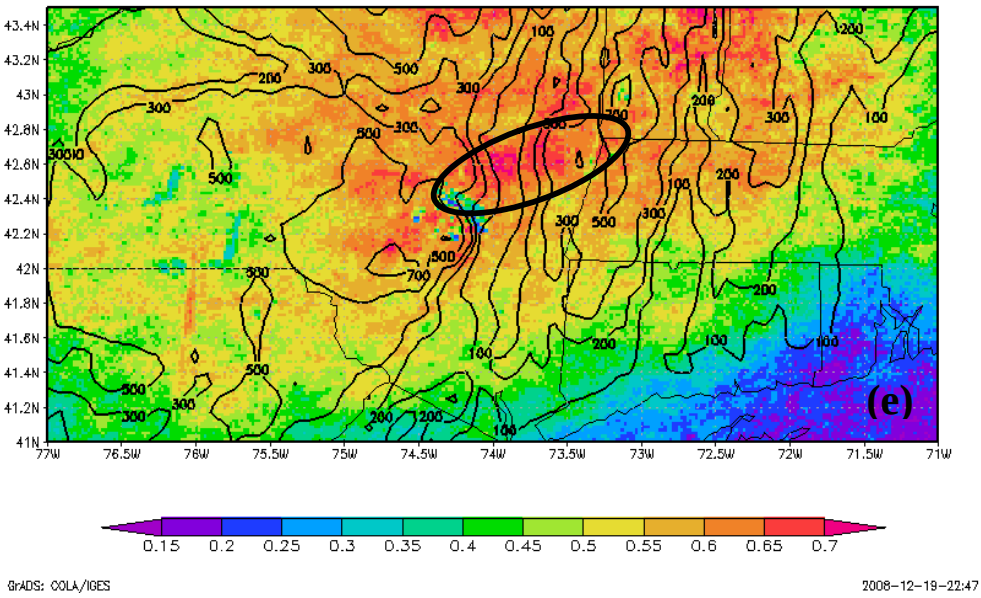

Figure 35. (e) Fraction of 45+dBZ occurrences occurring on severe weather days for forecast office ALY (Albany, NY) during the 1996-2007 warm seasons. Oval indicates convective maxima along terrain features.

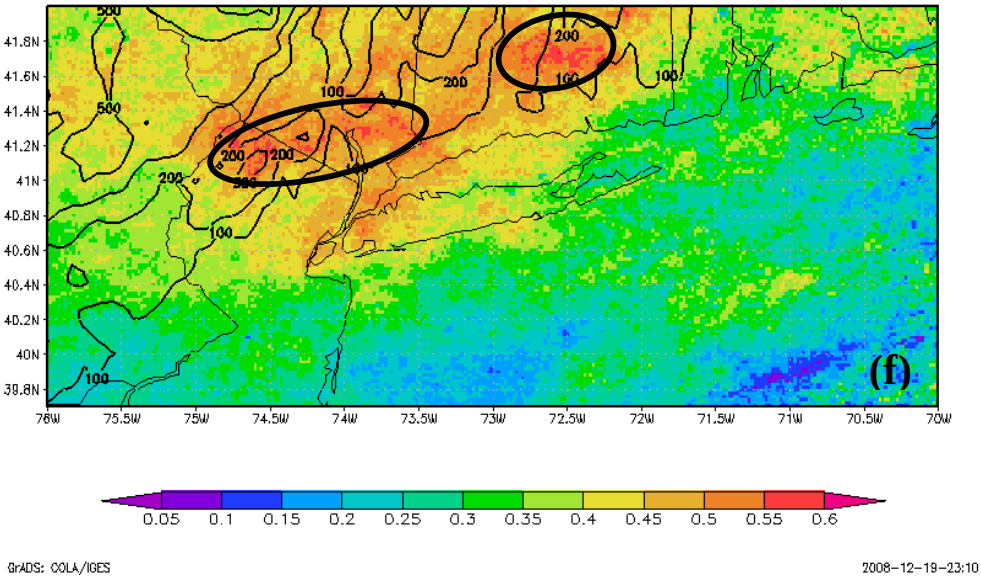

Figure 35. (f) Fraction of 45+dBZ occurrences occurring on severe weather days for forecast office OKX (New York, NY) during the 1996-2007 warm seasons. Oval indicates convective maxima along terrain features.

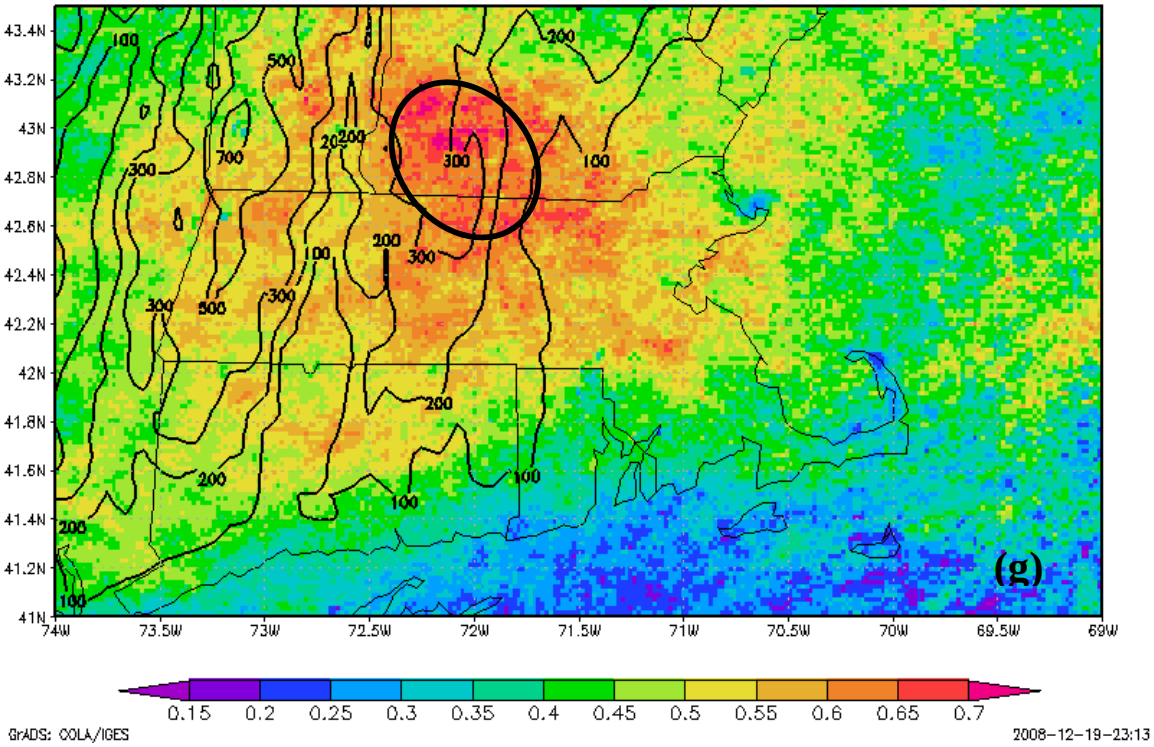

Figure 35. (g) Fraction of 45+dBZ occurrences occurring on severe weather days for forecast office BOX (Taunton, MA) during the 1996-2007 warm seasons. Oval indicates convective maxima along terrain features.

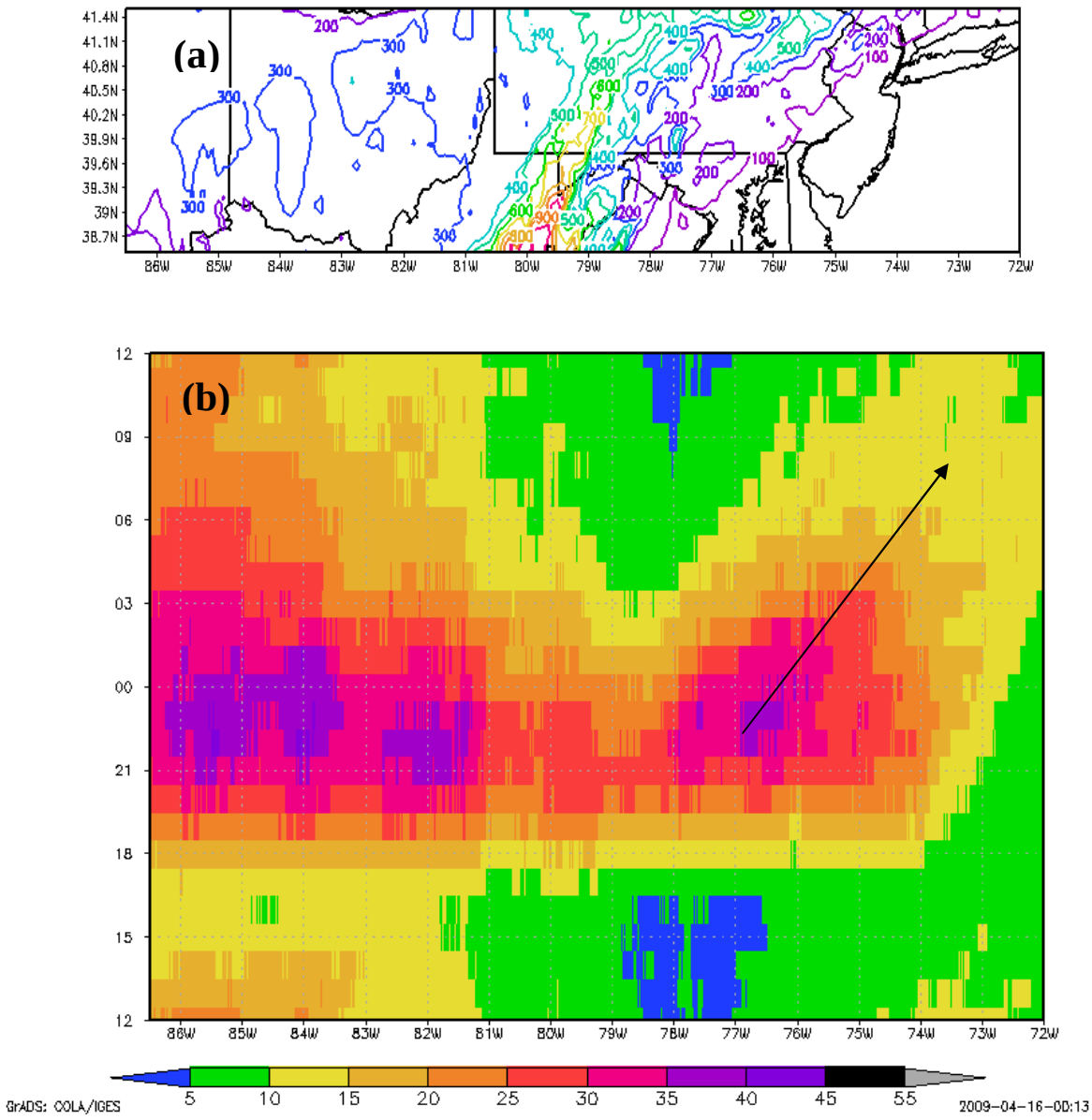

Figure 36. (a) 5 minute topography (every 100 m) from 38.5º N to 41.5ºN and from -86.4ºW to -72ºW. (b) Average echo frequency of 45+dBZ as a function of longitude and time (hovmoller diagram). Arrow pointing to the northeast indicates some propagation towards the later evening hours towards the coast.

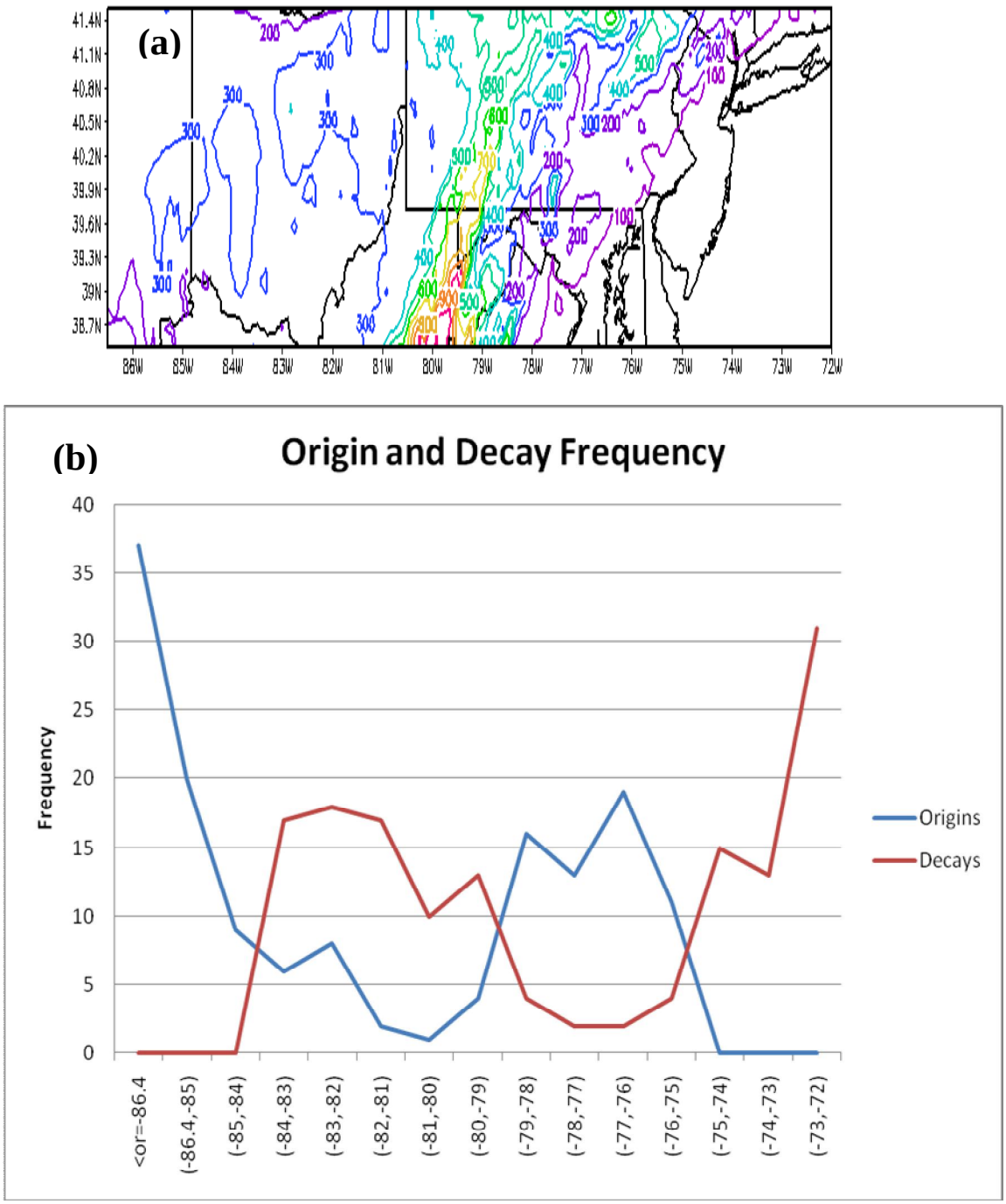

Figure 37. The sum of the starting (genesis) and ending (decay) of convection for 1º width longitudinal bands across 38.5º N to 41.5ºN from -86.4ºW to -72ºW.

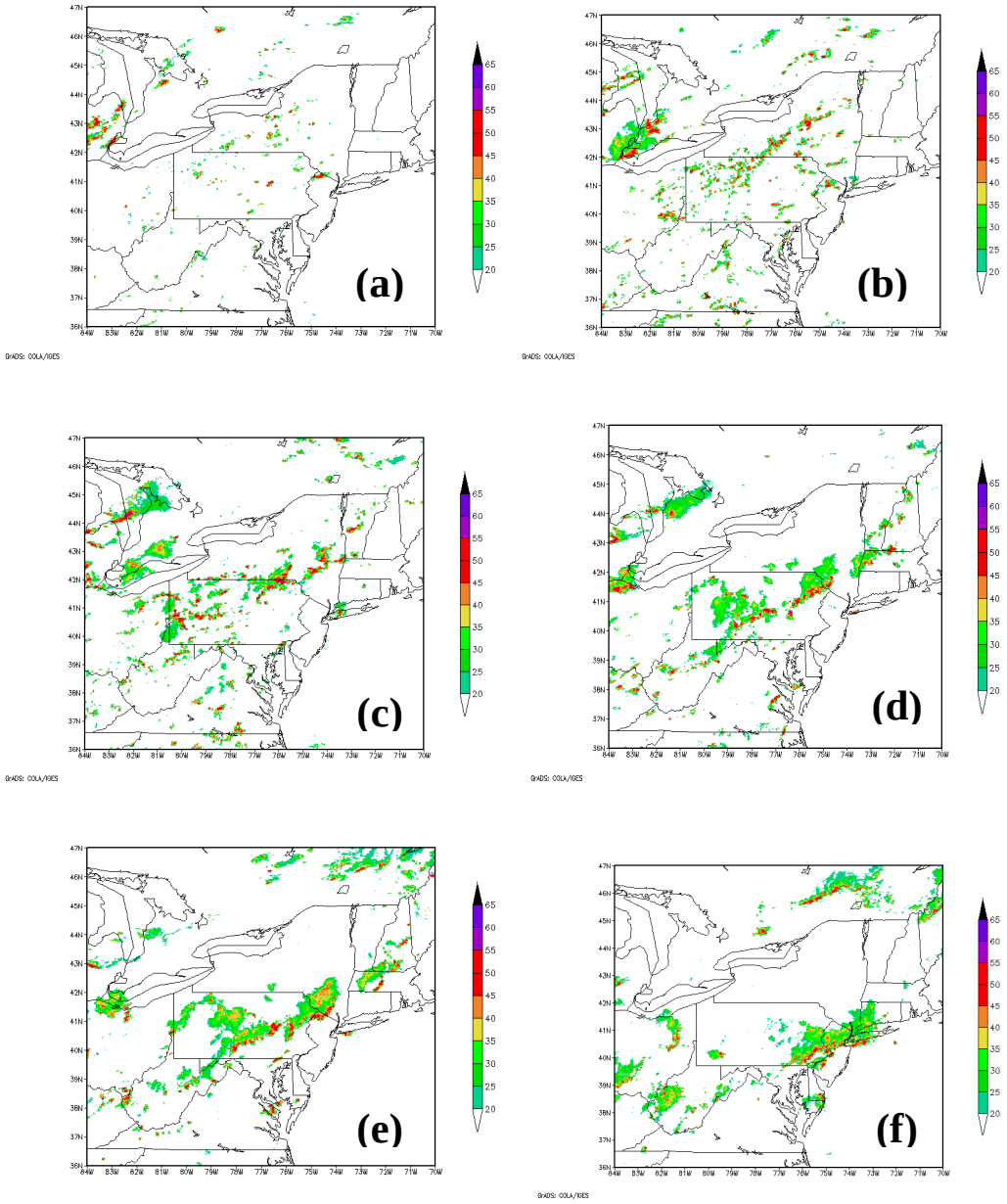

Figure 38. Composite reflectivity (shaded every 5 dBZ) images for the squall lines on 27 and 28 June 2007 at, (a) 17 UTC 27 June, (b) 19 UTC 27 June, (c) 21 UTC 27 June, (d) 23 UTC 27 June, (e) 01 UTC 28 June, and (f) 03 UTC 28 June.

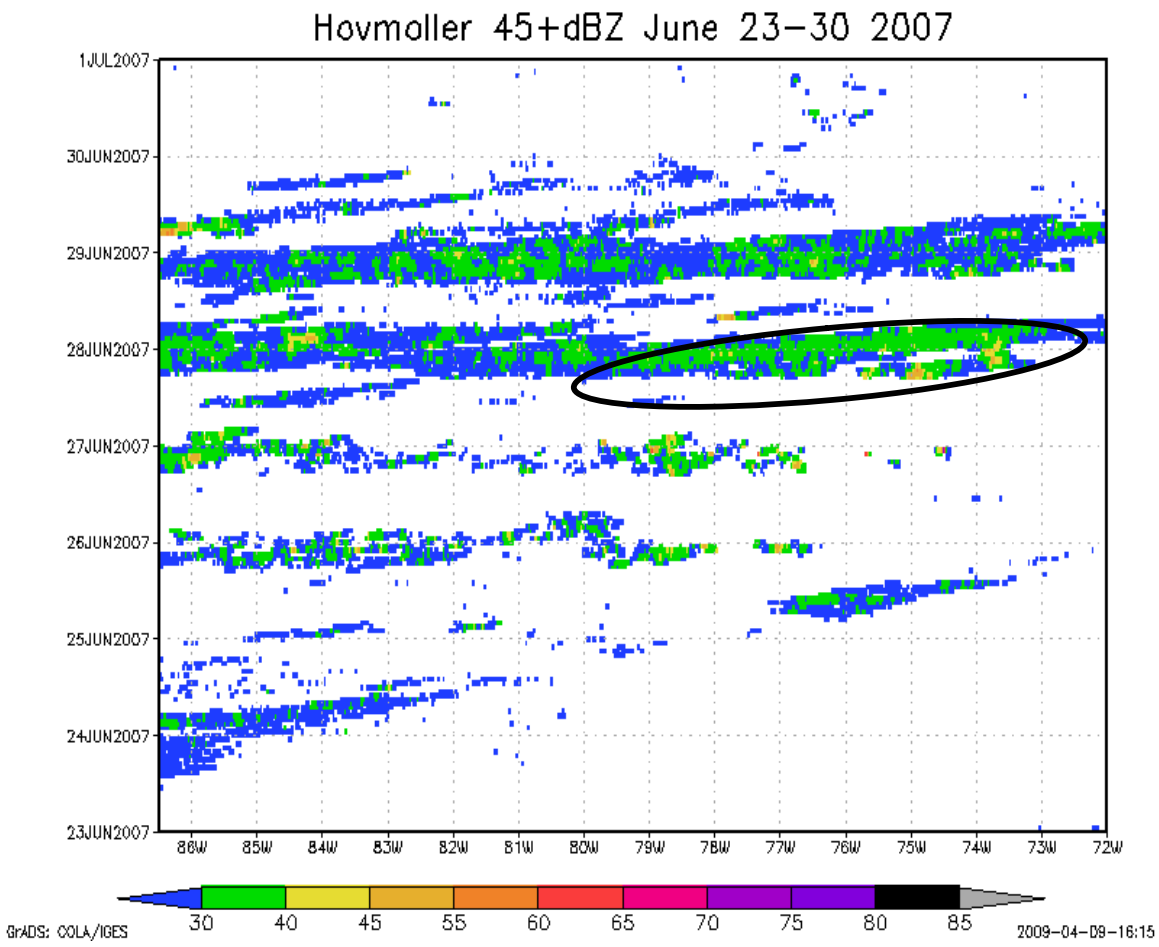

Figure 39. Hovmoller plot showing the echo frequency of 45+ dBZ for 23-30 June 2007. The object identified with the oval indicates the organized convection seen on figure 38.

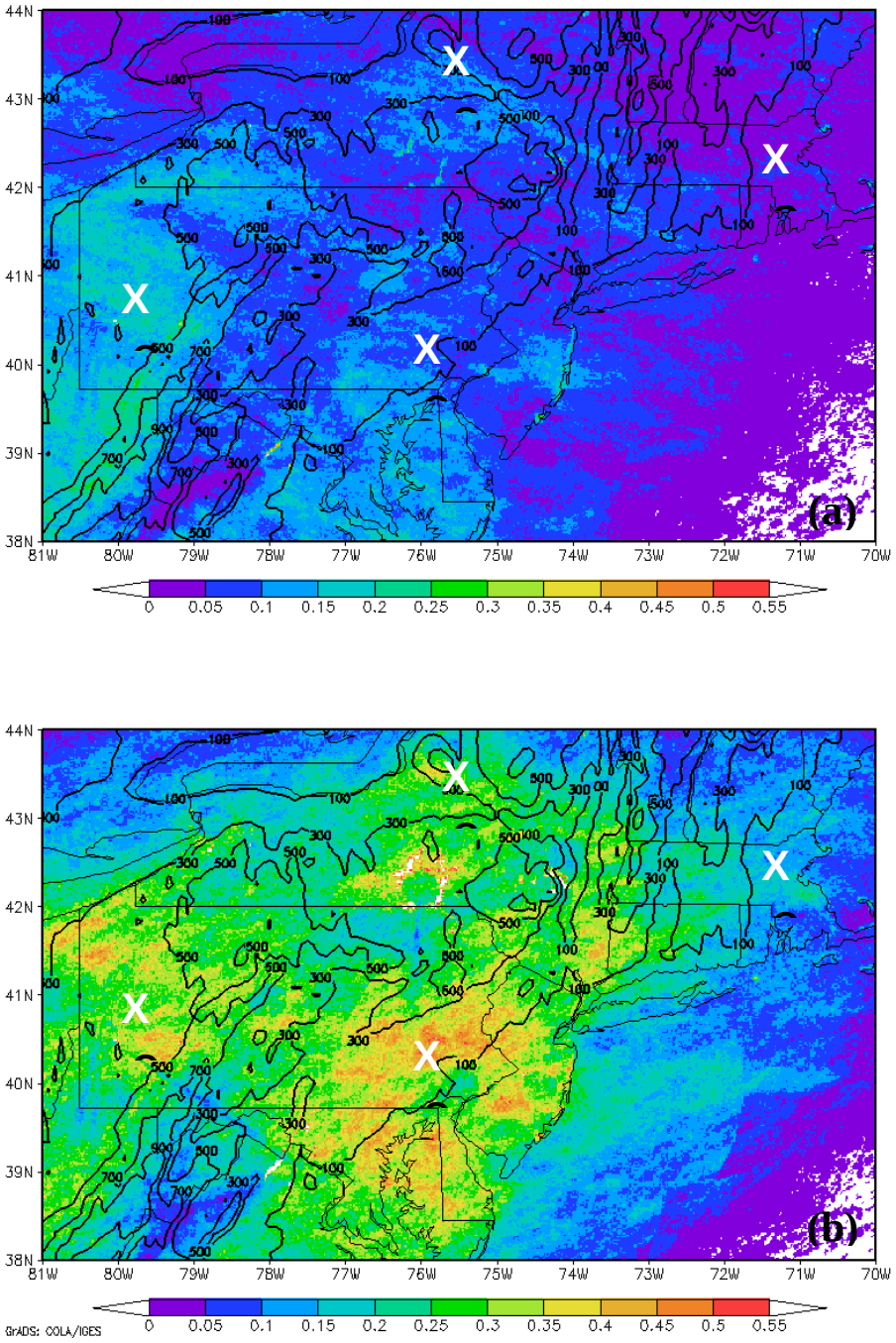

Figure 40. Pr_{storm} for all hours using the sampled NARR winds at 500 hPa for the 4 points in Fig. 9 for the (a) west to northwest (270º-315º) wind direction and (b) southwest to west (225º-270º) wind regime.

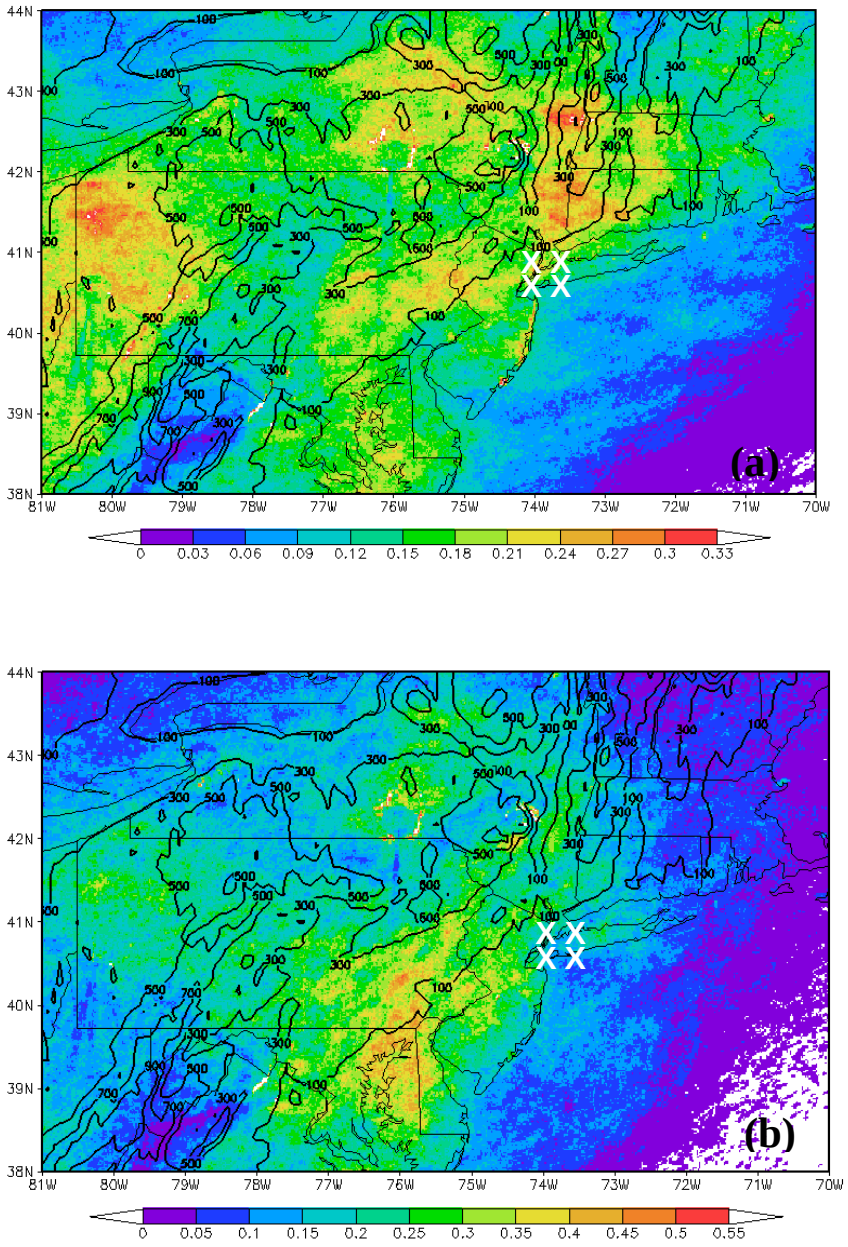

Figure 41. Pr_{storm} for all hours using the sampled NARR winds at 925 hPa for the 4 points in Fig. 9 for the (a) southwest to northwest (225º-315º) wind regime and for the (b) southeast to southwest (145º-225º) wind regime.

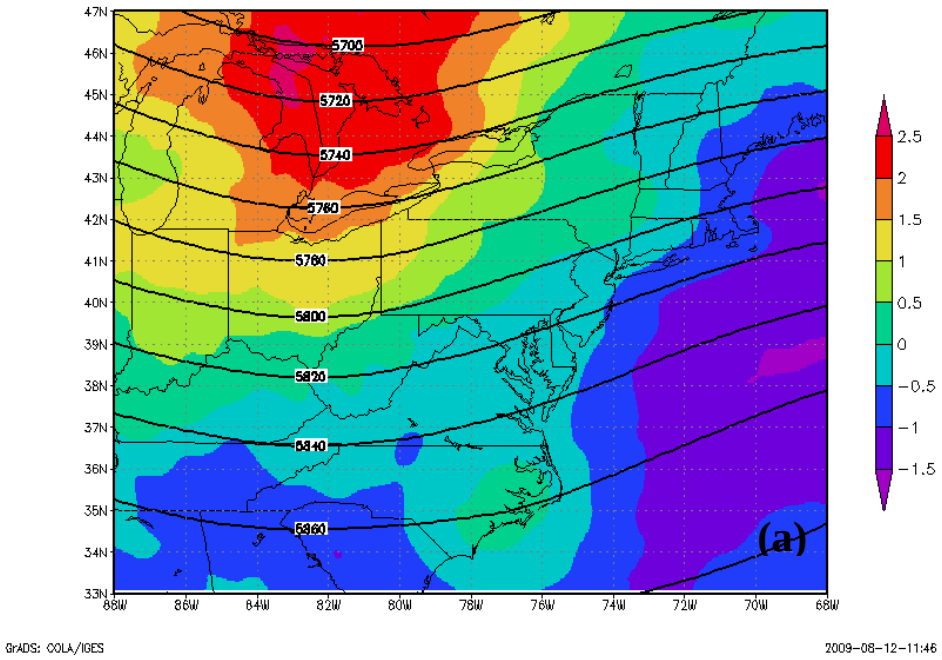

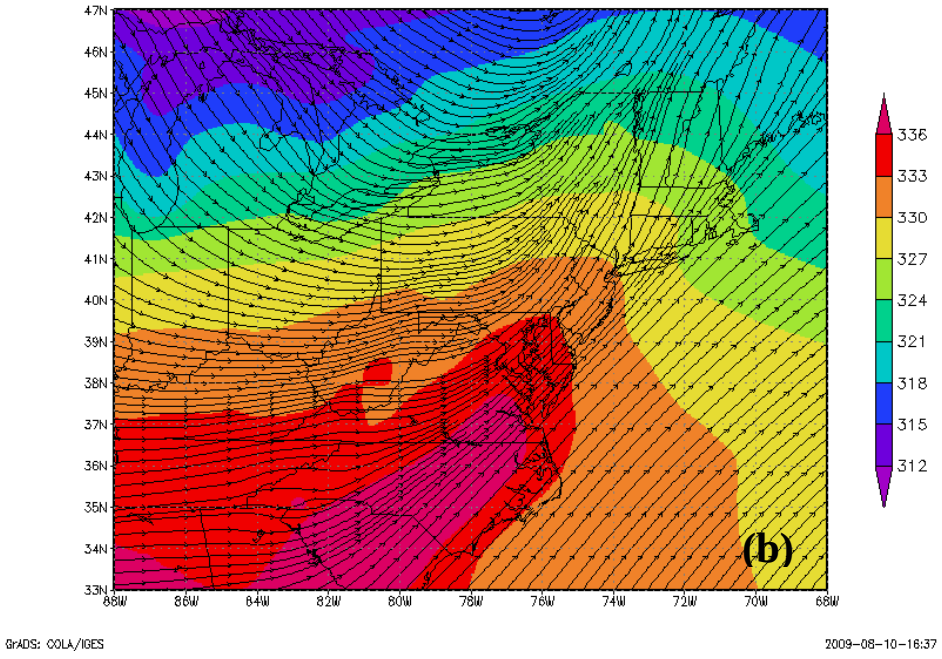

Figure 42. (a) 500-hPa geopotential height (contoured every 20 m) with absolute vorticity (x 10^{-5}) (shaded 0.5 x 10^{-5} s^{-1}) and (b) 925 hPa equivalent potential temperature Θ_e (shaded every 3 K) with streamlines at 925 hPa shown for all days with widespread convection across the domain that is greater than 1 standard deviation of the areal mean.

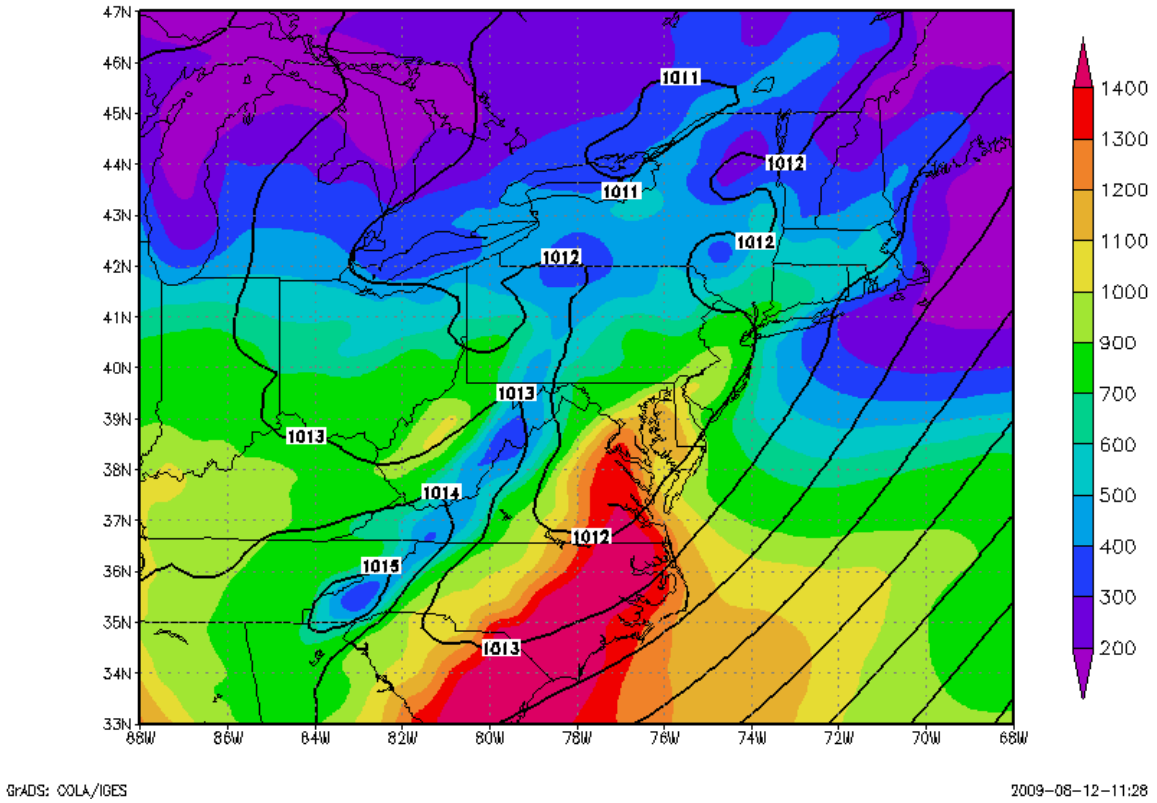

Figure 43. Mean sea level pressure (MSLP; contoured every 1 hPa) and average low level (0-180 hPa above the ground) CAPE (shaded every 100 J kg^{-1}) across the Northeast U.S. for all times of widespread convection across the domain that is greater than 1 standard deviation of the areal mean.

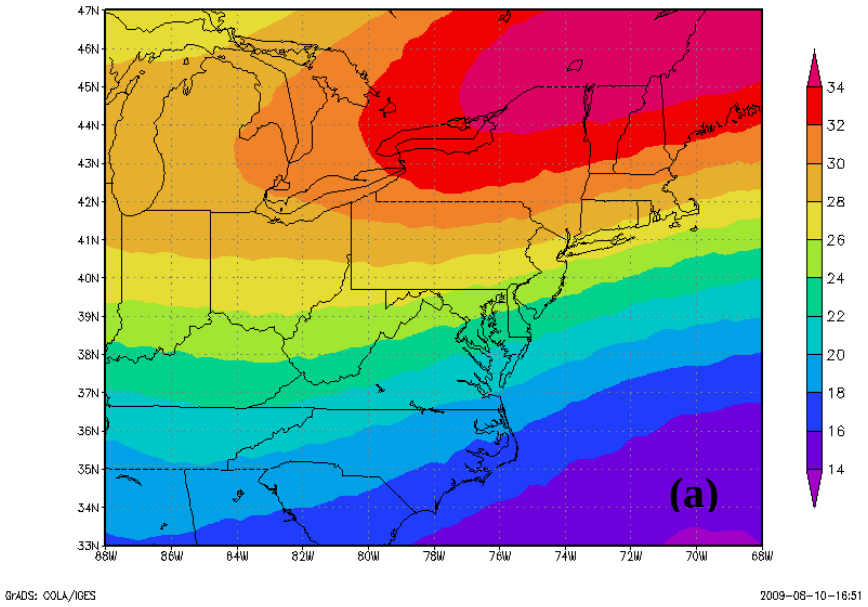

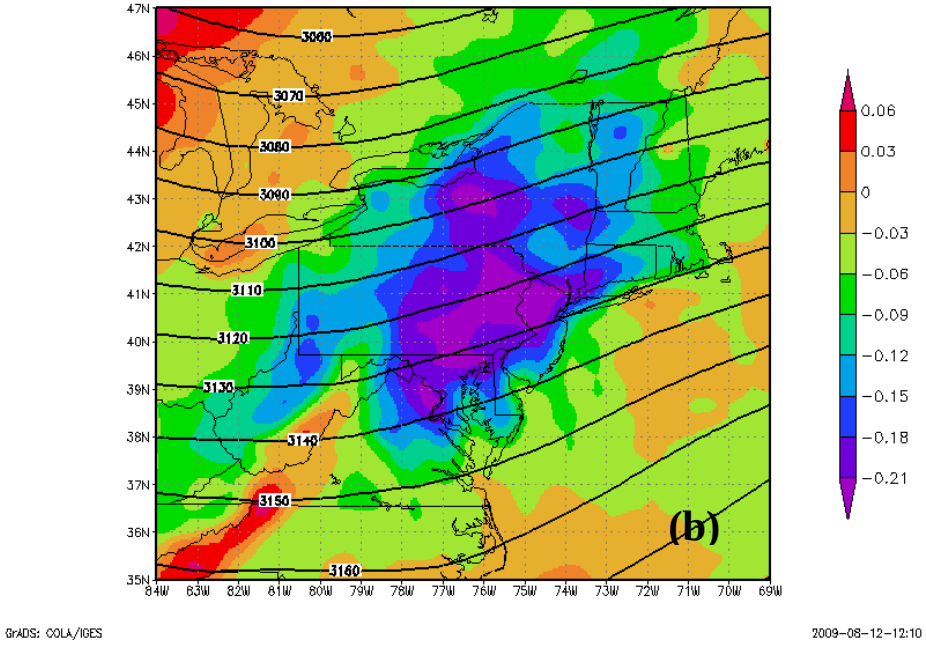

Figure 44. (a) Averaged 200 hPa wind speed (shaded every 2 m s^{-1}) across the Northeast U.S. for all times of widespread convection across the domain that is greater than 1 standard deviation of the areal mean and (b) averaged vertical velocity (shaded every 0.03 Pa s^{-1}) at 700 hPa for all days with widespread convection across the domain that is greater than 1 standard deviation of the areal mean.

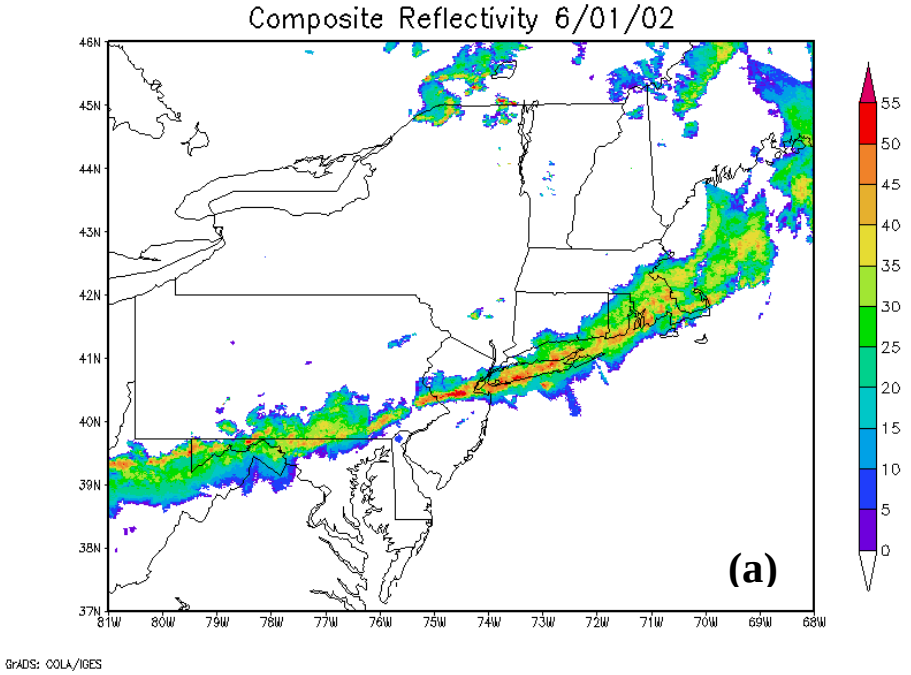

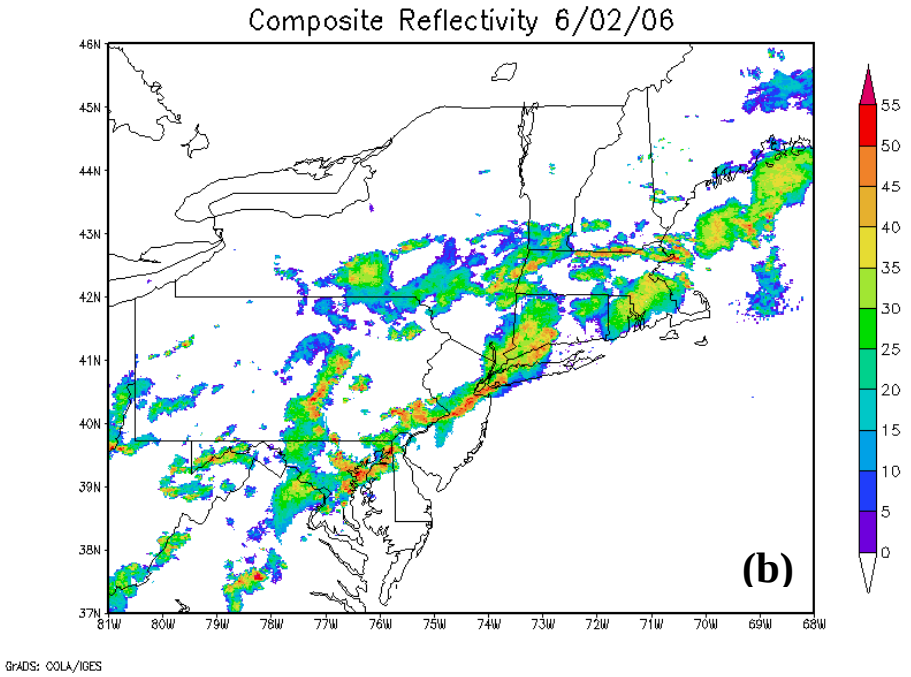

Figure 45. Composite reflectivity for two squall line cases (a) 0100 UTC on 1 June 2002 and (b) 0015 UTC on 2 June 2006.

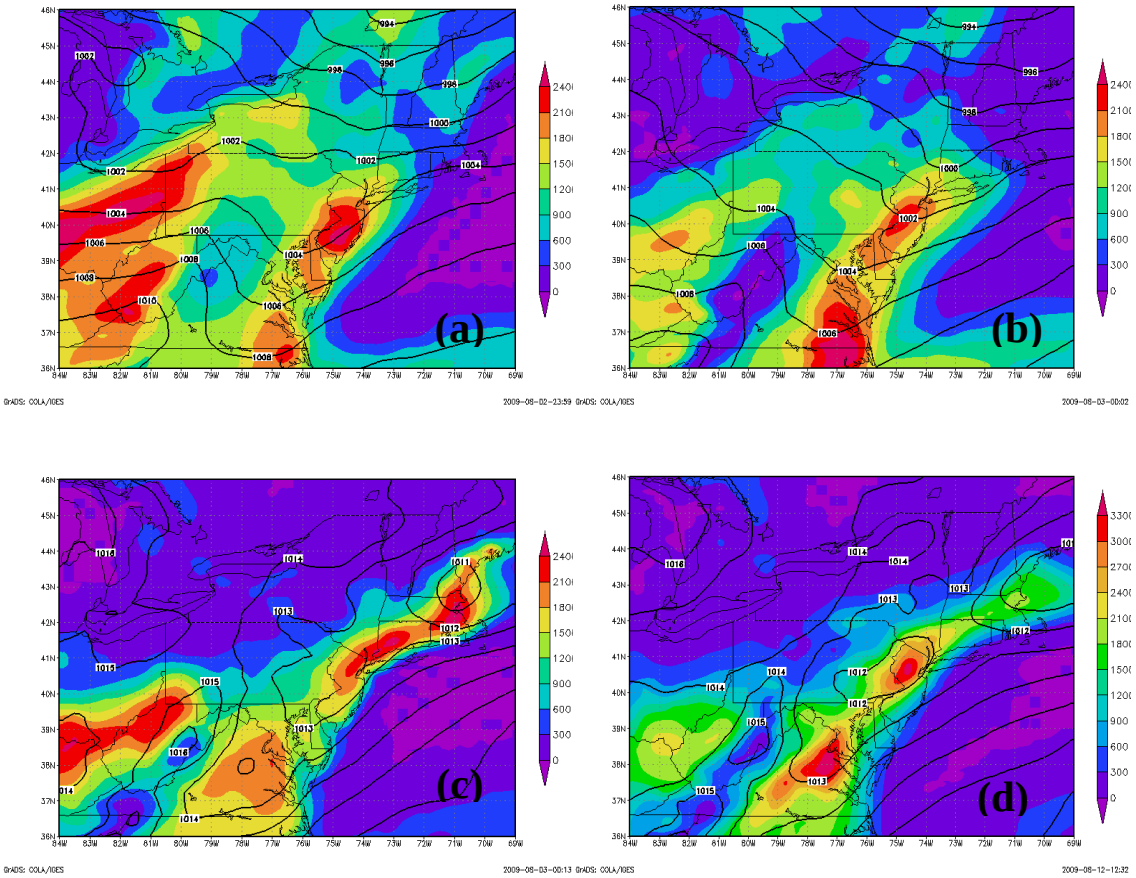

Figure 46. MSLP (contoured every 2 hPa) and Surface CAPE (shaded every 300 J kg^{-1}) for (a) 21 UTC 31 May 2002 (b) 00 UTC 1 June 2002 and MSLP (contoured every 1 hPa) and Surface CAPE (shaded every 300 J kg^{-1}) (c) 21 UTC 1 June 2006 (d) 00 UTC 2 June 2006.

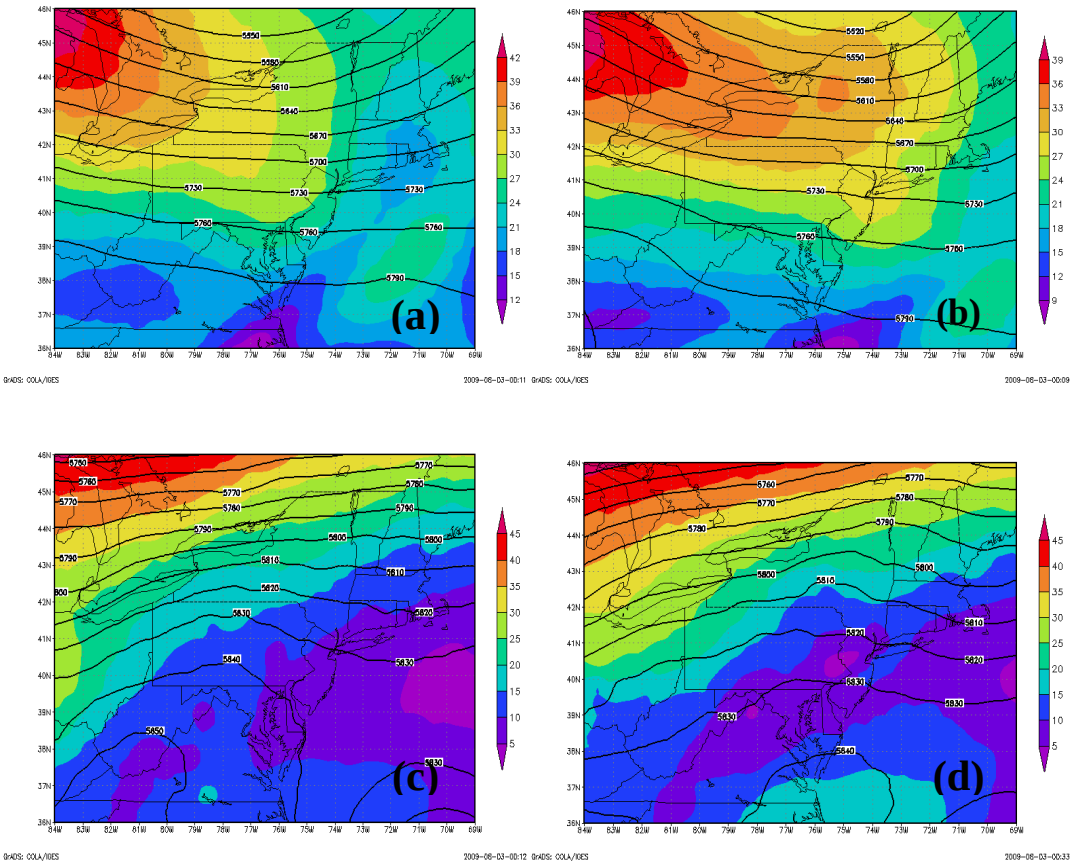

Figure 47. 500-hPa geopotential height (solid contours every 30 m) at 500 hPa and Wind Speed at 200 hPa (shaded every 3 m s^{-1}) for (a) 21 UTC 31 May 2002 (b) 00 UTC 1 June 2002 and 500-hPa geopotential height (solid contours every 10 m) and Wind Speed at 200 hPa (shaded every 5 m s^{-1}) for (c) 21 UTC 1 June 2006 (d) 00 UTC 2 June 2006.

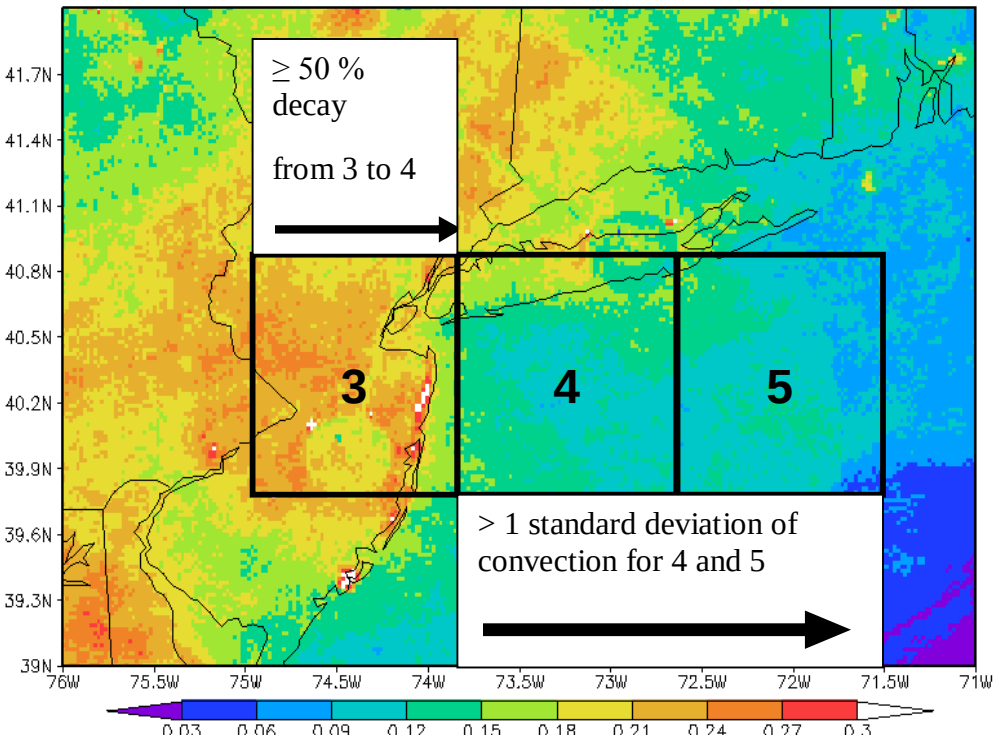

Figure 48. 1° latitude x 1° longitude boxes used for areal sums of convection in Fig. 8. The top text box describes the first scenario for days in which box 3 has convection that is at least 50 % more than the convection in box 4. The bottom text box describes the second scenario for days in which both box 4 and box 5 have greater than 1 standard deviation of their respective means.

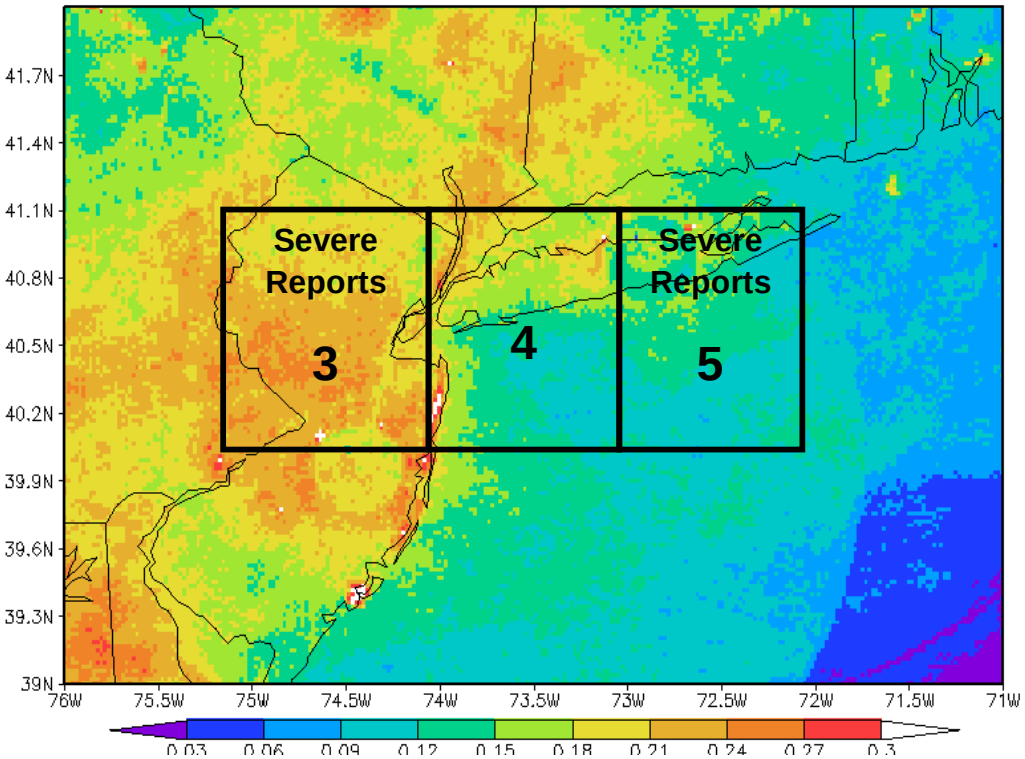

Figure 49. 1° latitude x 1° longitude boxes used for areal sums of convection in Fig. 8. Severe reports are counted within the area of each box between the warm seasons 1996-2007 exclusive for each of the boxes.

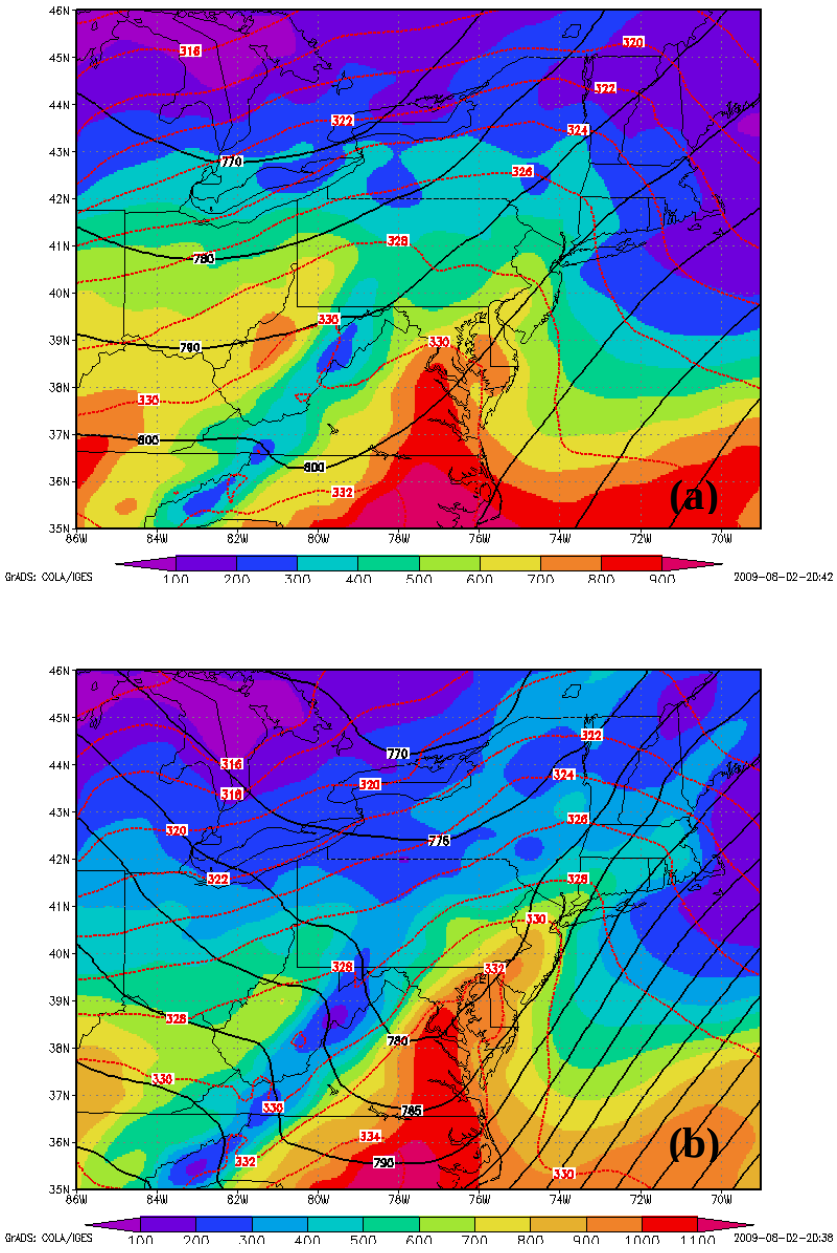

Figure 50. Composite for the scenario in which convection decays going from Box 3 (Northern New Jersey) to Box 4 (New York City and Western Long Island), (a) 925 hPa geopotential height (solid contours every 10 m) , θ_e (red dashed every 2 K), and average CAPE between 0 and 180 hPa above the surface (shaded every 100 J kg^{-1}) 12 hours before the peak hour of convection and (b) same as (a) but at the peak hour of convection and for the 925 geopotential height (solid contours every 5 m).

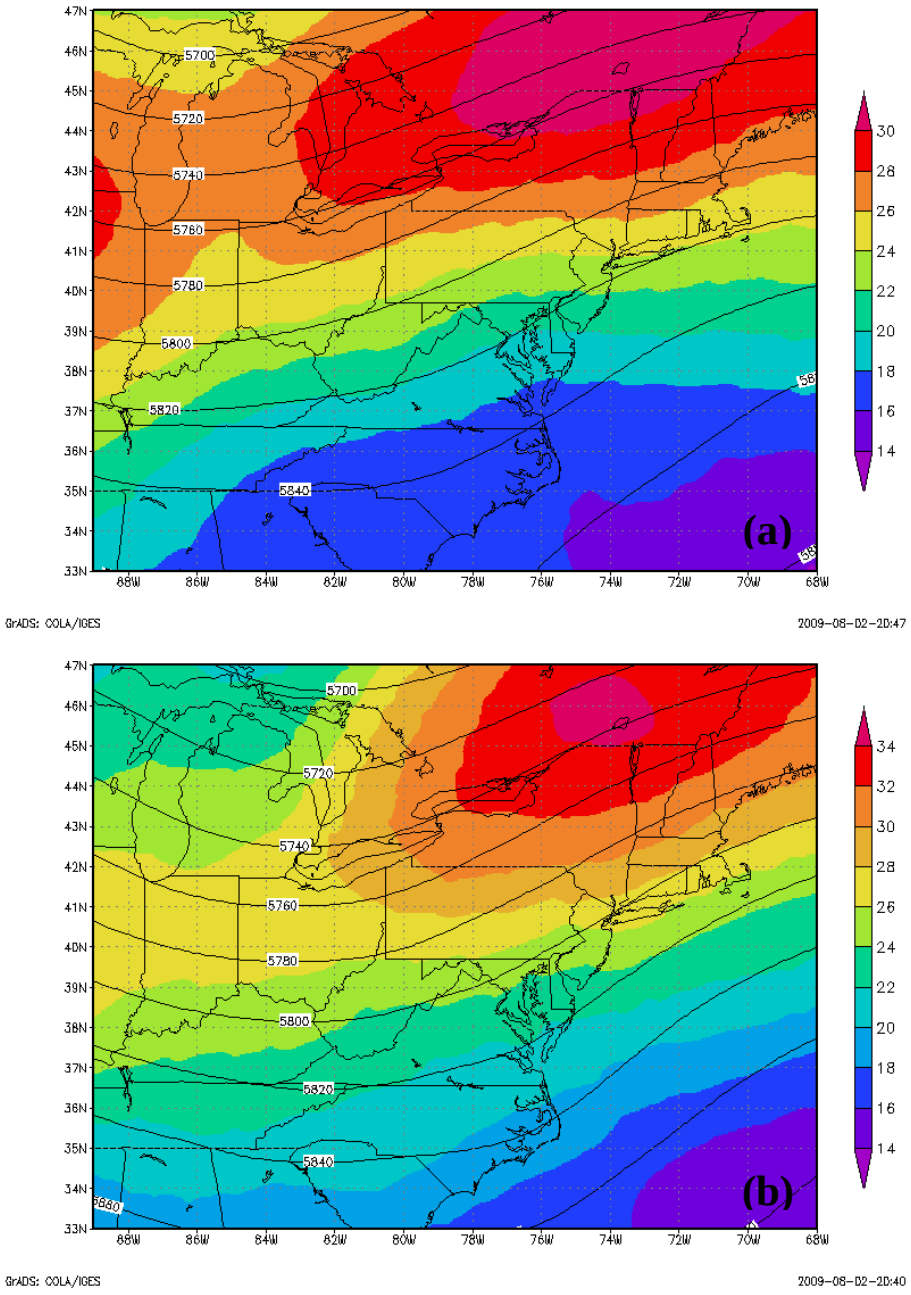

Figure 51. Same as Fig. 50 except for (a) geopotential height at 500 hPa (solid contours every 20 m) and wind speed at 200 hPa (shaded every 2 m s^{-1}) 12 hours before the peak hour of convection and (b) same as (a) but at the peak hour of convection.

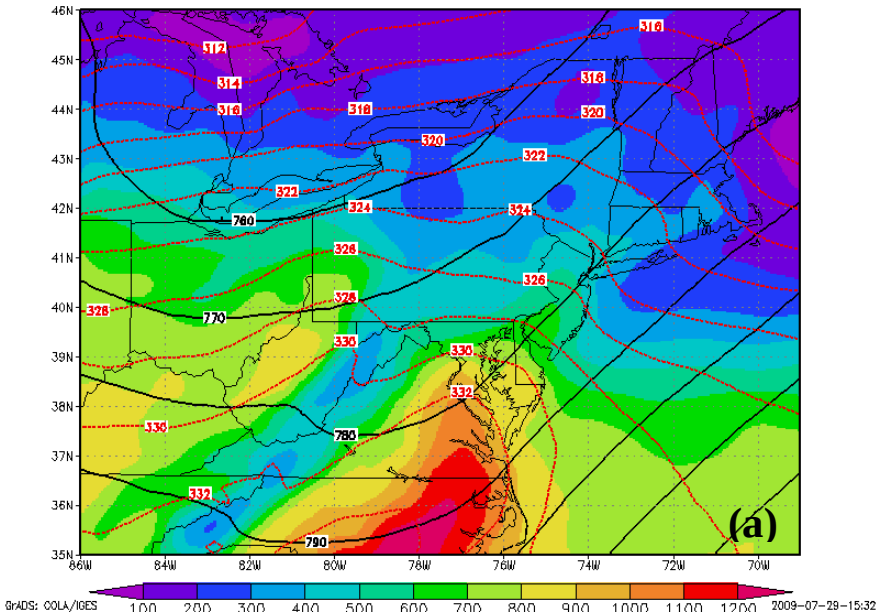

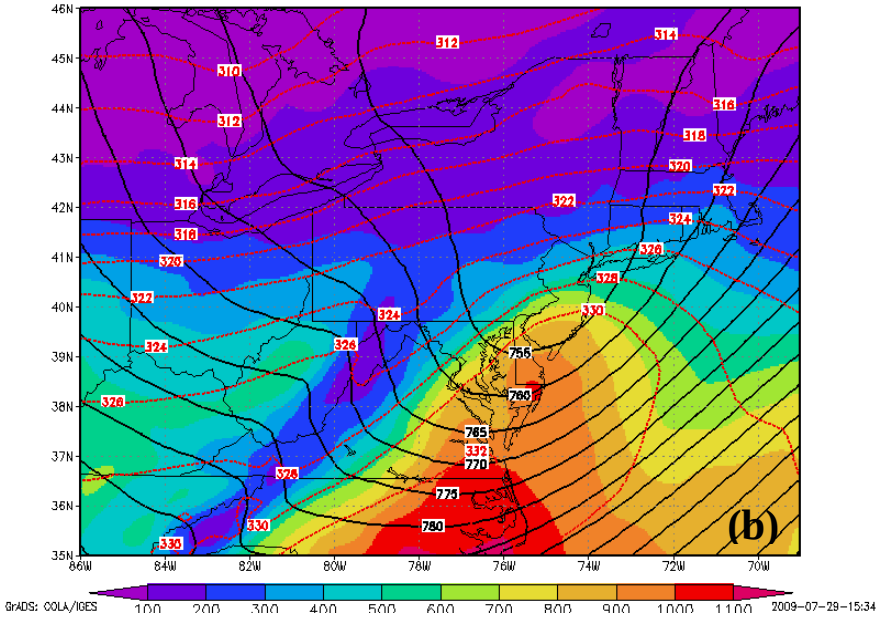

Figure 52. Same as Fig. 50 except for the scenario in which convection in Box 4 (New York City and Western Long Island) and Box 5 (Eastern Long Island) is greater than 1 standard deviation of each of their means.

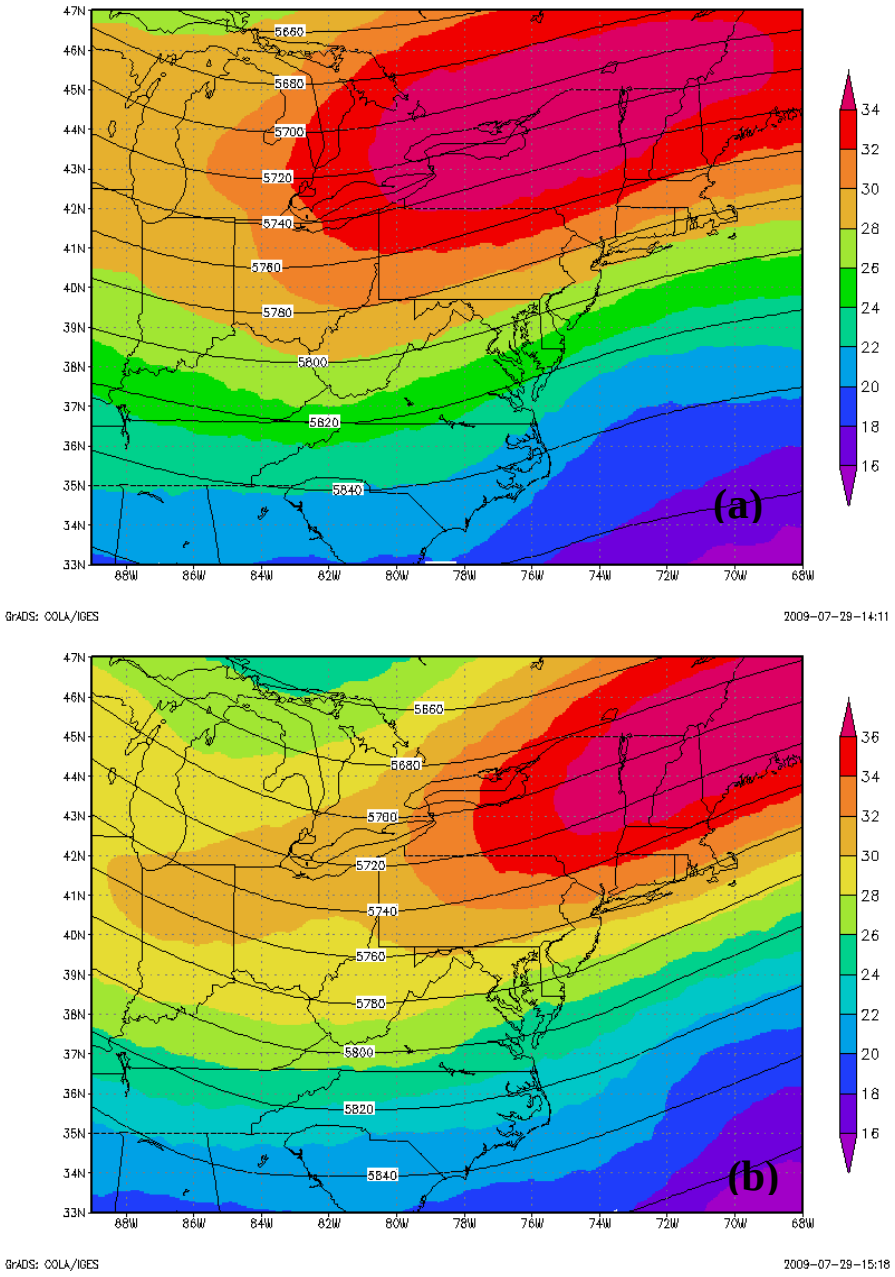

Figure 53. Same as Fig. 51 except for the scenario in which convection in Box 4 (New York City and Western Long Island) and Box 5 (Eastern Long Island) is greater than 1 standard deviation of each of their means.

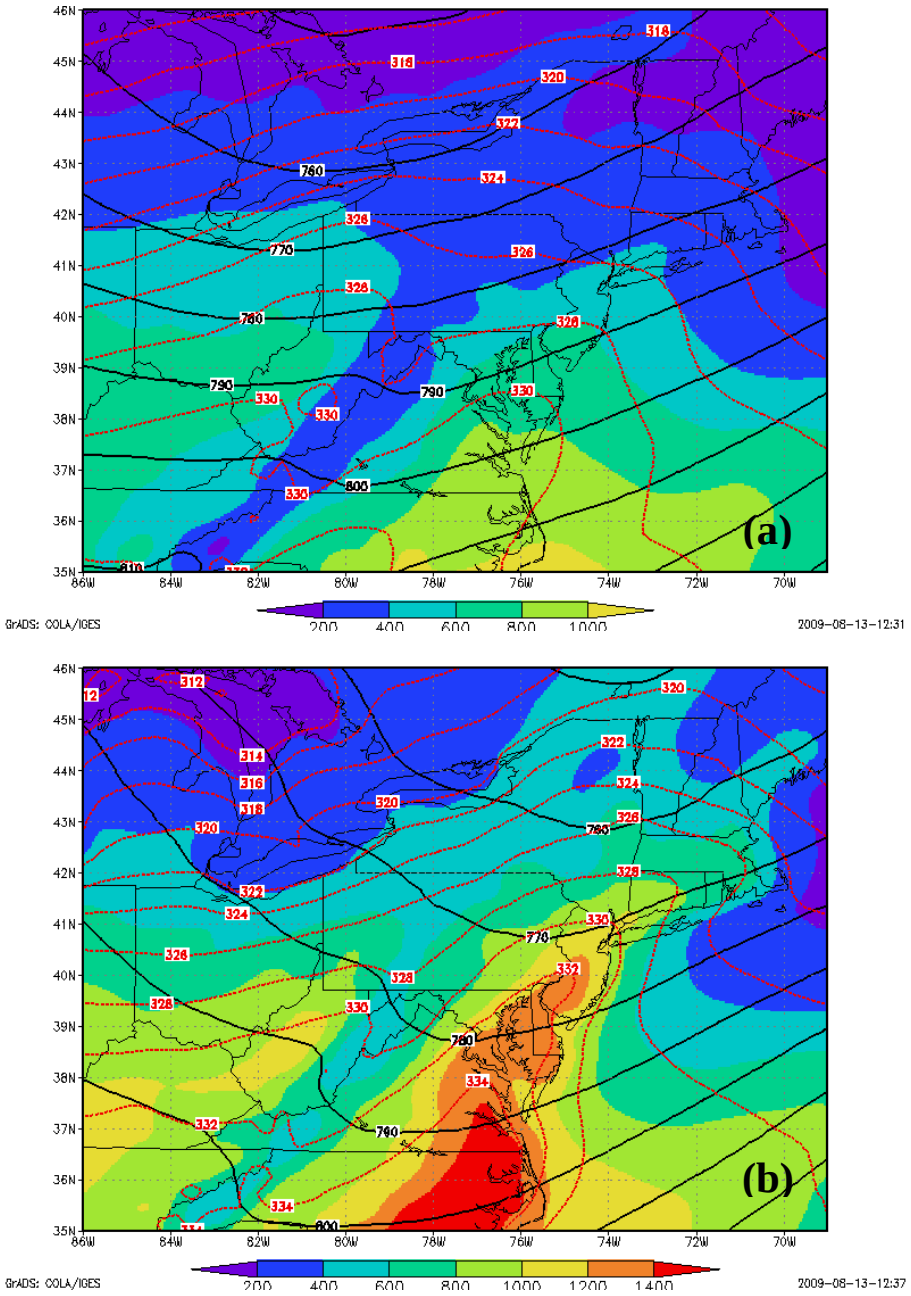

Figure 54. Composite for all severe weather reports for the warm seasons of 1996 through 2007 for northern New Jersey and not eastern Long Island showing, (a) 925 hPa geopotential height (solid contours every 10 m), θ_e (red dashed every 2 K), and average low level CAPE between 0 and 180 hPa above the surface (shaded every 200 J kg^{-1}) 12 hours before the time of the severe report and (b) same as (a) but at the time of the severe report.

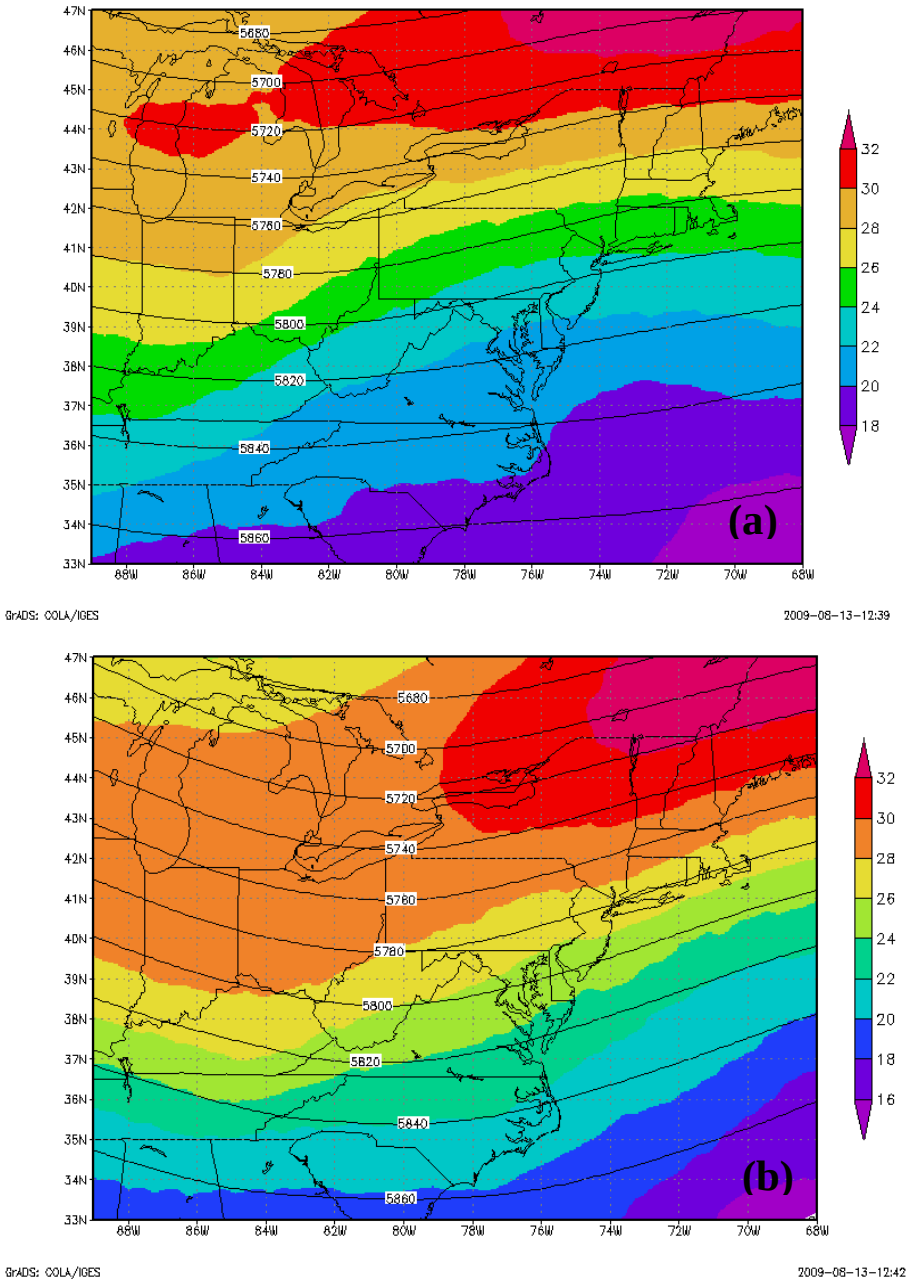

Figure 55. Composite for all severe weather reports during the warm seasons of 1996 through 2007 for northern New Jersey and not eastern Long Island showing, (a) geopotential height at 500 hPa (solid contours every 20 m) and wind speed at 200 hPa (shaded every 2 m s^{-1}) 12 hours before the severe report and (b) same as (a) but at the time of the severe report.

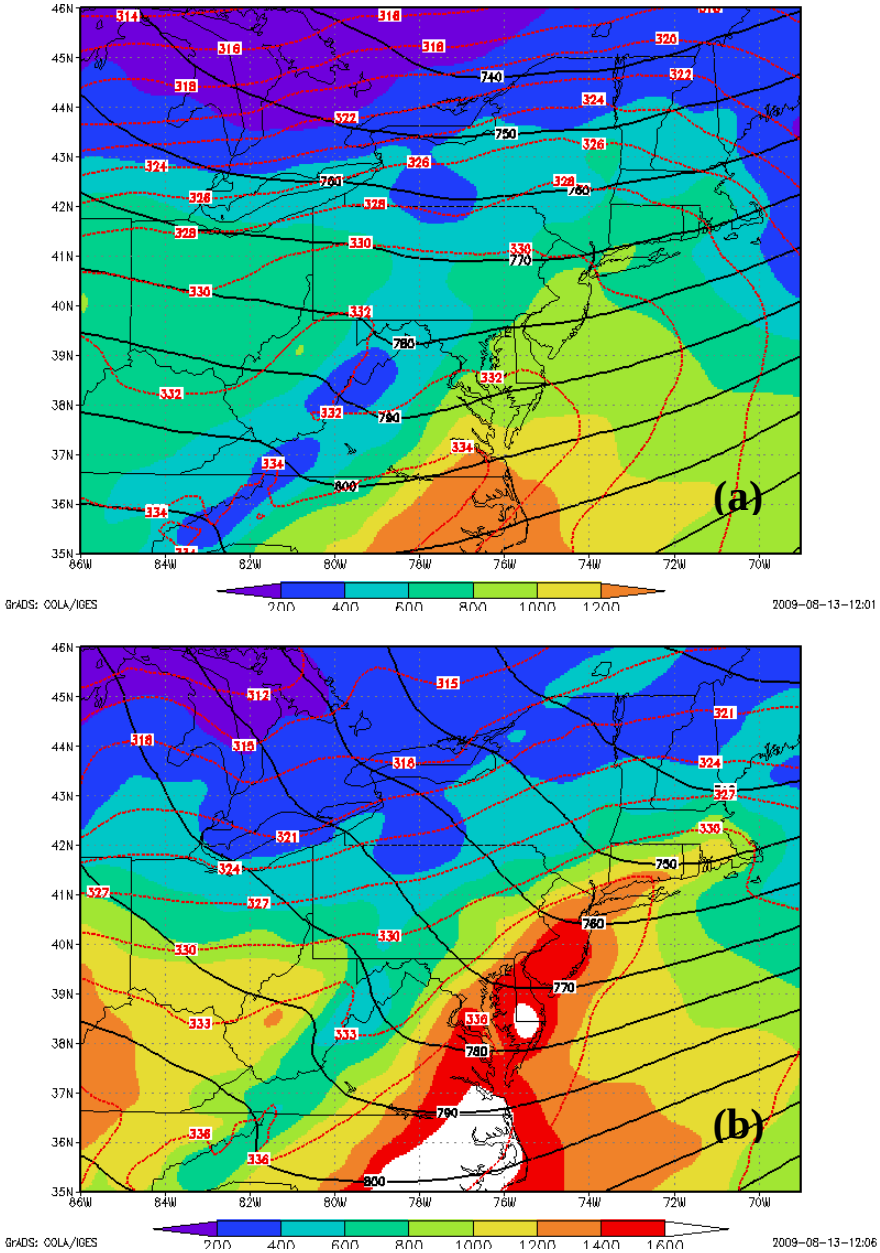

Figure 56. Same as Fig. 54 except for all severe weather reports during the warm seasons of 1996 through 2007 for eastern Long Island.

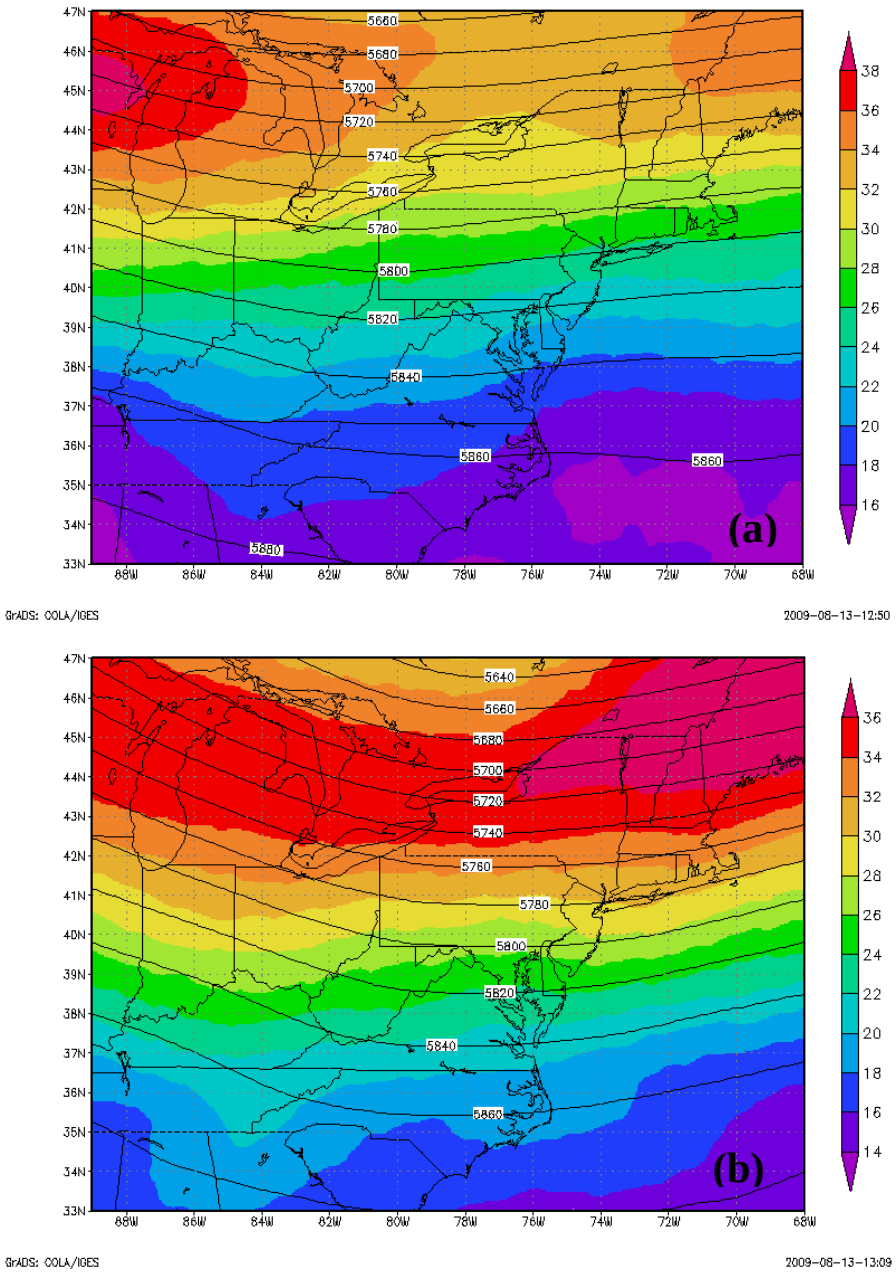

Figure 57. Same as Fig. 55 except for all severe weather reports during the warm seasons of 1996 through 2007 for eastern Long Island.

References

Allan, S.S., J.A. Beesley, J.E. Evans, and S.G. Gaddy. "Analysis of Delay Causality at Newark International Airport." 4th USA/Europe Air Traffic Management R&D Seminar, Santa Fe, New Mexico, December 2001.

Banacos, P and M. Ekster. "Elevated Mixed Layers and their Role in Significant Severe Thunderstorm Episodes in the Northeastern U.S." 1-2 Nov 2005. Online Powerpoint. Seventh Northeast Regional Operational Workshop. 10 Jan 2008. http://cstar.cestm.albany.edu/nrow/nrow7/Ekster%5CEML_Ekster.ppt#267,1,Elevated Mixed Layers and their Role in Significant Severe Thunderstorm Episodes in the Northeastern U.S.

Bornstein, R.D. and Q. Lin, 2000: Urban Heat Island and Summertime Convective Thunderstorms in Atlanta: Three Case Studies. *Atmospheric Environment*. **34**, 507-516.

Bosart L. F., A. Seimon, K. D. Lapenta, and M. J. Dickinson, 2006: Supercell Tornadogenesis over Complex Terrain: The Great Barrington, Massachusetts, Tornado on 29 May 1995. *Weather and Forecasting*. **21**, 897-922.

Cannon, John W, 2002: Characteristics of Recent Northern New England Tornadoes. *Eastern Region Technical Attachment*. **2002-04**, 1-16.

Carbone R. E., J. D. Tuttle, D. A. Ahijevych, and S. B. Trier, 2002: Inferences of Predictability Associated with Warm Season Precipitation Episodes. *Journal of the Atmospheric Sciences*. **59**, 2033-2056.

Changnon S. A., R. G. Semonin, and F.A. Huff, 1976: A Hypothesis for Urban Rainfall Anomalies. *Journal of Applied Meteorology*. **15**, 544-560.

Christian, Hugh J and M. A. McCook. "Lightning and Atmospheric Electricity Research at GHCC." NASA/Marshal Space Flight Center. 04 Aug 2009. http://thunder.msfc.nasa.gov/primer/primer4.html

Croft, P.J. and Shulman, M.D., 1989: A Five-Year Radar Climatology of Convective Precipitation for New Jersey. *International Journal of Climatology*. **9**, 581-600.

David, C. L., 1976: A Study of Upper Air Parameters at the Time of Tornadoes. *Monthly Weather Review*. **104**, 546-551.

Doswell III, C., H.E. Brooks, and M. Kay, 2005: Climatological Estimates of Daily Local Nontornadic Severe Thunderstorm Probability for the United States. *Weather and Forecasting*. **20**, 577-595.

Doswell III, C., 2001. Severe Convective Storms – An Overview. In C. Doswell III (Ed.) *Severe Convective Storms* (p. 13). Boston, MA: American Meteorological Society.

Doty, Brian,1995. The Grid Analysis and Display System (GrADS) V1.5.1.12. User manual.

Evans, J.E. Robinson, M. Allan S., 2005: Quantifying Convective Delay Reduction Benefits for Weather/ATM Systems. *6th USA/Europe Air Traffic Management R&D Seminar, Baltimore MD*.

Falconer, P. D., 1984: A Radar-Based Climatology of Thunderstorm Days Across New York State. *Journal of Climate and Applied Meteorology*. **23**, 1115-1120.

Federal Meteorological Handbook No. 11, 2007: Doppler Radar Meteorological Observations. Part A, System Concepts, Responsibilities and Procedures. FCM-H11A-2007, Office of the Federal Coordinator for Meteorological Services and Supporting Research.

Fowle, M. A. and P. J. Roebber, 2003: Short-Range (0-48 h) Numerical Prediction of Convective Occurrence, Mode and Location. *Weather and Forecasting* **18**, 785, 788.

Girodano, L. A. and J. M. Fritsch, 1991: Strong Tornadoes and Flash-Flood-Producing Rainstorms During the Warm Season in the Mid-Atlantic Region. *Weather and Forecasting*. **6**, 437-455.

Johns, R. H., 1984: A Synoptic Climatology of northwest-flow Severe Weather Outbreaks. Part II: Meteorological Parameters and Synoptic Patterns. *Monthly Weather Review*. **112**, 449-464.

Johnson and Mapes, 2001: Mesoscale Processes and Severe Convective Weather. In C. Doswell III (Ed.) *Severe Convective Storms* (pp. 78-80). Boston, MA: American Meteorological Society

Joss, J., 1990. Precipitation Measurement and Hydrology. In D. Atlas (Ed.) *Radar in Meteorology*. (p. 581) Boston, MA: American Meteorological Society.

Kelleher, K. E., K. K. Drogemeier, J. J. Levitt, C. Sinclair, D. E. Jahn, S. D. Hill, L. Mueller, G. Qualley, T. D. Crum, S. S. Smith, S. A. Del Greco, S.

Lakshmivarahan, L. Miller, M. Ramamurthy, B. Domenico, and D. W. Fulker, 2007: Project Craft: A Real-Time Delivery System for NEXRAD Level II Data Via the Internet: *Bulletin of the American Meteorological Society (BAMS)*. **88**, 1045-1057.

LaPenta, K.D., L.F. Bosart, T. J. Galarneau Jr., and M. J. Dickinson, 2005: A Multiscale Examination of the 31 May 1998 Mechanicville, New York, F3 tornado: *Weather and Forecasting*, **20**, 494–516.

Loose, T. and R. D. Bornstein, 1977: Observations of Mesoscale Effects on Frontal Movement Through an Urban Area. *Monthly Weather Review*. **105**: 563-571.

Hesterberg, T., D. S. Moore, S. Monaghan, A. Clipson, and R. Epstein, 2005: Bootstrap Methods and Permutation Tests, 2nd Edition. W.H. Freeman, N.Y.

Orville, R. E., G. Huffines, J. Nielson-Gammon, R. Zhang, B. Ely, S. Steiger, S. Phillips, S. Allen, and W. Read, 2000: Enhancement of Cloud-to-Ground Lightning over Houston, Texas. *Geophysical Research Letters*. **28**, 1-10.

Parker, M. D. and D. A. Ahijevych, 2007: Convective Episodes in the East-Central United States. *Monthly Weather Review*. **11**, 3707-3727.

Parker, M. D. and J. C. Knievel, 2005: Do Meteorologists Suppress Thunderstorms: Radar-Derived Statistics and the Behavior of Moist Convection. *Bulletin of the American Meteorological Society (BAMS)*. **86**, 341-358.

Riley, G.T., and L. F. Bosart, 1987: The Windsor Locks, Connecticut Tornado of 3 October 1979. An Analysis of an Intermittent Severe Weather Event. *Monthly Weather Review*. **115**, 1655-1677.

Shepard, J. M. and S. J. Burian, 2003: Detection of Urban Induced Rainfall Anomalies in a Major Coastal City. *Earth Interactions*. **7**, 1-17.

Wallace, J.M. 1975: Diurnal Variations in Precipitation and Thunderstorm Frequency over the Conterminous United States. *Monthly Weather Review*, **103**, 406-419.

Wasula, A. C., L. F. Bosart and K. D. Lapenta, 2002: The Influence on the Severe Weather Distribution across Interior Eastern New York and Western New England. *Weather and Forecasting*.**17**, 1280.

Weisman, R. A., 1990: An Observational Study of Warm Season Southern Appalachian Lee Troughs. Part II: Thunderstorm Genesis Zones. *Monthly Weather Review*. **118**, 2020-2041.

Wilson et al, 1994. "Boundary Layer Clear-Air Radar Echoes: Origin of Echoes and Accuracy of Derived Winds." *Journal of Atmospheric and Oceanic Technology*. **11**: 1184-1206.

Zajac, B. A. and S. A. Rutledge, 2001: Cloud-to-Ground Lightning Activity in the Contiguous United States from 1995 to 1999. *Monthly Weather Review*. **129**: 999-1019.